ELUCIDATING THE ROLE OF JASMONATE METABOLITES IN JASMONIC ACID SIGNALING

A Dissertation Submitted to the Faculty of the Graduate School
at the University of Missouri

In partial fulfillment of the requirements for the degree of
DOCTOR OF PHILOSOPHY

By
Arati Nepal Poudel

Dissertation Supervisor
Abraham J. Koo

December 2017

The undersigned, appointed by the dean of the Graduate School,
have examined the dissertation entitled

ELUCIDATING THE ROLE OF JASMONATE METABOLITES IN JASMONIC ACID SIGNALING

Presented by Arati Nepal Poudel

A candidate for the degree of doctor of philosophy
In Plant, Insect and Microbial Sciences
And hereby certify that, in their opinion, it is worthy of acceptance.

Dr. Abraham J. Koo, PhD

Dr. Walter Gassmann, PhD

Dr. Melissa Goellner Mitchum, PhD

Dr. David G. Mendoza-Cózatl, PhD

ACKNOWLEDGEMENTS

I would like to express my deepest appreciation to my advisor, Dr. Abraham J. Koo for introducing me in the area of plant molecular biology and biochemistry. Without his guidance and persistent help this dissertation would not have been possible. I also like to thank Professor Walter Gassmann for believing in me to be the part of Division of Plant Science. I will always be grateful for your kind support and thoughtful advice. I am equally thankful to my doctoral committee Dr. Melissa Goellner Mitchum and Dr. David G. Mendoza-Cózatl for their valuable comments and advice.

I am grateful to Dr. Misha Kwasniewski from Grape and Wine Institute, University of Missouri, Kazuki Saito group from Riken institute Japan, Lloyd Sumner and Zhentian Lei from Metabolomics Core, University of Missouri for facilitating me with the untargeted metabolomics. I am also thankful to Trupti Joshi's group for their help in analyzing RNA-seq data. I am also indebted to Dr. James Schoelz for guidance and advice throughout my time as a student.

Thanks are due to my colleagues in the lab, Tong, Athen and Rebekah for the interactive and nice lab environment. I am also grateful to all the undergraduates in the lab especially Hannah, Ben, Leslie and Eric for their help with my research work.

I am very grateful to my beloved husband and daughter for their positivity, encouragement and constant support throughout all my ups and downs. My special thanks goes to my parents, parents in laws, sister, brother and to all who babysitted my daughter while I was in research.

TABLE OF CONTENTS

LIST OF TABLES

LIST OF FIGURES

ELUCIDATING THE ROLE OF JASMONATE METABOLITES IN JASMONIC ACID SIGNALING

ABSTRACT

By Arati Nepal Poudel

Dr. Abraham J. Koo, Dissertation Supervisor

The plant hormone jasmonic acid controls immune responses against insect herbivory and regulates plant development. Jasmonic acid is synthesized upon wounding and herbivory and is converted to many derivatives collectively termed as jasmonate (JA). Jasmonoyl-isoleucine (JA-Ile), among the JA is the bioactive form that signals through a nuclear residing co-receptor complex via direct binding to the receptor and subsequent activation of downstream gene expression. Although the JA biosynthetic pathway is well known with almost all the biosynthetic enzymes identified and characterized in detail, the catabolic pathways leading to a diverse array of JA metabolites has only begun to be studied in recent years. One of those pathways catalyzed by the Arabidopsis cytochrome P450 enzymes CYP94B1 (B1) and CYP94B3 (B3) oxidizes JA-Ile to

12-hydroxy (OH)-JA-Ile. Further oxidation of 12OH-JA-Ile to 12-carboxy (COOH)-JA-Ile is carried out by CYP94C1 (C1) in the same CYP94 family. In a second pathway, the amidohydrolases ILL6 and IAR3 cleave JA-Ile at the amide bond into free jasmonic acid and -Ile. In contrast to the well-established function of JA-Ile in mediating JA-dependent responses, biological functions of other JA metabolites are less clear. Identification of additional metabolic pathways of JA and respective mutants blocked in such pathways are providing a unique opportunity to study the homeostatic regulation of JA and its biological function in plant stress responses. Two chapters of this thesis presents the physiological and signaling function of oxidized JA-Ile in plant growth and defense responses. The last chapter discusses a screening work aimed at identifying the novel enzyme group involved in JA metabolism. Collectively, the results extend our understanding of JA metabolism in plant growth and defense responses.

Chapter II presents a mechanism for the inactivation of the JA pathway and its relationship with plant response to wounding. Arabidopsis cytochrome P450 enzymes in the CYP94 clade metabolize JA-Ile, a major isoform of JA responsible for many biological effects attributed to the JA signaling pathway; thus, they are expected to contribute to the attenuation of JA-dependent wound responses. To directly test this, we created double and triple knock-out mutants of three *CYP94* genes, *CYP94B1*, *CYP94B3*, and *CYP94C1*. The mutations blocked the oxidation steps and caused JA-Ile to hyper-accumulate in the wounded leaves. Surprisingly, over accumulation of JA-Ile in the mutants did not result in a stronger wound response, but instead displayed a series of symptoms

reminiscent of JA-Ile deficiency, including increased susceptibility to insect. The mutants responded normally to exogenous JA treatments, indicating that JA-perception or signaling pathways were intact. Untargeted metabolite analyses revealed a global reduction in wound-induced metabolite production in the mutants consistent with the dampened wound-response and increased susceptibility to insects. These observations raise questions about the current JA-signaling model and point toward a more complex model perhaps involving other JA-Ile derivatives and/or feedback mechanisms.

Chapter III focuses on the signaling function of 12OH-JA-Ile which is the first metabolite in the JA-Ile signal catabolic pathway. Contrary to the widely held belief that 12OH-JA-Ile is largely an inactive signal, genetic analyses in chapter II, provided indirect evidence that 12OH-JA-Ile may function as an active signal. Consistently, Arabidopsis seedlings treated with 12OH-JA-Ile accumulated anthocyanin and were also increased in leaf trichome cell numbers to levels comparable to that induced by the same concentration of JA-Ile. Both anthocyanin and trichomes are anti-herbivory features known to be regulated by JA-Ile. In addition, expression of several JA-Ile responsive marker genes was upregulated by 12OH-JA-Ile. Genome-wide transcript analyses and untargeted metabolomics experiments showed that 12OH-JA-Ile could mimic a significant part of JA-Ile effects both at the transcriptional and metabolic levels. Mutation in *CORONATINE INSENSITIVE 1* (*COI1*) blocked 12OH-JA-Ile effects on anthocyanin and trichome induction, indicating that 12OH-JA-Ile signals through the common receptor and signaling mechanism as JA-Ile. 12OH-JA-Ile was able

to trigger anthocyanin accumulation in tomato seedlings in a COI1-dependent manner indicating that the 12OH-JA-Ile signaling system is likely to be conserved in eudicots. Increased endogenous 12OH-JA-Ile levels in a double T-DNA insertion mutant blocked in 12OH-JA-Ile hydrolysis, *ill6iar3*, and decreased 12OH-JA-Ile either by triggering hydrolysis or oxidation of 12OH-JA-Ile in transgenic line *ILL6-OE* or *CYP94C1-OE* displayed phenotypes proportionate with endogenous 12OH-JA-Ile, indicative of JA-Ile-like signaling in wounded plants. Together, these results show that 12OH-JA-Ile likely plays a prominent role in the JA-regulated wound response in plants than previously thought.

Chapter IV presents a genetic screening approach aimed at identifying novel genes in JA metabolism. JA-resistant phenotypes have been observed in most transgenic lines overexpressing catabolic enzymes of the JA pathway. Screening of a mutant population randomly overexpressing Arabidopsis genes was hypothesized to reveal other catabolic enzymes. Such a transgenic mutant population generated by Ichikawa and colleagues (2006) was screened for resistance to JA-inhibited root elongation and an altered JA-Ile profile in wounded leaves. Twenty two candidates were selected and the identity of cDNAs potentially responsible for the phenotypes in ten of those candidates was determined by PCR and DNA sequencing. A candidate gene encoding UDP-glucosyltransferase *86A1* (*UGT86A1*) and its close homolog *UGT86A2* were further characterized. Transgenic lines overexpressing *UGT86A1* or *UGT86A2* displayed reduced JA-Ile and increased 12-*O*-glucosyl-jasmonic acid levels in wounded leaves. T-DNA insertion mutants, *ugt86a1* and *ugt86a2*, however, did

not show JA profiles opposite to the overexpressing lines and a preliminary *in vitro* enzyme assay using purified glutathione *S*-transferase tagged UGT86A1 and UGT86A2 proteins failed to detect clear glucosyltransferase activities. Potential reasons for the discrepancies and future directions are discussed.

CHAPTER I: BACKGROUND AND GENERAL INTRODUCTION

1. An overview and brief history of the defense hormone jasmonic acid

Plants are constantly exposed to various environmental and biotic stresses throughout their life cycle. Their sessile lifestyle inevitably calls for robust defense mechanisms to compensate for their immobility in order to survive in nature. These survival strategies are mostly mediated by transcriptomic remodeling that brings about cellular and physiological changes and are orchestrated by hormones. The lipid derived hormone jasmonate (JA) is one such signal activated under external stress or internal developmental cues that controls stress adaptive responses against biotic aggressors as well as multiple aspects of plant growth and development. JA was first isolated in the 1960s as the essential oil of the jasmine flower in a volatile methylated form called methyl-JA (MeJA) (Demoli et al., 1962; Wasternack 2007). Since then various precursors and derivatives of JA were isolated from plants. It wasn't until the 1990s when JA was found to confer the insect resistance by inducing protease inhibitors in tomato (Farmer and Ryan 1990). Discovery of JA's ability to induce other defense traits, including synthesis of a large number of secondary metabolites that act as insecticides, fungicides, and toxins, followed and, before long, JA was recognized as one of the major plant hormones with an indispensable function in plant defense. JA research in the last decade or so is characterized by the elucidation

of its molecular perception and signaling mechanisms, including the identification of the JA receptors and a number of transcription factors that regulate downstream JA responsive gene expression. JA dependent transcription and defense responses are conserved in all higher plant species examined to date (Howe and Jander, 2008; Browse, 2009a; Wasternack and Hause, 2013). An area in JA biology that has lagged behind but has seen recent progress is the area that deals with JA catabolism and signal inactivation, and is the subject of this dissertation.

2. Jasmonic acid biosynthesis

Jasmonic acid biosynthesis begins in the chloroplast deriving its precursor from plastidial membrane lipids. The stress activated phospholipases such as DEFECTIVE IN ANTHER DEHISCENCE 1 (DAD1) hydrolyze α linolenic acid (C18:3) from the glycerol lipids, most likely the most abundant galactolipids (Ishiguro et al., 2001). This polyunsaturated fatty acid precursor is oxidized at the 13^{th} carbon position by 13-LIPOXYGENASEs (13-LOXs) to become 13(*S*)-hydroperoxytrienoic acid (13-HPOT). 13-LOX activity in Arabidopsis is provided by four nuclear encoded LOX genes (*LOX2*, *LOX3*, *LOX4* and *LOX6*) that are wound inducible (Bannenberg et al., 2009; Chauvin et al., 2013). The 13-HPOT is then metabolized to an epoxide, 12,13(*S*)-epoxyoctadecatrienoic acid (12,13-EOT) by a member of the cytochrome P450 (CYP74A) family, ALLENE OXIDE SYNTHASE (AOS) (Laudert et al., 1996; Howe et al. 2000). This is followed by the cyclization of 12,13-EOT to yield 12-oxo-phytodienoic acid (OPDA) by the

activity of ALLENE OXIDE CYCLASE (AOC). OPDA is both the intermediate in the JA biosynthetic pathway and a molecule with distinct signaling properties from JA (Bottcher and Pollmann 2009; Wasternack and Hause, 2013).

OPDA is then transported from the chloroplast to the peroxisome by yet an unknown mechanism. Entry into the peroxisome is facilitated by an ATP-binding cassette transporter (PXA1) (Zolman et al., 2001, Footitt et al., 2002). OPDA then undergoes reduction and activation by OPDA REDUCTASE 3 (OPR3) and OPC-8: COENZYME A LIGASE1 (OPCL1) respectively, before it undergoes β oxidation (Schaller et al., 2000; Koo et al., 2006). Three different classes of enzymes consisting of ACYL-CoA OXIDASE (ACX), multifunctional protein (MFP) and L-3-ketoacyl-CoA thiolase (KAT) catalyze the three rounds of β oxidation steps to give jasmonic acid (Cruz Castillo et al. 2004; Baker et al. 2006; Delker et al. 2007).

The newly formed jasmonic acid is then conjugated to an amino acid, -Ile, by a cytosolic acyl amide synthetase, JASMONATE RESISTANT 1 (JAR1) to form a bioactive JA, jasmonoyl-isoleucine (JA-Ile) (Fig. 1) (Staswick and Tiryaki, 2004; Suza et al., 2010). JAR1 is a member of 19 closely related proteins in Arabidopsis that belong to the auxin inducible GH3 family of proteins first described in soybean (Hagen and Guilfoyle 1985). Although JAR1 also uses other amino acids as substrates for conjugation reactions, the -Ile conjugate is the predominantly occurring form in plants and is the strongest binding ligand for the JA hormone receptor. The nascent endogenous JA-Ile is also produced as a *cis* stereoisomer, (3*R*,7*S*)-JA-Ile (also referred to as (+)-7-*iso*-JA-Ile). This isomer,

although less stable and thought to easily epimerize to the more stable trans isomer, is present in 9 out of 10 times in the stable form at an equilibrium, and was shown to be the most active receptor binding form of JA (Fonseca et al., 2009). The conjugated form as the active form of a hormone is unique in the case of JA since in all other cases known to date, conjugation is associated with inactivation, storage, or degradation of hormones.

3. JA signaling and wound perception

JA mediated downstream responses require molecular perception of JA-Ile by the nuclear residing co-receptor protein complex consisting of CORONATINE INSENSITIVE 1 (COI1) and JASMONATE ZIM DOMAIN (JAZ) proteins (Figure 1.1) (Chini et al., 2007, Thines et al., 2007; Koo et al., 2017). The Arabidopsis *coi1* mutant was first isolated in a mutant screen for insensitivity to the bacterial phytotoxin coronatine, a structural mimic of JA-Ile and a strong agonist of the COI1-JAZ co-receptor. Mutant *coi1* phenocopies several JA-deficient phenotypes, such as fertility defects, resistance to wound-induced growth inhibition, inability to induce JA-responsive marker gene expression and increased susceptibility to insects. Unlike JA-biosynthetic mutants (Sanders et al., 2000), *coi1* mutant phenotypes cannot be rescued by exogenous JA treatment (Feys et al., 1994; McConn and Browse, 1996; Stintzi and Browse 2000). COI1 is an F-box protein component of the E3 ubiquitin ligase complex, Skip1-Cul1-F-box protein (SCF^{COI1}) (Xie et al., 1998) that recognizes the target protein for ubiquitination. The knowhow of the F-box protein functioning in the

analogous hormone auxin (Santner and Estelle 2009) aided the discovery of JA repressor JAZ proteins as the target of COI1. Indeed, JAZ was found to physically interact with COI1 and was degraded by the 26S proteosomal pathway upon polyubiquitination by the SCF^{COI1}. JAZs are transcriptional repressors that interact with transcription factors (TFs) such as MYC2, a dominant TF for many JA-responsive genes (Boter et al., 2004; Lorenzo et al., 2004), and interfere with TF action to activate gene transcription (Kazan and Manners 2008). JAZ also recruits other co-repressor protein TOPLESS (TPL) either through direct interaction or through adaptor proteins known as NOVEL INTERACTORS OF JAZ (NINJA) and thereby further repressing the transcriptional activity (Pauwels et al., 2010). Proteolytic degradation of JAZ relieves the TFs (MYC2/3/4/5) to initiate gene transcription (Boter et al., 2004; Fernandez-Calvo et al., 2011; Figueroa and Browse, 2012; Zhang et al., 2015).

JA-induced gene expression patterns reveals a complex feedback regulation mechanism. Transcriptional induction of the early JA-responsive TF *MYC2* and almost entire JA-biosynthetic genes (at least 13 in Arabidopsis) constitute the positive feedback loop while induction of *JAZs* (10 out of 12 canonical *JAZs*), *JA-ASSOCIATED MYC2-LIKE* (*JAM1/2/3*) encoding negative TFs that compete with MYCs to repress JA-responsive gene expression, and genes encoding JA-Ile catabolic enzymes constitute the negative feedback loop (Thines et al., 2007; Chico et al., 2008; Chung et al., 2008; Koo and Howe, 2012; Nakata et al., 2013; Bhosale et al., 2013; Sasaki-Sekimoto et al., 2013). Among the 12 JAZs in Arabidopsis, non-canonical JAZs, such as JAZ8 and the splice

variants of JAZ10 are resistant to JA-Ile-mediated proteolytic degradation, have been proposed to desensitize the JA signaling system during the extended period of persisting levels of JA-Ile (Chung and Howe, 2009; Shyu et al., 2012; Moreno et al., 2013).

4. Other derivatives of JA and JA-Ile catabolism

Wounding or herbivory stimulates *de novo* synthesis of JA. JA-Ile typically peaks within 0.5-2 h of wounding, followed by gradual decline over time for about 10-12 h in Arabidopsis (Chung et al., 2008; Koo et al., 2009). The decline of JA-Ile indicates its metabolic turnover which has been the recent focus of research in the JA field (Koo and Howe, 2012; Koo 2017). These recent efforts have uncovered two major pathways of JA-Ile catabolism. The so-called ω-oxidation pathway mediated by a group of cytochrome P450 enzymes in the CYP94 clade oxidizes JA-Ile at the 12^{th} carbon position. The oxidation occurs in two consecutive steps. First, CYP94B1(B1) and CYP94B3 (B3) introduce a hydroxyl group to the methyl end of the pentenyl side chain of JA-Ile to form 12-hydroxy (OH)-JA-Ile (Koo et al., 2011, Kitaoka et al., 2011; Heitz et al., 2012; Koo et al., 2014). Subsequently, CYP94C1 further oxidizes the 12OH-JA-Ile to 12-carboxy (COOH)-JA-Ile (Heitz et al., 2012). The *in vitro* enzyme assays indicated that B1 is specific for only the first hydroxylation step while B3 and C1 can catalyze both steps sequentially (Koo et al., 2011; Heitz et al., 2012). However, genetic studies with knock-out mutants and transgenic lines overexpressing the enzymes have suggested that B1 and B3 together catalyze at least 95% of the first

hydroxylation step while B3 and C1 catalyze the second oxidation step (Koo et al., 2014). These oxidized forms of JA-Ile are largely thought to represent the degraded forms of JA, however, the precise function of these metabolites in plant growth and development have not been systematically tested. The second catabolic pathway termed, the hydrolytic pathway, involves cleavage of the JA-Ile molecule at the covalent amide bond that joins jasmonic acid with –Ile (catalyzed by JAR1). The enzyme catalyzing this reaction was first reported in tobacco (Woldemariam et al., 2012) and soon was followed by discoveries in Arabidopsis (Bhosale et al., 2013; Widemann et al., 2013; Zhang et al., 2016). The discovery in Arabidopsis was aided by a transcriptional co-expression analysis that identified a member of indole-3-acetic acid (IAA) amido hydrolase (IAH) family gene, *ILL6*, being a major candidate as a novel regulator of the JA pathway (Bhosale et al., 2013). The IAH family consists of seven members in Arabidopsis and has previously been studied with respect to IAA metabolism (Bartel and Fink, 1995; Davies et al., 1999; Ludwig-Müller, 2011). Subsequent studies confirmed the *in vitro* enzymatic activity as well as the *in vivo* function of both ILL6 and IAR3, in the same IAH family, in metabolizing JA-Ile (Widemann et al., 2013; Zhang et al., 2016). The dual substrate specificity of IAR3 towards both JA and IAA conjugates as well as the JA (and wound)-inducible feature of their gene expression raised the possibility of these amidohydrolases mediating cross-talks between the hormonal pathways (Zhang et al., 2016).

Both of the ω-oxidation and the hydrolytic JA-Ile turnover pathways are highly conserved among different plant species and their expression is

dependent on the JA receptor COI1 implying their importance in providing competitive edge to plants (Ludwid-Muller 2011; Koo and Howe, 2012; Koo 2017). This dissertation and associated work address the physiological importance of these catabolic pathways in balancing the growth-defense trade-offs during wound response.

JA comprises of other chemically modified forms of jasmonic acid (Figure 1.1). They include the methylated MeJA; the dehydrogenated 4,5-didehydro-, 3,7-didehydro-, 11,12-didehydro-JA; the reduced 9,10-dihydro-JA; the decarboxylated cis-jasmone; the C6 keto group of the cyclopentanone ring reduced cucurbic acid; the 11- and 12-hydroxylated 11OH-JA and 12OH-JA; the 12-carboxylated 12COOH-JA; the 11- and 12-glucosylated (Glc) 11- and12-*O*-Glc-JA; sugar esterified at the C1 carboxyl terminus JA-*O*-Glc and JA-*O*-gentiobiosyl esters; and the 12-sulfated 12HSO_4-JA (Sembdner and Parthier, 1993; Wasternack, 2007; Koo, 2017). These JA derivatives also conjugate to various amino acids (JA-Ala, JA-Val, etc.) and 1-aminocyclopropase-1-carboxylic acid (ACC) (Staswick and Tiryaki, 2004; Guranowski et al., 2007). Considering the stereochemistry variants of above mentioned metabolites, the list of naturally occurring JA increase exponentially. Functions of many of these metabolites as well as enzymes catalyzing their production are understudied. Some of the identified enzymes include the recently reported JASMONATE-INDUCED OXYGENASE/JASMONIC ACID OXIDASE (JOX/JAO) that catalyzes direct hydroxylation of jasmonic acid to produce 12OH-JA (Caarls et al., 2017; Smirnova et al., 2017). This is a second route to produce 12OH-JA in addition to

the already known pathway which is the cleavage of 12OH-JA-Ile at the amide bond catalyzed by ILL6 and IAR3. The blocked JA catabolism in *jao2* mutant boosted plant immunity against the necrotrophic fungal pathogen *Botrytis cinerea* (Smirnova et al., 2017). 12OH-JA on the other hand is an important virulence factor for the rice blast fungus *Magnaporthe oryzae* (Patkar et al. 2015). Implication of 12OH-JA-Ile and 12COOH-JA-Ile in host resistance against *B. cineria* has also been reported (Aubert et al. 2015). The methylation of jasmonic acid is catalyzed by *S*-adenosyl-L-methionine:jasmonic acid carboxylmethyl transferase (JMT) (Seo et al., 2001). Although MeJA is not the active ligand for the COI1-JAZ co-recepter *per se* (Thines et al., 2007), its volatile physical property makes it an effective intercellular long distance or air borne mobile signal (Farmer and Ryan 1990; Heil and Ton 2008). The Arabidopsis hydroxyjasmonate sulfotransferase (ST2A) was reported to have *in vitro* activity to convert 12OH-JA to the sulfated derivate of JA, 12HSO_4-JA (Gidda et al., 2003). Both 12OH-JA and 12-HSO_4-JA tested negative for inhibiting germination and root elongation, and were not able to induce JA-responsive marker gene expression (Miersh et al., 2008). The glucosyl derivative of JA, 12-*O*-Glc-JA was reported to have tuber inducing effects in potatoes (Yoshihara et al. 1989) and leaf movements in rain trees (*Samanea saman*) and legumes (*Medicago truncatula*) (Nakamura et al. 2011; Zhou et al. 2012). The enzyme responsible for the JA 12-*O*-glucosylation has not been identified in Arabidopsis; however, in maize, *silkless1* (*sk1*) gene encoding a predicted peroxisome localized uridine diphosphate (UDP) glycosyltransferase was reported to function in JA catabolism

even though the enzymatic function awaits to be verified (Hayward et al., 2016). Identification of the complete set of metabolic enzymes and their associated mutants will aid in understanding the biological function of each JA metabolite.

5. JA action in regulating plant growth and defense tradeoffs

JA regulates a wide range of physiological processes ranging from growth, development and defense responses. These processes appear to be coordinated rather than independent to one another. Sensing of JA changes the morphological features resulting from deposition of callose, cuticular lipids and phenolics; and increased number of glandular and non-glandular trichomes; and inhibition of root and shoot growth (Havko et al., 2016; Huot et al., 2013; Wu and Baldwin 2010; Yoshida et al. 2009; Zhang and Turner 2008). The reinforcement of protective cell barriers or biogenesis of hair-like structures loaded with defense compounds are the obvious defense strategy developed against herbivory attack. On the other hand, a contribution to the inhibition of growth to increase plant fitness in the face of attack is more controversial, since the immediate benefit of such measure is less clear and is viewed more as a mechanism at the expense of increased defense.

Emerging evidences indicate that multiple factors are contributing to the so-called fitness penalty in wounded or JA-treated plants. Resource reallocation of nutrients and energy to the production of defense metabolites has been the traditionally held reason behind ceassation of growth (Engelsdorf et al. 2013; Ohnmeiss and Baldwin 1994; Ullmann-Zeunert et al. 2013; Zhang et al. 2017).

However, there is evidence supporting a more active program “wired” into the defense system such as interference with cell cycle progression, cell division, and cell elongation (Noir et al. 2013; Pauwels et al. 2008; Zhang and Turner 2008). Adding weight to this argument, recent transcriptomics data revealed widespread active repression of genes associated with photosynthesis (Attaran et al. 2014; Kerchev et al. 2012; Mitra and Baldwin 2014; Nabity et al. 2013). Still another major factor playing a role in growth-defense tradeoff regulation appears to be the crosstalk between JA and other signaling pathways. For example, an elegant mechanism of hormone cross-talk between JA and the major growth hormone, gibberellin (GA), has been described to occur through protein-protein interaction between JAZ and DELLA proteins, which are, similar to JAZ, transcriptional repressors of the GA-regulated transcriptional system (Hou et al., 2010; Yang et al., 2012). Another example comes from the interaction between defense and light response pathways (Moreno et al., 2009). Plant exposed to shade light grow faster but are compromised in insect resistance in a process famously termed the “shade avoidance syndrome” (Ballare, 2014). At the molecular level, under far-red light conditions the active Pfr form of phyB is decreased while JAZs are stabilized (Leone et al., 2014; Campos et al., 2016).

The molecular mechanism of JA-mediated growth-defense tradeoff is an area of research that will continue to see more development in the near future partly due to important implications in crop engineering. Our unique observation of uncoupling of JA accumulation and plant growth in the JA catabolic mutants

described in Chapter II is relevant in this regard and may contribute to closing the knowledge gap in the growth-defense regulation.

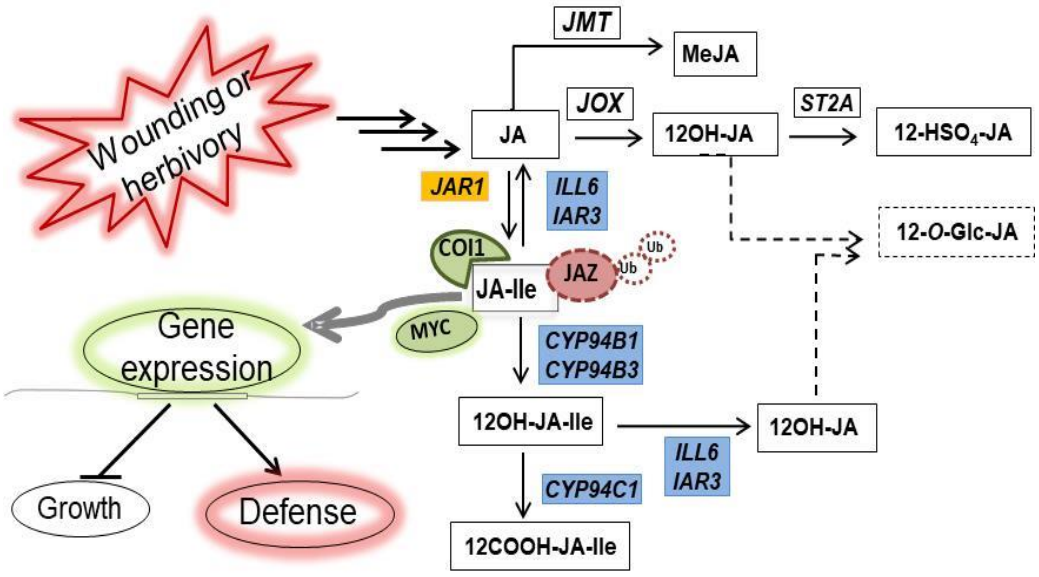

Figure 1.1. Overview of JA-Ile metabolic and signaling pathways.

Enzymes in blue and orange colored boxes in the metabolic pathways represent their subcellular localization in endoplasmic reticulum and cytoplasm, respectively. Enzymes in non colored boxes have not been reported for their subcellular localization. Solid lines in the enzymatic pathway denote the confirmed enzymatic steps, while dashed lines represent without known enzymes. Wounding or herbivory activates JA-Ile biosynthesis which promotes complex formation between COI1 and JAZ co-receptors which results in polyubiquitination of JAZ followed by its degradation by 26S proteasome pathway (not shown). JAZ degradation releases transcription factors such as MYC2/3/4/5 to activate JA responsive gene expression that results in increase defense traits and suppression of growth.

CHAPTER II: MUTATIONS IN JASMONOYL-L-ISOLUCINE-12-HYDROXYLASES SUPPRESS MULTIPLE JA-DEPENDENT WOUND RESPONSES IN ARABIDOPSIS THALIANA

This chapter has been published in Biochemica et Biophysica Acta (BBA) – Molecular and Cell Biology of Lipids, Volume 1861, Issue 9, part B, 2016 Sept. 1396-1408

ABSTRACT

Plants rapidly perceive tissue damage, such as that inflicted by insects, and activate several key defense responses. The importance of the fatty acid-derived hormone jasmonate (JA) in dictating these wound responses has been recognized for many years. However, important features pertaining to the regulation of the JA pathway are still not well understood. One key unknown is the inactivation mechanism of the JA pathway and its relationship with plant response to wounding. Arabidopsis cytochrome P450 enzymes in the CYP94 clade metabolize jasmonoyl-L-isoleucine (JA-Ile), a major isoform of JA responsible for many biological effects attributed to the JA signaling pathway; thus, they are expected to contribute to the attenuation of JA-dependent wound responses. To directly test this, we created the double and triple knock-out mutants of three CYP94 genes, *CYP94B1*, *CYP94B3*, and *CYP94C1*. The

mutations blocked the oxidation steps and caused JA-Ile to hyper-accumulate in the wounded leaves. Surprisingly, over accumulation of JA-Ile did not lead to a stronger wound response, rather the mutants displayed a series of symptoms reminiscent of JA-Ile deficiency, including increased susceptibility to insects. The mutants responded normally to exogenous JA treatments, indicating that JA-perception or signaling pathways were intact. Untargeted metabolite analyses revealed a global reduction in wound-induced metabolite production in the mutants consistent with the dampened wound-response and increased susceptibility to insects. These observations raise questions about the current JA-signaling model and point toward a more complex model perhaps involving other JA-Ile derivatives and/or feedback mechanisms.

1. Introduction

Across kingdoms, oxylipins function as important regulators of cell differentiation, immune response, and wound healing (Andreou et al., 2009; Blancaflor et al., 2014; Blee, 2002; Funk, 2001; Kachroo and Kachroo, 2009; Shah, 2005). In animals, arachidonic acid-derived eicosanoids, such as leukotrienes and prostaglandins function as mediators in wounding, asthma, arthritis, and other inflammatory diseases (Funk, 2001; O'Byrne et al., 1997). In plants, linolenic acid-derived jasmonate (JA) carry out similar functions in stress-related processes (Acosta and Farmer, 2010; Browse, 2009a; Koo and Howe, 2009; Wasternack and Hause, 2013). JA plays an essential role in wound response and plant resistance against insects (Erb et al., 2012; Halitschke and

Baldwin, 2005; Howe and Jander, 2008). Unlike animals, tissue injury in plants does not mobilize specialized cells such as leukocytes that are the principal cellular components of the mammalian inflammatory responses. Plants instead activate defense responses in each cell that mostly depend on genome wide transcriptional remodeling (León et al., 2001; Pauwels et al., 2008; Reymond et al., 2000). Some of the documented JA-regulated wound responses in plants are: synthesis of chemical toxins and insect deterrents (e.g., glucosinolates, nicotine, etc.), production of anti-nutritive compounds (proteinase inhibitors), release of volatiles that attract predatory insects, reinforcement of structural barriers, formation of specialized defense cells (e.g., trichomes), priming of immune system for future attacks, and growth inhibition (Baldwin, 1996; Biggs, 1985; De Geyter et al., 2012; Engelberth et al., 2004; Erb et al., 2012; Farmer and Ryan, 1992b; Heil and Karban, 2010; Kliebenstein et al., 2002b; Martin et al., 2002; Mithofer and Boland, 2012; Sonderby et al., 2010; Yoshida et al., 2009; Zhang and Turner, 2008). These responses occur locally at the site of damage as well as in neighboring cells and in the regions remote to the damaged tissues. JA's roles in mediating these systemic responses have been implicated in a number of experimental systems (Heil and Ton, 2008; Koo and Howe, 2009; Li et al., 2002; Wasternack and Hause, 2013). JA also serves other important signaling roles in normal plant growth and development, including reproductive organ development (Browse, 2009a; Wasternack and Hause, 2013).

JA exerts its function by regulating the transcription of many genes (Devoto et al., 2005; Lorenzo and Solano, 2005; Memelink, 2009; Pauwels et al.,

2008; Reymond et al., 2000). The number of genes changing their expression in response to wounding is on the order of several hundred to thousands (Attaran et al., 2014; Devoto et al., 2005; Pauwels et al., 2009; Stintzi et al., 2001; Strassner et al., 2002; Zhao et al., 2003). Undamaged leaves of mature plants contain very low levels of JA (Glauser et al., 2008; Koo et al., 2009). Wounding such as that inflicted by insects can activate rapid *de novo* synthesis of JA (Chung et al., 2008; Glauser et al., 2008; Koo et al., 2009). The speed of this induction is measured to be less than a few minutes of tissue injury, indicating that all biosynthetic enzymes are constitutively present in unstressed cells (Chung et al., 2008; Farmer et al., 2014; Glauser et al., 2008; Koo et al., 2009). Synthesis of JA is quickly followed by induction of JA-responsive gene expression (Chung et al., 2008). This happens when one of the isoforms of JA, jasmonoyl-isoleucine (JA-Ile), is perceived by a receptor complex in the nucleus (Chini et al., 2007; Thines et al., 2007). In cells containing low levels of JA-Ile, the activity of transcription factors (TFs), such as MYC2 that positively regulates JA-responsive gene expression (Dombrecht et al., 2007; Lorenzo et al., 2004), is repressed by transcriptional repressors called JASMONTE ZIM-DOMAIN (JAZ) proteins and their associated co-repressors (Katsir et al., 2008a; Pauwels et al., 2010). Elevated JA-Ile levels promote recruitment of JAZ to be flagged (ubiquitinated) for degradation by the 26S proteasome system. The CORONATINE INSENSITIVE1 (COI1), which is an F-box protein component of the E3 ubiquitin ligase SCF^{COI1} interacts with JAZ by a protein-protein interaction (Katsir et al., 2008b; Xie et al., 1998). This physical interaction between COI1 and JAZ has

been shown to occur only in the presence of JA-Ile and its closely related structural variants (e.g., JA-Val), but not in the absence these small molecule ligands nor in the presence of other precursors or derivatives of JA-Ile, such as 12-oxo-phytodienoic acid (OPDA), jasmonic acid, methyl-JA (MeJA), or 12-carboxy-JA-Ile (12COOH-JA-Ile) (Fonseca et al., 2009; Katsir et al., 2008b; Thines et al., 2007). Among the genes with increased transcripts are genes encoding positive regulators of the JA pathway (e.g., JA biosynthetic enzymes and TFs) and negative regulators (e.g., JA catabolic enzymes and transcriptional repressors). Thus, the JA pathway is under both positive and negative feedback regulations (Chini et al., 2007; Chung et al., 2008; Katsir et al., 2008a; Thines et al., 2007).

JA synthesis is initiated in the plastid through the so-called ‘octadecanoid pathway’ using α-linolenic acid (18:3) as the main precursor (Farmer and Ryan, 1992a; Ishiguro et al., 2001; Schaller, 2001; Wang, 2004). Following the release from membrane lipids by A1-type phospholipases, 18:3 is oxygenated and cyclized to produce a cyclopentenone intermediate, 12-oxo-phytodienoic acid (OPDA) by a series of enzymatic reactions in the plastid (Bell et al., 1995; Chauvin et al., 2013; Laudert et al., 1996; Stenzel et al., 2003; Ziegler et al., 2000). OPDA is found both as a free carboxylic acid form as well as those esterified to the complex glycerol lipids (Andersson et al., 2006; Buseman et al., 2006; Nilsson et al., 2015). The second stage of JA biosynthesis takes place in the peroxisomes where OPDA, upon entry into the peroxisome, assisted by a membrane-localized ATP-binding cassette transporter and its associated protein,

is oxidized through multiple rounds of ω-oxidation cycles to yield jasmonic acid (Koo et al., 2006; Park et al., 2013; Schaller et al., 2000; Schilmiller et al., 2007; Schneider et al., 2005; Theodoulou et al., 2005; Zolman et al., 2001). The active signal JA-Ile is produced when jasmonic acid is conjugated to isoleucine by a cytosolic acyl-amido synthetase, JAR1 (Staswick and Tiryaki, 2004).

The initial burst of JA-Ile is followed by its slow decline overtime, indicating a metabolic turnover (Glauser et al., 2008; Koo et al., 2009; Miersch et al., 2008). Compared to the well-studied JA biosynthetic pathways, the metabolic processes used to turn JA over are only beginning to be elucidated. Two major pathways for JA-Ile catabolism have been described recently. One pathway involves oxidation of the C_{12} position of JA-Ile to generate 12-hydroxy-JA-Ile (12OH-JA-Ile). This reaction is catalyzed by two members of the CYP94 family of cytochrome P450 in Arabidopsis, CYP94B1 (94B1) and CYP94B3 (94B3) (Heitz et al., 2012; Kitaoka et al., 2011; Koo et al., 2011; Koo et al., 2014). Together 94B1 and 94B3 contribute ca. 95% of the activity for conversion of JA-Ile to 12OH-JA-Ile in Arabidopsis leaves (Koo et al., 2014). 12OH-JA-Ile is further oxidized to a carboxy-derivative, 12COOH-JA-Ile by CYP94C1 (94C1) and 94B3 (Heitz et al., 2012). In the second turnover pathway, JA-Ile is hydrolyzed at the amide bond to free jasmonic acid and Ile by IAR3 and ILL6 in the family of ILR1-like amidohydrolases (Bhosale et al., 2013; Widemann et al., 2013; Woldemariam et al., 2012; Zhang et al., 2016). Some members in this family, including IAR3, hydrolyze amino acid conjugates of auxin, another major plant hormone (Davies et al., 1999), creating a hormone signaling crosstalk node

between JA and auxin pathways (Zhang et al., 2016). In addition, JA is metabolized into a wide variety of other derivatives (Gidda et al., 2003; Matsuura et al., 2001; Miersch et al., 2004; Sembdner and Parthier, 1993; Wasternack and Hause, 2013).

Sequences that are homologous to the CYP94s and IAHs have been found in most higher-plant genomes, indicating the evolutionary conservation of the catabolic pathways and the existence of selection pressures to limit JA overproduction (Campanella et al., 2003; Koo and Howe, 2012). Compared to JA-deficiency or insensitivity, which has been well-characterized at the molecular and organismal levels (through the use of various mutants defective in JA-biosynthesis or signaling pathways) (Browse, 2009b), physiological impacts of blocked JA turnover have not been studied in detail. Identification of genes involved in JA-Ile catabolism has provided an opportunity to address this issue.

Here, we report biochemical, molecular, and physiological characterization of Arabidopsis mutants disrupted in JA-Ile turnover with the question in mind: “Why do plants need to get rid of JA?” An obvious hypothesis is that plants will suffer chronic stress symptoms due to the constitutive activation of JA-mediated defense signaling pathway. However, CYP94 knock-out mutants displayed an array of phenotypes that were the opposite of this expectation as they became less responsive to wounding. Given the unexpected nature of these results, more careful studies were carried out using multiple allelic mutants and genetic complementation lines, as well as by examining several JA-dependent wound response phenotypes and molecular characteristics of the mutants.

2. Material and methods

2.1. Plant materials and growth conditions

Arabidopsis thaliana ecotype Columbia-0 was used as the wild-type (WT) for all experiments. CYP94 T-DNA insertion lines used in this study were *cyp94b1-1* (*b1-1*)(SALK_129672), *cyp94b1-2* (*b1-2*) (SALK_132621), *cyp94b3-1* (*b3-1*) (CS302217), *cyp94b3-2* (*b3-2*) (SALK_018989c), *cyp94c1-1* (*c1-1*) (SALK_011290), and *aos* (SALK_017756). These were obtained from the Arabidopsis Biological Resource Center and have been described earlier (Koo et al., 2011; Koo et al., 2014; Schilmiller et al., 2007). Genetic crosses were made to generate double and triple homozygous mutants, *b1-1b3-1*, *b1-1b3-2*, *b1-2b3-1* (Koo et al., 2014) and *b1-1b3-1c1-1* (Figure 2.3). The *b1b3aos* mutant was generated by using *b1-1b3*-2 pollen to pollinate sterile *aos* flowers. The cross F2 progeny was first selected for double homozygous *b1-1b3-2* by PCR genotyping then selected for sterile plants (*aos*). The *b1-1b3-2aos* seeds were maintained by spraying the developing flowers with 100 μM jasmonic acid methyl ester (MeJA) solution every other day. Primers used for genotyping *c1-1* are listed along with all other primers used in this study in Table 1. Plants were grown in environmental growth chambers at 22 °C with a long-day photoperiod condition of 16 h light (100–120 μE m^{-2} s^{-1}) except for the plants used for insect feeding assays, which were grown under a short-day photoperiod of a 12 h day. Transgenic lines were created to complement *b1b3* (*b1-2b3-1*) with the WT copy of *CYP94B3* (*94B3*) gene controlled by its native promoter. A 3.5 kb region containing a 1.5 kb open reading frame of *94B3* and a 2 kb upstream region was

PCR amplified using primers indicated in Table 1 and was cloned into a gateway vector pENTR/D-TOPO (Life Technologies). Following sequence verification, the insert was recombined by the LR reaction into the pGWB501 vector (Nakagawa et al., 2007) kindly provided by Dr. Tsuyoshi Nakagawa of Shimane University-Matsue, Japan. The *b1b3* plants were transformed by the floral dipping method (Clough and Bent, 1998) using a C58C1 strain of *Agrobacterium tumefaciens* harboring above constructed plasmids. Seeds harvested from resulting plants were screened for resistance to hygromycin. Twenty seedlings that survived the antibiotics selection were tested for JA profile. Three of the T2 lines with the JA-Ile and 12OH-JA-Ile levels restored to the WT levels were retained for subsequent experiments (Figure 2.7).

2.2. Wounding and growth assays

Wounding for time course JA profiling and transcript analyses was administered on 4–5 week-old plants by crushing the fully expanded leaves across the midrib twice using a pair of hemostats with serrated teeth (Herde et al., 2013). Wounding for wound-induced growth inhibition (WIGI) assays was modified from previously described methods (Yan et al., 2007; Zhang and Turner, 2008) and is illustrated in Figure 2.1. Overall, six rosette leaves were wounded ten times over the course of eight days beginning from the 17–18-d old stage. Each time, a pair of leaves was wounded once with a hemostat across the midrib. On day one, leaves numbered 1 and 2 were wounded; on day two, leaves numbered 3 and 4 were wounded; and on day three, leaves numbered 3 and 4

received a second set of wounding. Leaves were numbered counting from the first true leaf as leaf 1. After the first three days of wounding, plants were allowed to recover for three days without wounding. On day seven, leaf number 5 and 6 were wounded; and finally, on day eight, leaf number 5 and 6 received a second set of wounding. After three days from the final wounding, fresh weight of the above-ground tissue was determined. Dry weight was determined after drying the harvested plants in an oven at 55 °C for at least three days. For root length assays, seedlings were grown vertically on solid Murashige and Scoog (MS) medium in square Petri plates either with or without JA (10 μM) (Koo et al., 2011). Root length was determined on the seven-day old plants for those grown on plain MS media, and on the nine-day old plants for those on the JA-containing plates.

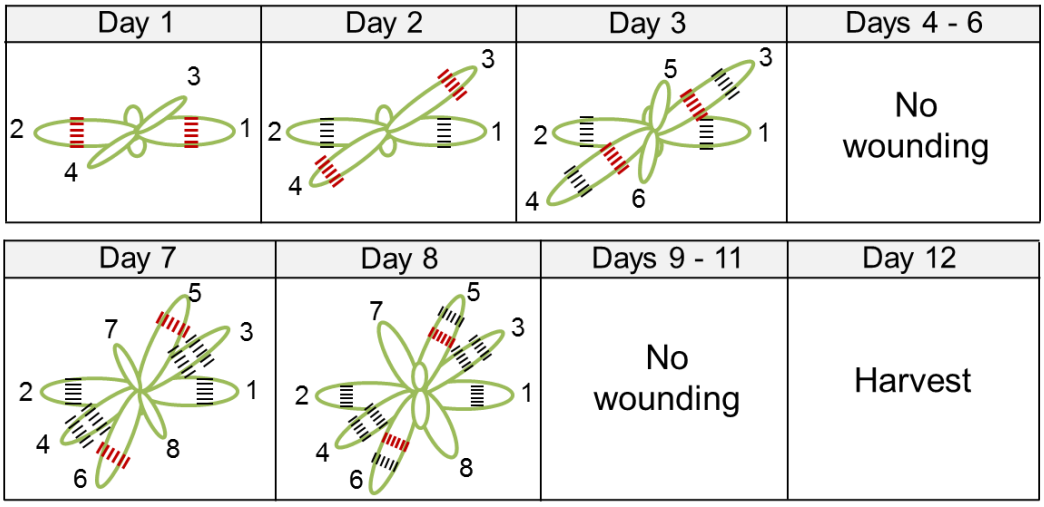

Figure 2.1. Schematic illustration of wounding for the WIGI assay. Schematic illustration of wounding for the WIGI assay. Red and black dashed lines across leaves (numbered) denote fresh and old (previously wounded) wounding marks, respectively. Day 1 starts at 17-18-d-old. The illustration is not to the scale.

Table 2.1. Oligonucleotides used in this study.

Use	Primer name	Primer sequences (5' – 3')
T-DNA genotyping		
T-DNA	LBb1	GCGTGGACCGCTTGCTGCAACT
cyp94c1	jh1cko RP	TGATAAACCGGTTAGCTGGTG
	jh1cko LP	AAACTCAGATTCTTCAATCCGC
B3promoter:B3 cloning		
	JH2_compl_F1	CCACGTCATGGATTGAGGCTAAAAGGCTA
	JH2_compl_R1	CCCTTAAACGTTGTTAAGGATGTGACTTCT
RT-PCR and qRT-PCR		
94B1	P4503koF1	AACCGCCACCGTCTTCTCCAAT
	Jh3ckoR2	CCATGTGAGCGGTTAGAAGAGG
94B3	P4502GABIkoRP	GCAAAGCAAGATCTTTTGTCG
	JH2 taa R	TTAAACGTTGTTAAGGATGTGACTTCTTCTC TTG
94C1	jh1cko RP	TGATAAACCGGTTAGCTGGTG
	JH1_XhoI R	TTCTCGAGCTAACTCCTTTCTTGGATCATAA CC
ACTIN8	rt ACTIN8 F	GAGACAACTTACAACTCGATC
	rt ACTIN8 R	CTGTGGACAATGCCTGGAC
JAZ8	rt JAZ8 F	ATGAAGCTACAGCAAAATTGTG
	rt JAZ8 R	GACCCGTTTGAGGATGACTTG
JAZ10	rt JAZ10 F	CCGATTCATCGGCTAAATCTCG
	rt JAZ10 R	GCGACCTTCATAATTTCACCAGC
OPR3	rt OPR3 F	GCATGGAAGCAAGTTGTGGAAG
	rt OPR3 R	CGAGGTTTCGGGTACTTCACG
MYC2	rt MYC2 F	TGGCAACCGTCGTATGATTTCT
	rt MYC2 R	TCACCTCCTCATCAACAGCGTC
PAP1	rt PAP1 F	TGCTGGAAGATTACCTGGTCG
	rt PAP1 R	AGTGCCGGTGTTGTAGGAATG
DFR	rt DFR F	TGGTGGTCGGTCCATTCAT
	rt DFR R	GAGAGAGCGCGGTGATAAGG

2.3. Anthocyanin measurement and trichome counting

Relative anthocyanin contents were determined using a spectrophotometry-based method described previously (Rabino and Mancinelli, 1986). The entire above ground tissue was submerged in methanol:water:HCl = 85:14:1 (v/v/v) and gently rocked overnight in 4 °C. Absorption at wavelengths 530 and 657 nm was determined in the supernatant. Anthocyanin content was calculated by the formula $A_{530} - (A_{657} \times 0.25)$ and was normalized by the tissue weight. For trichome assays, plants were wounded according the wounding scheme of WIGI (described in Section 2.2). Trichomes within a predefined 5×5 mm^2 area were counted from the adaxial surface of leaf 8, which had not been directly wounded, using photo images taken under a stereomicroscope (SZ-PT Olympus).

2.4. Insect feeding trials

The no-choice insect feeding assay was performed as described earlier (Herde et al., 2013). Newly hatched neonates of *Spodoptera exigua* (Benzon Research, PA, USA) were transferred onto 5-week old plants grown under the short-day condition. Each feeding unit contained eight insect larvae and two plants of the same genotype in a cage made out of an inverted bottomless clear plastic cup placed on a pot of soil. The interface between the cup and the pot was sealed by Parafilm to prevent the insects from escaping, and the top opening was capped with Miracloth to allow air exchange. In a typical assay, 10-12 feeding units were set up per genotype. Larvae weight was determined individually after 14-d of feeding. For the choice assay (Green et al., 2012),

Spodoptera larvae were hatched and raised on an artificial beet armyworm diet (Southland Products, AR, USA) for 7-10 days. Fifteen similar sized larvae were released in the middle of a Petri dish containing leaves of genotypes under examination. An equal number of leaves (typically six) from each genotype were arranged alternately around the periphery of the Petri dish surrounding the larvae in the middle. The cut leaf petioles were covered with wet papers to keep leaves hydrated during the entire time of the assay. Several of these choice-assay units were set up in parallel. After 15 h of feeding, the number of larvae on each genotype leaf was counted.

2.5. RNA analysis

Total RNA was extracted using TRIzol reagent (Invitrogen) according to the manufacturer's instructions. Tissue (50-100 mg) was first ground into a fine powder while frozen in a vial containing metal ball bearings using TissueLyser II (QIAGEN). One μg of the total RNA treated with DNaseI (QIAGEN) was reverse transcribed using the Moloney murine leukemia virus (M-MLV) reverse transcriptase (Promega) and oligo$(dT)_{20}$ primers. Five ng of cDNA was used as a template for subsequent PCR reactions. Taq-Pro Red Complete (Denville) was used as Taq polymerase for semi-quantitative RT-PCR experiments while Phusion Taq Polymerase (Thermo Scientific) was used for all cloning purposes. Quantitative (q) RT-PCR was performed on a CFX96 Touch™ real-time PCR detection system (Bio-Rad) using SsoFast™ EvaGreen® Supermix (Bio-Rad) as described previously (Zhang et al., 2016). A complete list of primers used for

PCR is listed in Table 1. *ACTIN8* (AT1G49240) gene was used as an internal reference gene, and transcript levels were expressed as fold changes relative to untreated WT control (0 h).

2.6. JA quantification

JA extraction and quantification were completed according to methods described earlier (Koo et al., 2014; Zhang et al., 2016). Briefly, 20–50 mg of frozen tissue was homogenized with metal beads using TissueLyserII. A 200 μL methanol:water:acetic acid = 70:29:0.5 (v/v/v) mixture containing internal standards, dihydro-JA(dhJA) and [$^{13}C_6$]-JA-Ile, was added and vigorously shaken for 20 min at 4 °C. After removing the metal beads, the homogenates were centrifuged at 18,000 *g* for 30 min at 4 °C, and the cleared supernatant was collected in LC vials. For the experiments where a whole plant was used for JA extraction, plants were manually ground with a mortar and pestle followed by the large-scale extraction method described previously (Chung et al., 2008). An electrospray ionization (ESI) triple quadrupole mass spectrometer (Xevo TQ-S, Waters) interfaced with the ACUITY Ultra Performance Liquid Chromatography (UPLC) system (ACUITY H-class, Waters) was used to quantify JA metabolites. Five μL of samples were separated on a UPLC BEH C18 column (1.7 μm, 2.1 × 50 mm; Waters) maintained at 40 °C using a 3-min gradient program with 0.1% aqueous formic acid and methanol as mobile phase solvents (flow rate 0.4 mL/min). Multiple reaction monitoring under ESI negative ion mode was used to detect characteristic MS transitions for jasmonic acid (*m*/*z*, 209 > 29), dhJA (211

> 59), 12OH-JA (225 > 59), JA-Ile (322 > 130), [$^{13}C_6$]-JA-Ile (328 > 136), 12OH-JA-Ile (338 > 130), and 12COOH-JA-Ile (352 > 130). Data were analyzed using MassLynx 4.1 and TargetLynx software (Waters), and the quantification was based on standard curves generated using known amounts of analytes and internal standards.

2.7. Untargeted metabolite profiling

Plant metabolites were extracted from ca. 25 mg of freeze-dried tissues by homogenizing with 80% aqueous methanol (5 μL per mg tissue) containing 2.5 μM lidocaine and 10-camphorsulfonic acid as internal standards in a mixer mill (MM300, Retsch) together with a zirconia bead for 10 min at 20 Hz. Following centrifugation at 12,000 *g* for 10 min and filtration through an Ultrafree-MC (MILLIPORE UFC30LG00) filters, 1 μL was separated on a bridged ethyl hybrid (BEH) C18 column (1.7 μm, 2.1 × 100 mm, Waters) and analyzed using UPLC-QTOF-MS (AQUITY/Xevo G2 Q-Tof, Waters). The analytical conditions including the inlet methods and MS parameters were the same as previously described (Tamura et al., 2014). Chemical assignment of metabolites were conducted by comparing the *m/z* values of MS/MS or MS and retention times to the in-house database, KNApSAcK database and published works (Afendi et al., 2012; Bottcher et al., 2008; Tohge et al., 2005).

3. Results

3.1. The loss-of-function mutants *b1b3* and *b1b3c1* hyperaccumulate JA-Ile

The enzymatic functions of CYP94B1 (94B1), CYP94B3 (94B3), and CYP94C1 (94C1) have been characterized in detail using both *in vivo* and *in vitro* experimental systems (Heitz et al., 2012; Kitaoka et al., 2011; Koo et al., 2011; Koo et al., 2014). The 94B1 and 94B3 enzymes mainly catalyze hydroxylation of JA-Ile at the terminal carbon (C_{12}) of the pentenyl side chain to yield 12OH-JA-Ile, whereas the 94C1's main function is to oxidize the resulting 12OH-JA-Ile to 12COOH-JA-Ile (Figure 2.2.A). Over 95% of the JA-Ile conversion to 12OH-JA-Ile was blocked in wounded leaves of *cyp94b1cyp94b3* plants (henceforth called *b1b3*) compared to that of the wild type (WT) (Figure 2.2.C) consistent with a recent report (Koo et al., 2014). Adding *94C1* mutation to the *b1b3* double mutant to create the *cyp94b1cyp94b3cyp94c1* triple mutant (*b1b3c1*) (Figure 2.3.A) did not further reduce the 12OH-JA-Ile level (Figure 2.3.C) but completely blocked the 12COOH-JA-Ile synthesis (Figure 2.2.D). Near complete blockage of this, so-called 'ω-oxidation pathway' of the JA-Ile catabolism pathways, resulted in hyperaccumulation of JA-Ile (Figure 2.2.B). Close to 3–4-fold increases at the peak (2h post wounding) of JA-Ile accumulation were detected in *b1b3* and *b1b3c1* compared to that in the WT. However, the large quantity of JA-Ile that had been accumulated in the double and triple mutants gradually declined overtime with kinetics similar to that found in the WT (Figure 2.2.B), indicating its turnover via alternative pathways such as the 'hydrolytic pathway' catalyzed by

ILL6 and IAR3 enzymes (Bhosale et al., 2013; Koo et al., 2014; Widemann et al., 2013; Zhang et al., 2016).

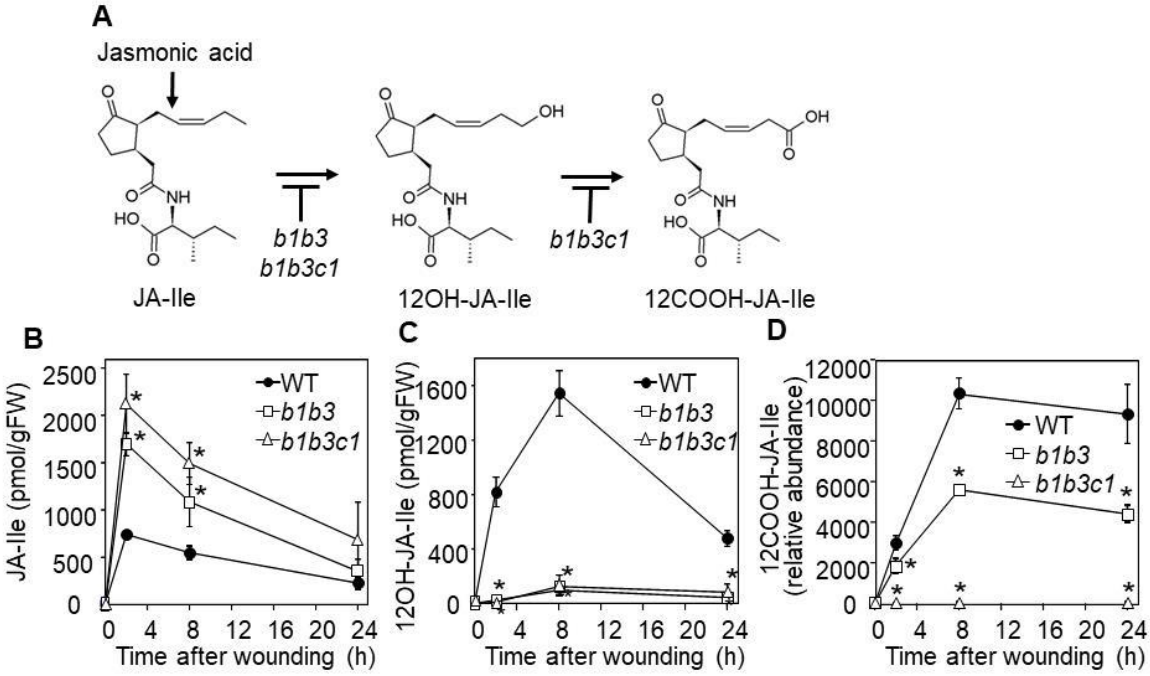

Figure 2.2. JA-Ile metabolism in WT, *b1b3*, and *b1b3c1* plants. (A) Schematics of the metabolic steps blocked in *b1b3* and *b1b3c1*. The *b1b3* mutant is mainly blocked in JA-Ile 12-hydroxylation to 12OH-JA-Ile whereas the *b1b3c1* is blocked in two consecutive oxidation steps converting JA-Ile to 12OH-JA-Ile and 12COOH-JA-Ile. (B–D) Time course accumulation of JA-Ile, 12OH-JA-Ile and 12COOH-JA-Ile in the wounded leaves of WT, *b1b3* and *b1b3c1*. Each data point is mean ± SD of three biological replicates.

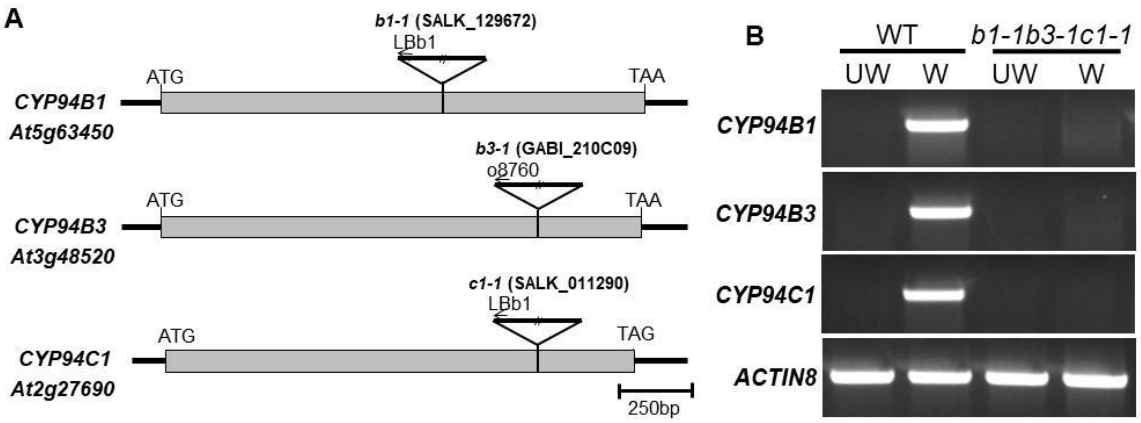

Figure 2.3. Molecular characterization of the *b1b3c1* triple mutant. (A) Schematics of the genomic structures of *CYP94B1*, *CYP94B3*, and *CYP94C1* genes, and the location of T-DNA insertions. Exons are represented by grey rectangles, and arrows indicate the direction of the T-DNA left border primers (LBb1 and o8760) used for PCR genotyping. (B) Semi-quantitative RT-PCR analysis of the *CYP94B1*, *CYP94B3*, and *CYP94C1* transcripts in unwounded (UW) and wounded (W) (1 h) leaves of WT and *b1-1b3-1c1-1* plants. *ACTIN8* serves as a loading control.

3.2. *b1b3* and *b1b3c1* are resistant to the growth inhibitory effects of wounding

The growth of *b1b3* and *b1b3c1* plants was observed to see if the disrupted JA-Ile turnover had any effect on normal plant growth and development. Under standard growth conditions, no obvious differences were detected among the WT, *b1b3*, and *b1b3c1* plants in their overall statures, and the biomass gain over the course of development was indistinguishable between the three genotypes (unwounded controls in Figure 2.4.A–C and growth curves in Figure 2.5). No quantifiable differences in root growth were observed among the

three genotypes grown on solid MS media (Figure 2.9.A–B). The absence of any measurable change in growth of the *b1b3* and *b1b3c1* was not surprising because JA levels in unstressed rosette leaves are known to be low in WT plants, and the *b1b3* and *b1b3c1* mutants do not accumulate high JA under normal growth conditions without stress treatments (Glauser et al., 2008; Koo et al., 2009) (Figure 2.2.C). Thus, in order to reveal the impacts of differential JA accumulation, plants were first elicited to synthesize JA. Wounding is an effective means to trigger JA biosynthesis (Figure 2.2). Furthermore, wounding is known to inhibit plant growth, and a significant part of this growth inhibition depends on an active JA-signaling pathway (Noir et al., 2013; Yan et al., 2007; Zhang and Turner, 2008). We predicted that wounding drove JA-Ile to higher levels in *b1b3* and *b1b3c1* (Figs. 2B and 2D), will cause more severely stunted phenotypes. In order to magnify the effects, wounding treatment (termed WIGI for Wounding Induced Growth Inhibition assay) was given multiple times during the course of plant development (see Section 2.2 for detailed wounding scheme). Upon induction by wounding, JA-Ile levels typically return to the basal level after about 24 h (Figs. 2B and 4D). Similarly, JA-Ile in the *b1b3* and *b1b3c1* declined over 24 h albeit maintaining a significantly higher level than that of the WT. When the plants were wounded additionally at this point (24 h, marked as ‘W2’ in Figure 2.4.D), JA-Ile increased to a new high. A third set of wounding at 48 h (‘W3’) pushed the JA-Ile level in the *b1b3* higher still. JA-Ile levels in the WT also rose in response to the repeated wounding but even after the third wounding (51 h) its

JA-Ile levels had barely reached that of the singularly wounded *b1b3* (at 3 h) (Figure 2.4.D).

Wounding caused a clear reduction in plant size of the WT plants (Figure 2.4.A). Under the wounding conditions we have used (WIGI), ca. 50–60% reduction in plant masses (both dry and fresh weights) were routinely observed with the WT plants consistent with what other groups have reported (Noir et al., 2013; Yan et al., 2007; Zhang and Turner, 2008). However, surprisingly, wounded *b1b3* and *b1b3c1* plants were visibly bigger and significantly heavier than the equally treated WT plants (Figure 2.4.A–C), indicating resistance to the growth-inhibitory effects of wounding. No significant differences were detected between *b1b3* and *b1b3c1* (Figure 2.4.B), and the single mutants, *b1* and *b3*, did not show obvious phenotypes (Figure 2.5.C), indicating that *b1b3* is necessary and sufficient for the phenotype. This decreased sensitivity to the wound-induced growth inhibition was highly reproducible in multiple wounding trials (Figures 2.4.B-C and 2.5.C).

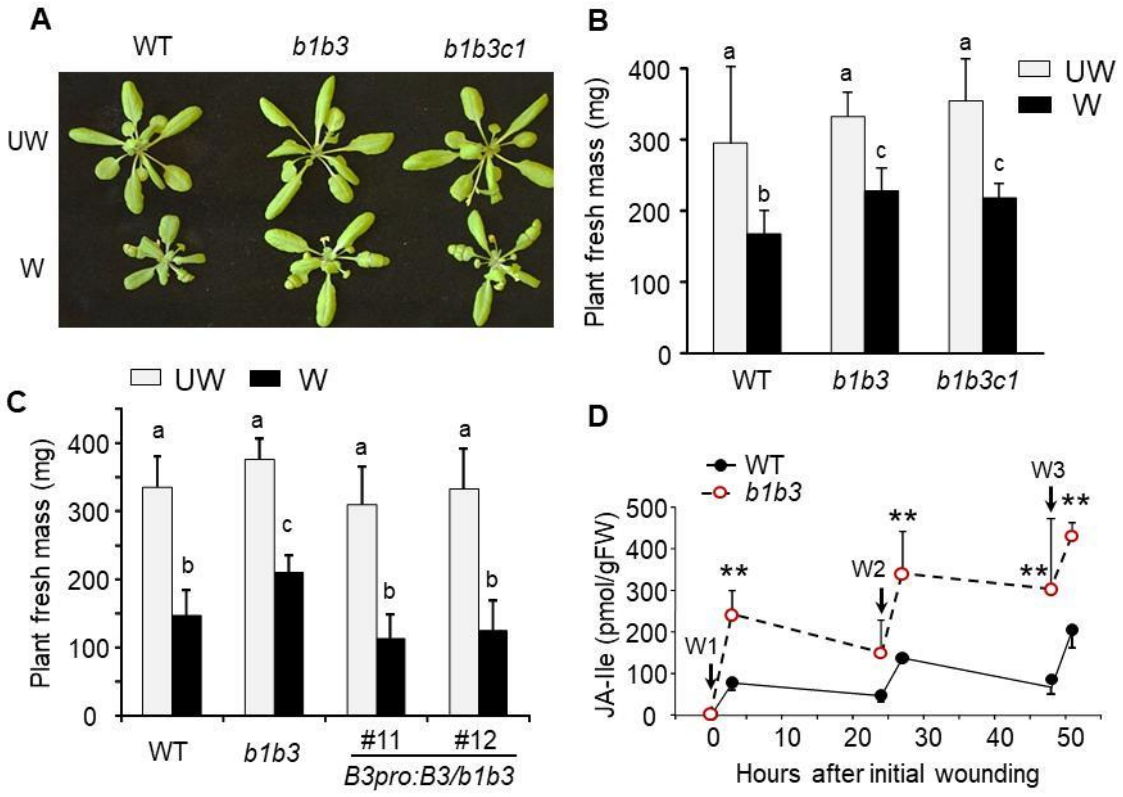

Figure 2.4. *b1b3* and *b1b3c1* mutants are resistant to the growth inhibitory effects of wounding. (A) Photographs of the representative WT, *b1b3*, and *b1b3c1* plants at the end of wound-induced growth inhibition (WIGI) assay. Top row, unwounded (UW) control; bottom, wounded (W). (B–C) Fresh weights (mg) of the indicated genotypes treated with WIGI. Two different allelic mutants, *b1-2b3-1* and *b1-1b3-1* were used as *b1b3* double mutants for (B) and (C), respectively. Two complemented transgenic lines of *b1b3* harboring the WT copy of *CYP94B3* gene are designated as *B3pro:B3/b1b3* (lines #11 and #12). Values represent average weights from 15–20 plants and SD. Asterisks (B) indicate significant difference compared to the wounded WT ($p < 0.01$; Student's *t* test). Numbers above bar graphs (C) denote percent inhibition of growth compared to the unwounded controls of each genotype. (D) JA-Ile accumulation in the WT and b1b3 during the first three days of WIGI treatment. Arrows indicate when

the plants received the first (W1), second (W2), and third (W3) wounding. Data show the mean and SD of three biological replicates.

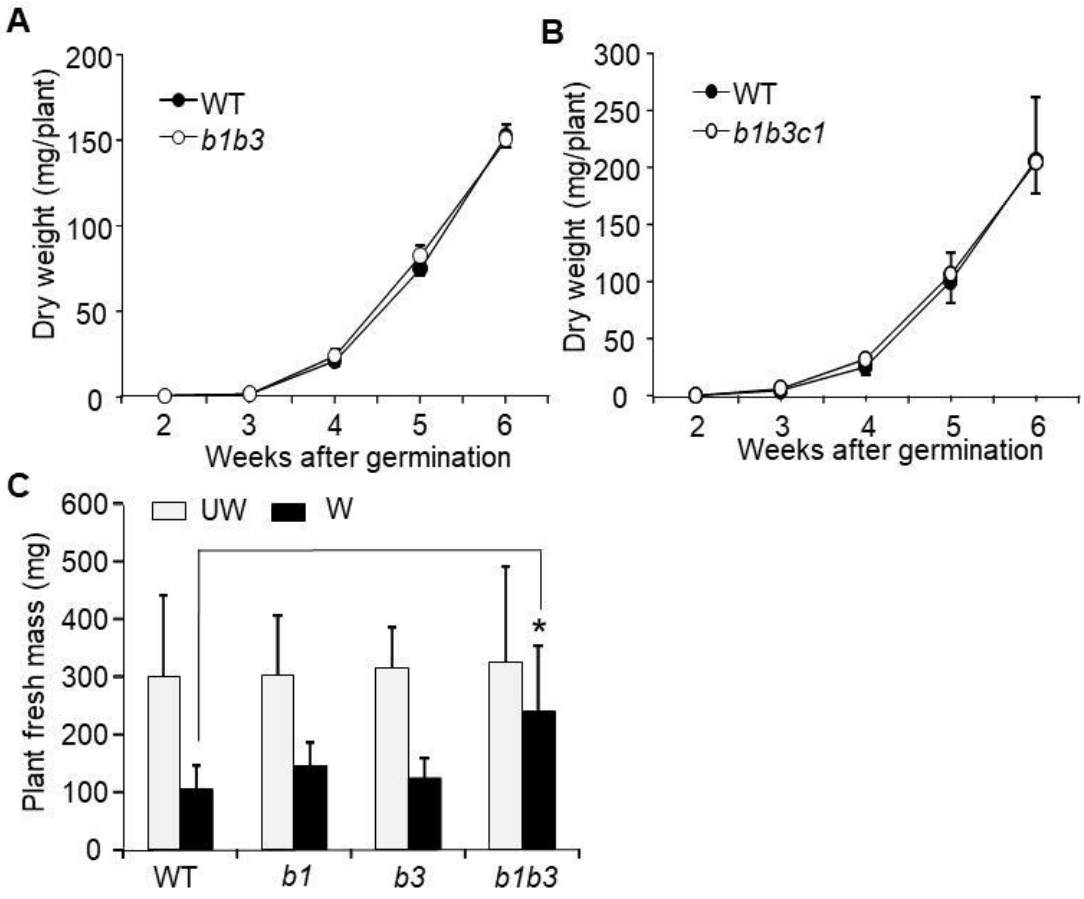

Figure 2.5. The unstressed *b1b3* and *b1b3c1* mutants have similar biomass as the WT plants but are less sensitive to the growth inhibitory effects of wounding. (A–B) Growth curves of WT, *b1b3* (*b1-2b3-1*), and *b1b3c1* plants showed overall similar weights throughout the development. Data show the mean ± SD of the dry mass (n = 16) of above-ground tissues at indicated time points. (C) Fresh weights of unwounded (UW) and wounded (W) WT, *b1* (*b1-2*), *b3* (*b3-1*), *b1b3* (*b1-2b3-1*) after WIGI treatment. Data represent an average and SD from 12 plants. *, $p < 0.01$; Student's t test.

In order to eliminate the potential artefactual contributions by off-target T-DNA insertions in genes other than *94B1*, *94B3*, and *94C1*, we took two separate genetic verification approaches. First, we isolated several independent T-DNA alleles of *b1* and *b3*, i.e., *b1-1*, *b1-2*, *b3-1* and *b3-2* (Koo et al., 2011; Koo et al., 2014), and created double mutants between them (*b1-1b3-1*, *b1-2b3-1*, *b1-2b3-2*). Replication of the phenotype in these multiple independent allelic mutants indicated that the phenotypes are caused by the mutation in *94B1* and *94B3* (shown in Figure 2.4.B, 2.6.C, and 2.5.C, which represent results using *b1-2b3-1* and *b1-1b3-1*). Second, transgenic lines complementing *b1b3* were generated. This was accomplished by introducing a wild type copy of the *94B3* gene (controlled by a 2 kb *94B3* native promoter) into a *b1b3* background (*B3pro:B3*/*b1b3*). *94B3* was chosen because of its dominant role over *94B1* (Koo et al., 2014). Two *B3pro:B3*/*b1b3* lines (#11 and #12), which are restored in the JA-Ile conversion of 12OH-JA-Ile (Figure 2.7) were subject to the WIGI assay, and the results showed that the WT-level of growth inhibition by wounding occurred in these lines (Figure 2.4.C). These two experiments unequivocally confirmed that the resistance to the growth inhibitory effects of wounding in *b1b3* is caused by mutations in *94B1* and *94B3* genes.

3.3. *b1b3* and *b1b3c1* accumulate less anthocyanin in response to wounding

The unexpected insensitivity to wounding despite very high levels of JA-Ile made us wonder whether this symptom applies to the plant growth only or can be

observed in other JA-dependent wound responses. Wounding is known to cause anthocyanin accumulation in plants, and this response is also known to be mediated by the JA pathway (Nakata et al., 2013; Pourcel et al., 2013; Qi et al., 2011).

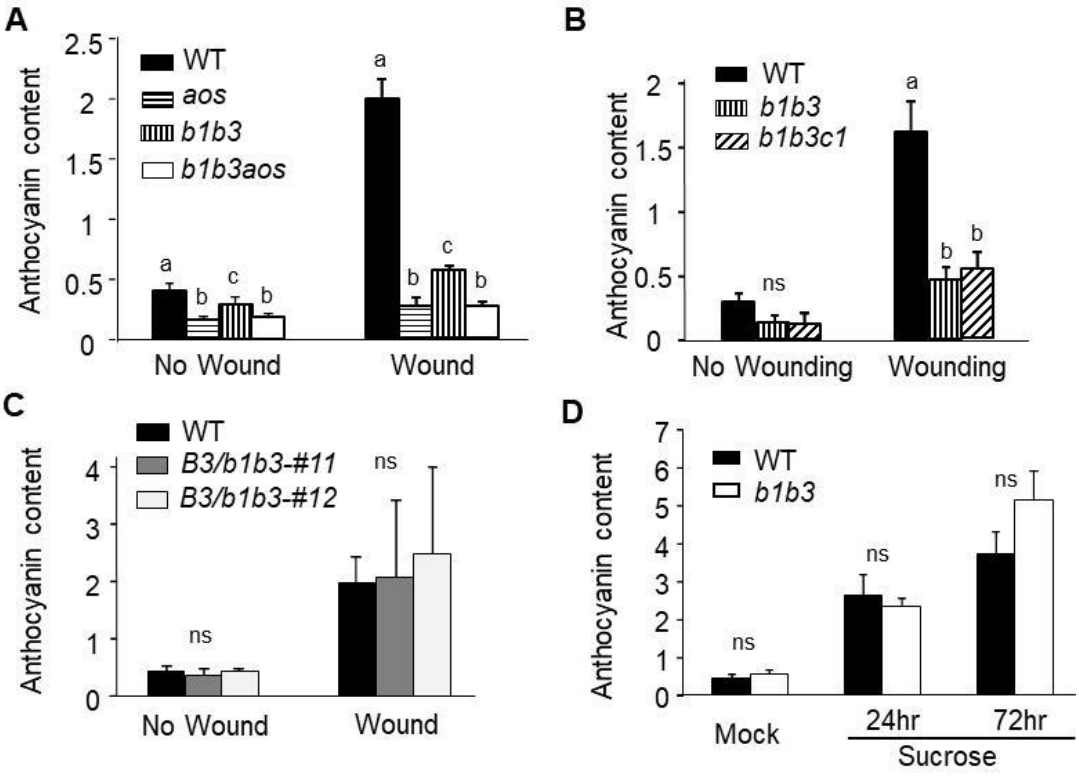

Figure 2.6. *b1b3* and *b1b3c1* are strongly impaired in wound-induced anthocyanin accumulation. (A–C) Anthocyanin content in unwounded (UW) and wounded (W) WT, *aos*, *b1b3* (two different allelic mutants, *b1-2b3-1* and *b1-1b3-1* were used in (B) and (C), respectively), *b1b3aos*, *b1b3c1*, and *B3pro:B3/b1b3* (lines #11 and #12). Wounding was administered according to the WIGI treatment method. Relative anthocyanin content was estimated by a spectrophotometric based method. Each error bar indicates SD of results obtained from five to six biological replicates. (D) Sucrose-induced anthocyanin accumulation in WT and *b1b3* plants. Ten-day old plants grown on

plain MS plates were transferred to plates with or without (Mock) 100 mM sucrose, and grown for 24 and 72 hrs. Data show mean and SD of four biological replicates.

Consistently, wounding (by the WIGI treatment) strongly induced anthocyanin in the WT plants (Figure 2.6.A). This induction was almost completely abolished in the JA-biosynthesis mutant, *aos*, demonstrating the absolute requirement of JA for the wound-induced anthocyanin accumulation (Figure 2.6.A). These results predict that JA-Ile hyperaccumulation in *b1b3* and *b1b3c1* is likely to induce stronger anthocyanin accumulation. However, anthocyanin levels in wounded *b1b3* and *b1b3c1* were markedly lower compared to that of WT (less than 30% of the WT) (Figure 2.6.A–C). The small increase of anthocyanin by wounding in *b1b3* was abolished in the *b1b3aos* triple mutant, which cannot synthesize JA, indicating that the wound induction of anthocyanin in the *b1b3* (albeit minor) requires JA production. Similar to the case of the growth-inhibition, no additive effects were observed with the *b1b3c1* triple mutant compared to the *b1b3* (Figure 2.4.B), and the phenotypes were highly reproducible in experimental iteration using same and independent allelic versions of *b1b3* mutants (Figures 2.4.B–C and Figure 2.8.), whereas the *b1* and *b3* single mutants did not display obvious changes (Figure 2.8.A). In addition, the anthocyanin defect was rescued by the *B3pro:B3*/*b1b3* complementation (Figure 2.6.C).

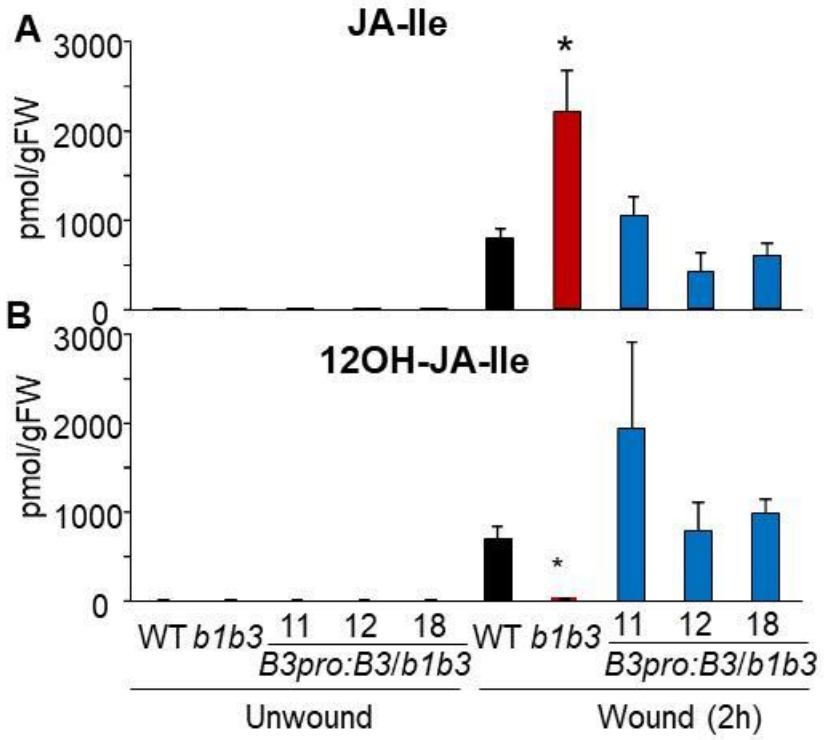

Figure 2.7. Transgenic complementation of *b1b3*. The *b1b3* plant was transformed with a WT copy of *CYP94B3* gene controlled by its native promoter (*B3pro:B3*/*b1b3*). (A) JA-Ile hyperaccumulation in the wounded leaves of *b1b3* is reduced back to the WT level in the three *B3pro:B3*/*b1b3* lines 11, 12, and 18 (T2 generation). (B) 12OH-JA-Ile deficiency of *b1b3* is restored to the WT level or higher in the complemented lines. Endogenous JA levels were quantified using UPLC-MS/MS. Data show the mean and SD of three biological replicates. Significant difference between wounded WT and *b1b3* are indicated by asterisks at $p < 0.05$ (Student's *t* test).

Since the reduction in anthocyanin content was so strong, we questioned whether *b1b3* is defective in anthocyanin biosynthesis. To test this, WT and *b1b3* plants were subjected to another anthocyanin-inducing condition separate from wounding, i.e. a high concentration of sucrose which is commonly used to induce

anthocyanin production (Mita et al., 1997; Teng et al., 2005; Tsukaya et al., 1991). WT and *b1b3* plants were first germinated and grown on plain MS media for 10 days and then moved to the MS media supplemented with 100 mM sucrose. For the mock treatment, the germinated plants were transferred to the plain MS instead. Anthocyanin levels were determined after 24 h and 72 h. As expected, anthocyanin in the WT plants grown on the sucrose media increased 4–5-fold compared to the control on the mock media within 24 h, and the level continued to rise to over 8-fold by 72 h (Figure 2.9.D). The *b1b3* responded to sucrose similarly as the WT, accumulating equivalent levels of anthocyanin. This data clearly demonstrated that *b1b3* plants have full capacity to synthesize anthocyanin indicating that its low induction by wounding was not due to any inherent defect in anthocyanin biosynthetic pathway.

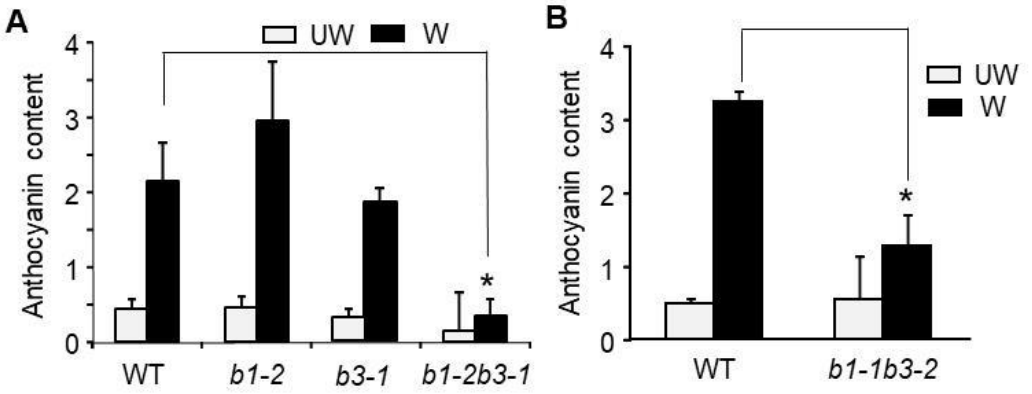

Figure 2.8. Wound-induced anthocyanin levels are strongly reduced in the *b1b3* mutant. (A–B) Anthocyanin content in unwounded (UW) and wounded (W) WT, *b1* (*b1-2*), *b3* (*b3-1*), *b1b3* (two different allelic mutants, *b1-2b3-1* and *b1-1b3-2* were used in (A) and (B), respectively). Wounding was administered according to the WIGI treatment.

Data show the mean and SD of six and four biological replicates for (A) and (B), respectively. Asterisks denote statistical difference between WT and mutant at $p < 0.01$.

3.4. *b1b3* and *b1b3c1* possess intact JA-perception and signaling system

Since *b1b3* and *b1b3c1* showed dampened wound-responses known to be controlled by the JA pathway, we questioned whether *b1b3* and *b1b3c1* are compromised in JA-response. To test this, *b1b3* and *b1b3c1* were subjected to three exogenous JA-induced response assays, namely, root growth inhibition, anthocyanin accumulation, and JA-responsive marker gene expression. As noted earlier, there were no differences in root lengths between the WT and *b1b3* or *b1b3c1* plants grown on plain MS media (Figure 2.9.A–B). When plants were grown on JA-containing media, root elongation was inhibited in all three genotypes to a similar degree, indicating that both *b1b3* and *b1b3c1* mutants were responding similarly to the exogenous JA as were the WT plants with respect to their root growth inhibition (Figure 2.9.A–B).

In a second response phenotype to exogenous JA, anthocyanin contents sharply rose in the 10-d-old WT seedlings when they were transferred to JA-containing media (Figure 2.9.C). Red coloration indicative of anthocyanin was also apparent in *b1b3* and *b1b3c1* similar to WT as early as within 48 h of incubation on the JA-containing plate. Even after 96 h of incubation there was no detectable difference in the anthocyanin content between WT, *b1b3*, and *b1b3c1* (Figure 2.9.C).

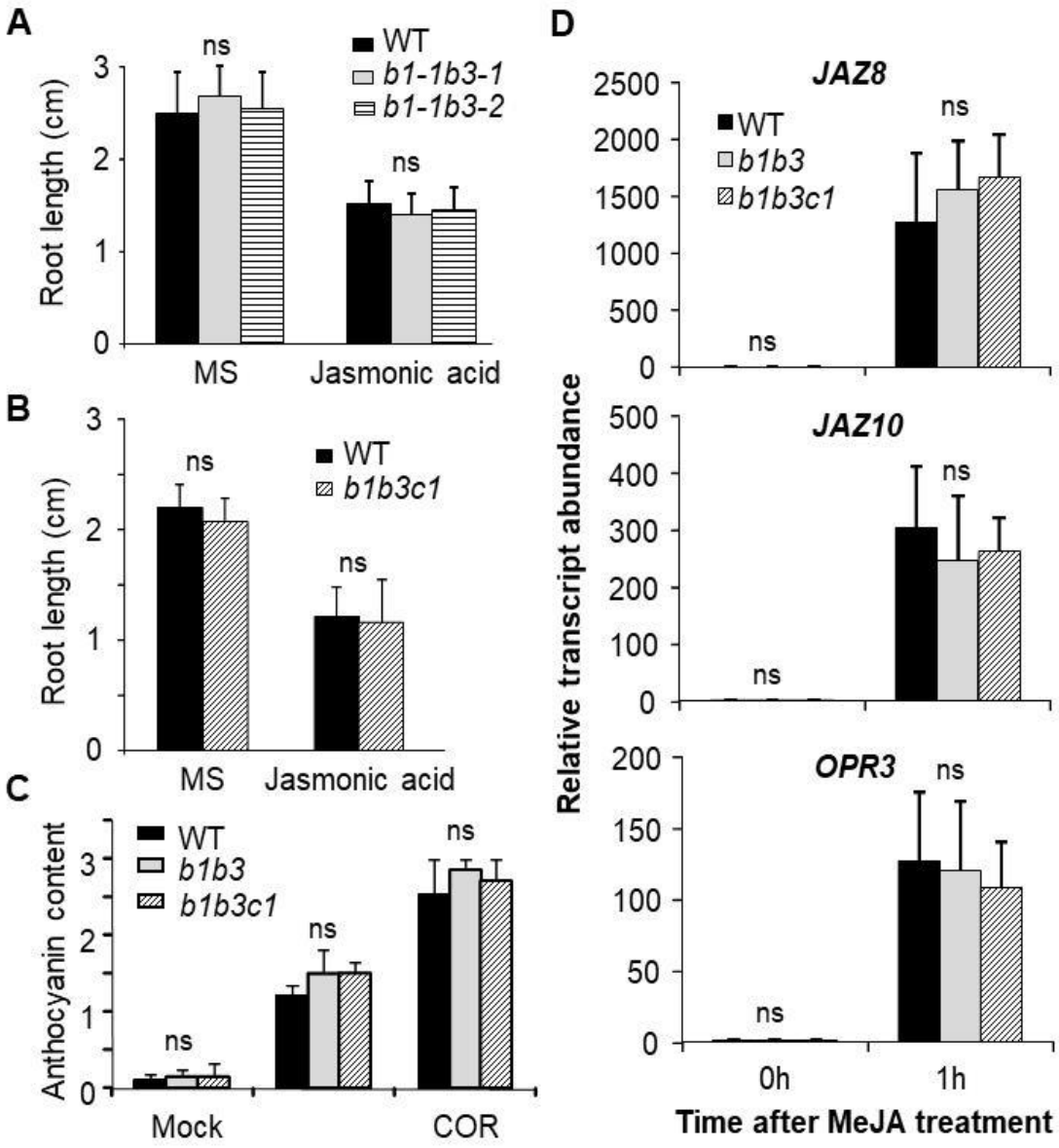

Figure 2.9. *b1b3* and *b1b3c1* have an intact JA signaling pathway. (A–B) Root growth inhibition assays. The WT, *b1b3* (*b1-1b3-1* and *b1-1b3-2*), and *b1b3c1* were grown on solid MS media with or without 10 μM jasmonic acid. Root length was determined on the 8-d or 10-d old plants for the MS or JA treated plants, respectively. Data show the mean and SD ($n > 12$). (C) The anthocyanin content in the WT, *b1b3*, and *b1b3c1* plants grown on solid MS media containing the Mock, 50 μM jasmonic acid or 5 μM coronatine. Ten-day old plants grown on plain MS plates were transferred to plates

with or without the shown substances and grown for 96 h. Data are mean and SD of four biological replicates. (D) Expression of JA-responsive marker genes *JAZ8*, *JAZ10*, and *OPR3* in the mature rosette leaves of WT, *b1b3*, and *b1b3c1* sprayed with 100 μM of MeJA. Relative transcript abundance was determined by qRT-PCR. *ACTIN8* was used as an internal reference gene, and the relative expression is shown as fold-changes compared to the untreated (0 h) WT values. Each data show mean and SD of three biological replicates.

Similar results were obtained when coronatine (COR) (a structural mimic of JA-Ile) was used in place of JA as an anthocyanin-elicitor (Figure 2.9.C). Earlier studies have established that COR binds to the JA-Ile receptor (Katsir et al., 2008b; Thines et al., 2007; Withers et al., 2012), but that, unlike JA-Ile, it is not metabolized by the CYP94 enzymes (Koo et al., 2011; Koo et al., 2014). The anthocyanin accumulation in the *b1b3* and *b1b3c1* that is similar to the WT in response to exogenous JA and COR, clearly indicates that the JA-perception and signaling pathway leading to the anthocyanin-accumulation is unaltered in *b1b3* and *b1b3c1* compared to WT. This also confirms the earlier conclusion from the sucrose treatment experiment where anthocyanin biosynthetic pathway is normal in the mutants.

As a third response phenotype to exogenous JA, expression of JA marker genes was examined by quantitative (q)RT-PCR. *JAZ8*, *JAZ10*, and *OPR3* are early-responsive genes that are rapidly induced by JA or wounding (Chung et al., 2008; Thines et al., 2007). Fully expanded rosette leaves of the WT, *b1b3*, and *b1b3c1* were evenly sprayed with a solution containing 100 μM MeJA. After 1 h

there was a sharp increase in all three gene transcripts in the WT. Comparable increases of all three gene transcripts were detected in *b1b3* and *b1b3c1* (Figure 2.9.D), demonstrating that the transcriptional activation system by JA is normal in the *b1b3* and *b1b3c1* leaves.

Together, these results indicate that *b1b3* and *b1b3c1* respond normally to exogenous JA treatment, and that the wound-induced growth inhibition and anthocyanin phenotypes are not due to the defects in the mutants' ability to perceive or respond to JA.

3.5. *b1b3* and *b1b3c1* are reduced in trichome density in response to wounding and are more susceptible to *S. exigua*

The results so far showing that *b1b3* and *b1b3c1*, despite increased JA-Ile and intact JA-signaling system, display dampened response to wounding prompted us to seek additional evidence that the mutants are indeed unresponsive to all major JA-dependent wound responses. The number of trichomes increases when plants are wounded in a JA-dependent fashion, i.e., the inducible trichome formation is blocked in JA-biosynthetic or perception mutants (Li et al., 2004; Yoshida et al., 2009). Similar assay was conducted on *b1b3* and *b1b3c1*. No significant difference in trichome numbers was detected in the unwounded controls indicating that the developmentally regulated trichome formation is not altered by the mutations. The WT, *b1b3*, and *b1b3c1* plants were then wounded according to the WIGI wounding schedule, and trichomes were counted. A defined area (25 mm^2) on a newly emerging leaf (the eighth true leaf)

which was not directly wounded during WIGI treatment was assessed for the trichomes. Wounding caused a 1.5-fold increase in the number of trichomes in the WT leaf 8 (Figure 2.10.A–B). In contrast, only a 1.2-fold increase was observed in both *b1b3* and *b1b3c1*.

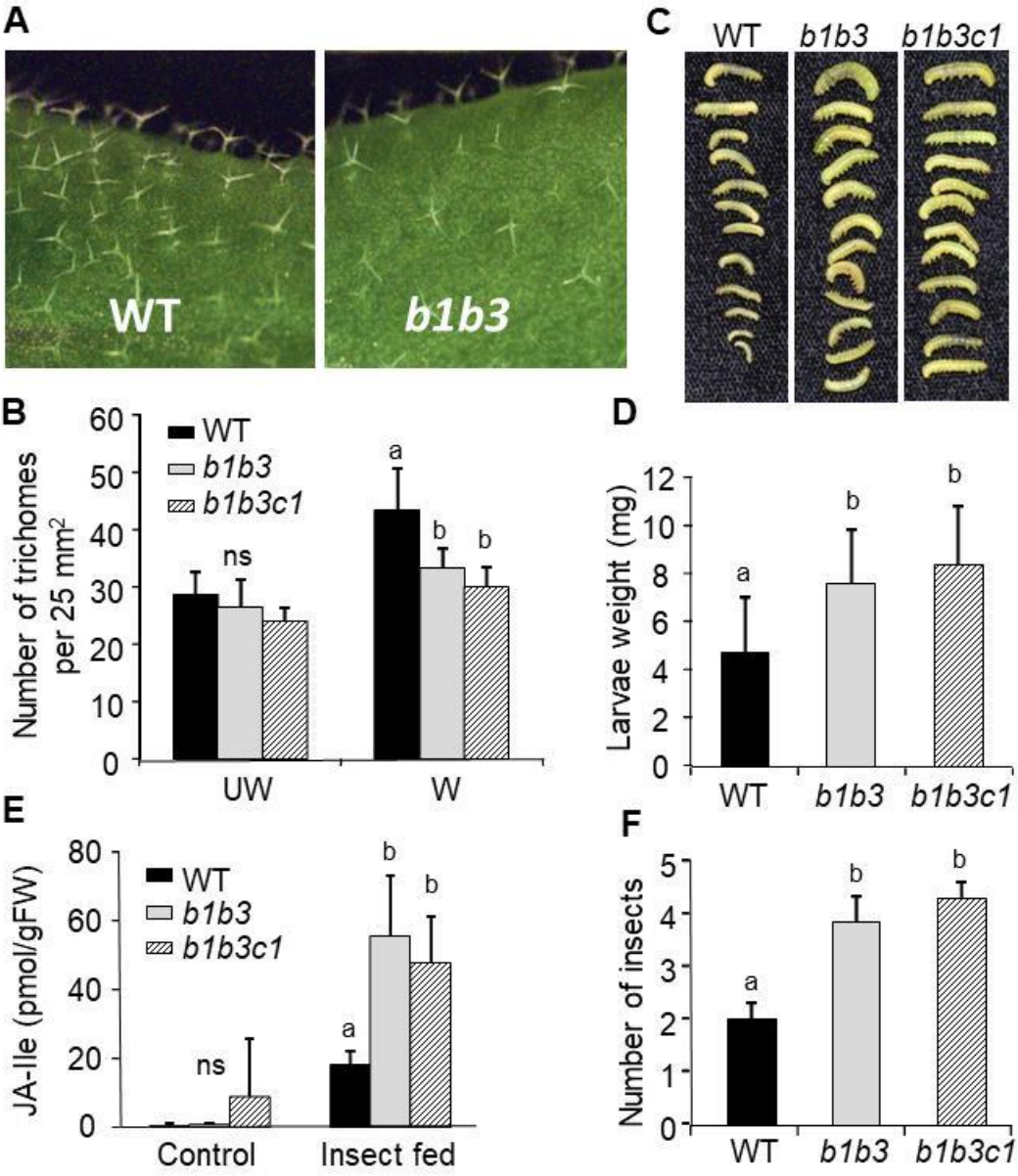

Figure 2.10. *b1b3* and *b1b3c1* plants make fewer trichomes in response to wounding and are more susceptible to the *S. exigua* feeding. (A) Photographs

showing trichomes on the leaf 8 of wounded WT and *b1b3* plants. (B) Number of trichomes on unwounded (UW) and wounded (W) WT, *b1b3*, and *b1b3c1*. Plants were wounded according to the WIGI treatment method. Trichomes within a 25-mm^2 area of undamaged Leaf 8 were counted (n = 6 plants). (C–D) No-choice insect feeding assay. A photo image and weight measurements of *S. exigua* larvae after 14-d of feeding. Values indicate the mean and SE of larval mass (n > 40). (E) JA-Ile levels in the control and *S. exigua* fed plants. Average of three biological replicates is shown with error bars denoting SD. (F) Insect choice assay. Fifteen *S. exigua* larvae were allowed to choose between the WT, *b1b3*, and *b1b3c1* leaves in an enclosed container. Number of larvae on each genotype was counted after 16 h. Data show the mean and SD of seven independent assays. Asterisks (B–F) denote a significant difference compared to the equally treated WT, $p < 0.01$; Student's t test. FW; fresh weight.

Plant resistance to insect herbivory is another well-established function of JA (Howe and Jander, 2008; Thaler et al., 2002). Plants deficient in JA are highly susceptible to insect attacks, and thus, plants with more JA-Ile are expected to be either more resistant or, at the minimum, similar to the WT. To test this, two commonly used feeding assays, termed 'no-choice' and 'choice' assays, were employed (Green et al., 2012; Herde et al., 2013). In the no-choice assays, insects were caged in with a single genotype of plants so that the insects would not have any choice for other food source other than the given plant genotype. Insects were allowed to feed for a defined period of time, and at the end of the trial, insects were recovered and individually weighed for their body mass. Just-hatched neonates of the generalist herbivore *Spodoptera exigua* (beet army

worm) (N>40) were raised on WT, *b1b3*, and *b1b3c1* for 14 d. It was apparent already during the early stage of feeding, that the *b1b3* and *b1b3c1* leaves were receiving more damage by the insects than the WT. After 14 d, larvae fed on *b1b3* and *b1b3c1* plants were visibly bigger and weighed almost twice as much as those fed on the WT plants (Figure 2.10.C–D). Quantification of JA-Ile content in the remaining plant tissues showed that the insect damaged *b1b3* and *b1b3c1* leaves contained much higher levels of JA-Ile (ca. 3 fold) than the WT (Figure 2.10.E).

For the 'choice' assays, insects were allowed to choose among the three genotypes. Fifteen *Spodoptera* larvae raised on an artificial diet for 7-10 days were released in the middle of a Petri dish containing leaves from all three genotypes arranged alternately encircling the insects. After 15 h, the number of insects on each genotype leaves was counted. The average insect count from seven such trials showed that more than twice as many insects were recovered from the *b1b3* and *b1b3c1* than from the WT plants ($p < 0.01$) (Figure 2.10.F). Although the design of this assay does not allow use to distinguish between the possibilities whether the larvae were more attracted to the mutants from the beginning (for example, by volatile cues) or they randomly chose leaves initially but that later migrated more to the mutants, what is clear is that if enough time is allowed (15 h), more insects will end up feeding on *b1b3* or *b1b3c1* than on WT.

3.6. Untargeted metabolomics revealed global reduction in wound-inducible metabolites in *b1b3*

The dramatically increased susceptibility to insects may be a reflection of global shifts in metabolism of *b1b3* and *b1b3c1* since metabolites play an important role in plant-insect interactions. Reduced anthocyanin levels in the mutants may be part of a much bigger scale metabolic changes. To address this question, an untargeted metabolic profiling experiment was carried out on WT and *b1b3*. Methanolic extracts from the entire above ground tissues of wounded (WIGI) and unwounded WT and *b1b3* (in six biological replicates) were analyzed using LC quadrupole time-of-flight mass spectrometry (LC QTOF MS) (Tamura et al., 2014). Principal component analysis (PCA) was carried out using around 600 detected MS peaks (ESI negative ion mode). The first component (PC1, 66.4% variance) mainly reflected the difference in treatments (i.e., wounding) while the second component (PC2, 10.4% variance) was largely a reflection of the variation between replicates (Figure 2.11.A). Six wounded WT samples formed a distinct cluster separated from the others. Wounded *b1b3* samples also clustered together, but they were not as well separated from the unwounded samples as the wounded WT. Unwounded WT and *b1b3* overlap indicated that there was not much difference between the two genotypes in the absence of wounding. However, wounding caused a massive change in metabolite abundance in WT plants (Figure 2.11.B). As much as 45% of the total metabolome was either induced or repressed by WIGI treatment. About 70% of the changed metabolites (31% of the total metabolites) were increased (>1.5-fold compared to unwounded

samples) whereas 30% were repressed by wounding (14% of total). Metabolites from *b1b3* were also changed in response to wounding, but fewer metabolites (ca. 30% total) were induced or repressed, and even the ones that were induced were induced to a lesser degree than those in WT. For example, up to 77% of the wound-induced metabolites in the WT were induced more than two-fold, whereas only 41% were induced above two-fold in the *b1b3* (Figure 2.11.B). The majority of wound-induced metabolites in *b1b3* (84%, 105 of 125 metabolites) was also induced in WT, whereas many induced in WT were not induced or did not make the cutoff (1.5-fold) in *b1b3*. The large overlap between the wound-induced metabolites of WT and *b1b3* indicated that similar rather than distinct metabolites were induced in *b1b3* compared to WT (Figure 2.11.C). Thus, wounding inflicted quantitative rather than qualitative differences in *b1b3*, consistent with other phenotypes observed in *b1b3* showing an overall weakened response to wounding. Among the metabolites that were induced by wounding in WT yet were less abundant or not induced in *b1b3* (< 1.5-fold compared to WT) were many compounds related to the phenylpropanoid and glucosinolate metabolism (Figure 2.11.D). These metabolites have important roles in plant-resistance to insects and are known to be regulated by the JA pathway (Howe and Jander, 2008; Kliebenstein et al., 2002a; Mithofer and Boland, 2012; Pourcel et al., 2013; Wasternack and Hause, 2013). Results from the ESI-MS positive ion mode analysis showed largely similar trends (Figures 2.11.D and 12).

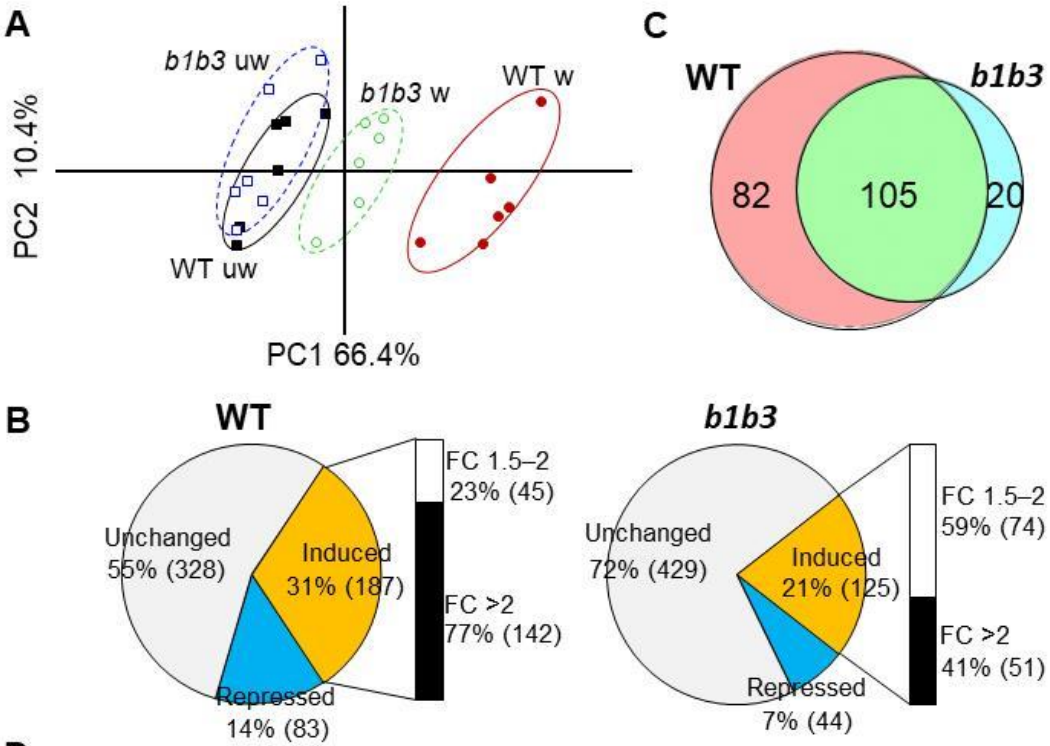

D

Compound name	RT (min)	ESI-MS (*m/z*)	Normalized peak intensity ratio		
			WT (w/uw)	*b1b3* (w/uw)	WT(w)/*b1b3*(w)
Phenylpropanoid compounds					
Cyanidin derivative	4.22	1181*	10.2	1.8	15.2
Kaempferol derivative	4.47	577	4.4	0.9	6.7
Cyanidin derivative[1,2]	3.97	975*	2.2	1.0	4.7
Cyanidin derivative	3.55	1343*	4.3	2.6	3.3
Syringaldehyde[1]	3.64	181	3.2	1.4	2.4
Salicylic acid[1]	2.18	137	4.5	2.5	2.3
Sinapoyl glucose	3.35	385	2.1	1.0	2.1
Glucosinolates					
3-Indolylmethyldesulfoglucosinolate[1]	4.88	367	11.5	1.1	10.8
Indole-3-carboxaldehyde	3.89	146*	4.1	1.8	2.3
Indolylmethylthiohydroximate[1]	3.35	205	2.1	1.0	2.0
8-Methylsulfinyloctyl glucosinolate[1,3]	3.05	494*	3.1	1.8	1.8
Neoglucobrassicin	3.97	477	6.4	4.6	1.8
5-Methylsulfinylpentyl glucosinolate	1.93	450	1.8	1.3	1.8
Glucoraphanin	1.73	436	1.6	1.1	1.6
2-(4'-Methylthio)butylmalic acid[1]	3.98	237*	5.0	4.0	1.6
Amino acids					
Tryptophan	2.83	203	2.4	1.6	1.9
L-Arginine[1,3]	2.54	175*	2.9	1.6	1.7
Pyroglutamic acid[1]	3.27	130*	1.6	1.2	1.6
Isoleucine / Leucine[1]	1.88	130	1.5	1.1	1.6
Lipids					
13S-Hydroperoxyoctadecatrienoic acid[1]	7.67	311*	2.3	1.0	2.3
12-Oxo-10,15(Z)-phytodienoic acid[1]	7.01	291	2.1	1.3	1.6

0.9 3 15

Figure 2.11. Untargeted metabolite profiling shows global reduction of wound-inducible metabolites in *b1b3*. Methanolic extracts of unwounded (uw) and wounded (w) WT and *b1b3* plants treated with WIGI were analyzed by LC-qTOF. (A) Principal component analysis (PCA) of the data obtained from six replicates of unwounded and wounded WT and *b1b3*. (B) Distribution of the metabolites induced (fold change (FC, wound/unwound) > 1.5), repressed (FC < 0.67) or unchanged (FC=0.67-1.5) by wounding in WT (left) and *b1b3* (right). The number of MS peaks (parenthesized) in each category is displayed with the percent total MS peaks. (C) Venn diagram showing an extensive overlap between the wound-induced metabolites of WT and *b1b3*. (D) Metabolites differentially accumulating between WT and *b1b3*. Wound-inducible metabolites that are at least 1.5-fold different in MS peak intensity between the two genotypes with known identity are displayed with heat maps visualizing the fold difference. Asterisks denote data from the ESI positive ion mode while all others are from negative ion mode. [1,2,3]These metabolites have been tentatively assigned based on the m/z values and retention times from the from the [1]KNApSAcK database (Afendi et al., 2012) and published data from [2](Tohge et al., 2005) and [3](Bottcher et al., 2008).

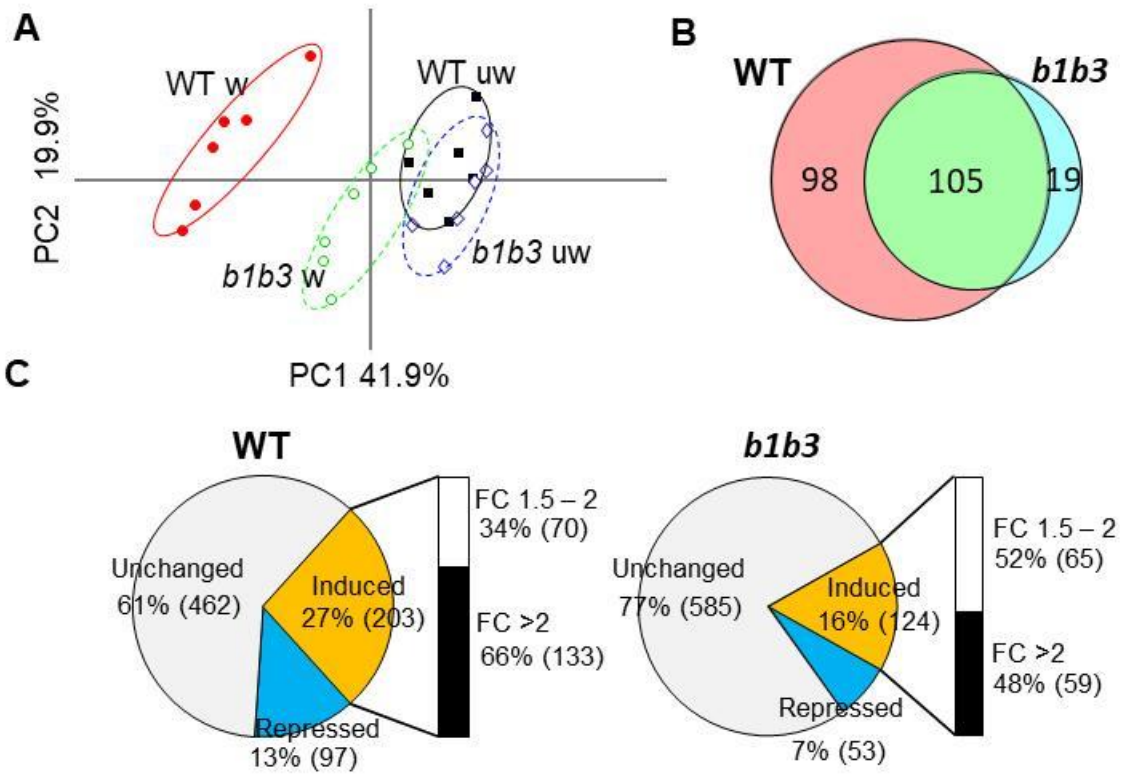

Figure 2.12. Statistical analyses of untargeted metabolite profiling data from the LC-qTOF operated at ESI positive ion mode. (A) PCA of the data obtained from six replicates—each of unwounded (uw) and wounded (w, by WIGI) WT and *b1b3*. (B) Distribution of the metabolites induced (fold change (FC, wounded/unwounded) > 1.5), repressed (FC < 0.67) or unchanged (FC 0.67-1.5) by wounding in WT and *b1b3* plants. The number of MS peaks (parenthesized) is displayed for each category with the percent total MS peaks. (C) Venn diagram showing a large overlap between the wound-induced metabolites of WT and *b1b3*.

3.7. Some JA-responsive genes are differentially regulated between WT and *b1b3*

Weaker response to wounding of *b1b3* may have been caused by changes occurring at the transcriptional level. Although we have shown earlier

(Figure 2.9.D) that transcriptional response to exogenously applied JA was not altered in *b1b3*, wounding may yield a different result because it causes differential accumulation of JA-Ile in the mutant. Since JA-Ile hyperaccumulates in *b1b3*, enhanced expression of JA-responsive genes were expected in response to wounding. Expression of six JA-responsive maker genes was examined using qRT-PCR in leaves at different times after wounding. All six genes were strongly induced by wounding, but different patterns emerged between WT and *b1b3*. Three of the six genes (i.e., *OPR3*, *MYC2*, *DFR*) were expressed with similar kinetics and levels in WT and *b1b3*. *JAZ8* and *JAZ10* transcripts were induced in both genotypes but that they accumulated to a much higher level (three-fold) in *b1b3* compared to WT. Expression of *PAP1*, which is a transcription factor for several anthocyanin biosynthetic genes (Qi et al., 2011; Teng et al., 2005), was initially (2 h) induced both in WT and *b1b3*, but then was differentially regulated afterwards in the two genotypes. Whereas the WT transcripts continued to rise until 7 h after wounding, they declined to the basal level in *b1b3* by 7 h. These results show that there are variations in gene expression among JA-responsive genes between WT and *b1b3* in response to wounding. While higher levels of JA-Ile in *b1b3* did not have an additive effect on certain genes, it boosted the expression of some genes, and for still others, it had a negative effect.

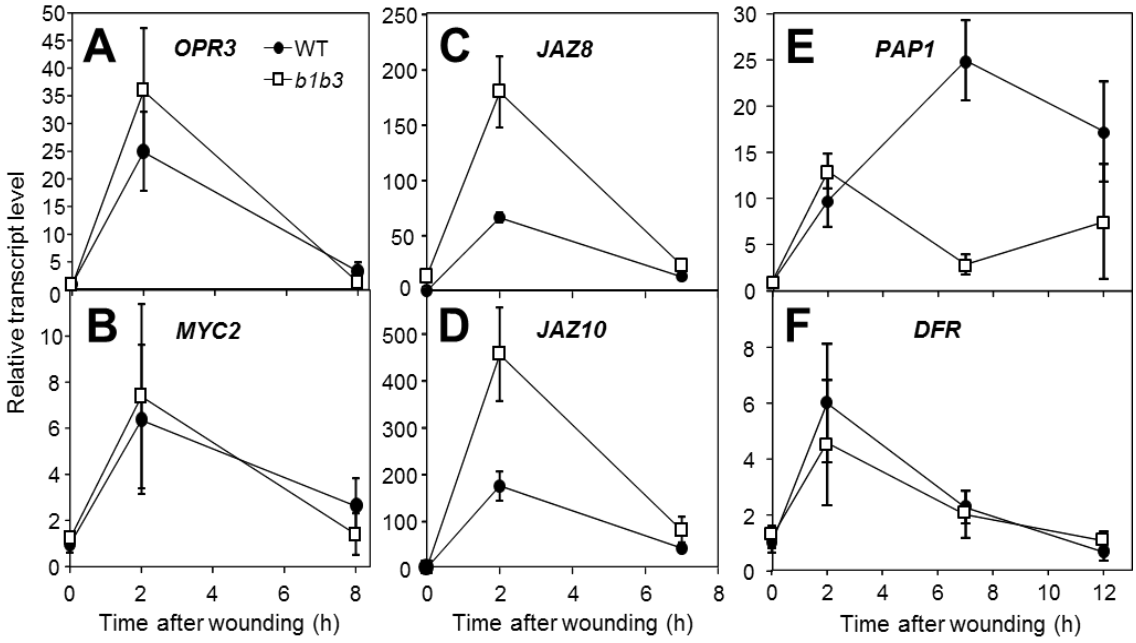

Figure 2.13. Time course of JA-responsive marker gene expression in wounded leaves of WT and *b1b3*. Rosette leaves of fully grown plants were wounded twice across the midrib with a hemostat, and the damaged leaves were harvested at indicated times for RNA isolation. (A-F) Transcript levels were determined by qRT-PCR using primers specific for *OPR3*, *MYC2*, *JAZ8*, *JAZ10*, *PAP1*, and *DFR*. *ACTIN8* was used as an internal reference gene and the expression levels are displayed relative to the unwounded (0 h) WT. Data represent the mean ± SD of three biological replicates.

4. Discussion

Compared to the well-studied JA biosynthetic pathways, the metabolic processes to turn JA over is only beginning to be elucidated. Our results using mutants defective in JA-Ile turnover demonstrated how misregulation of its catabolism can have a tremendous impact on plant's physiological responses to stresses. Despite having higher and sustained levels of JA-Ile, *b1b3* and *b1b3c1*

displayed significantly reduced responsiveness to wounding in a number of JA-Ile-dependent wound-response traits. This is counterintuitive because JA-Ile is expected to constitutively activate or enhance those responses. Through rigorous genetic analyses it was confirmed that these phenotypes are due to mutations in *CYP94* genes and not caused by any other off-target mutations in the genome. Comparisons between the *b1b3* and *b1b3c1* indicated that the mutation in *94C1* adds little or nothing to the *b1b3* phenotypes. Between *94B1* and *94B3*, loss-of-function in both genes was required for the wound-response defects, indicating functional redundancies between the two genes.

Although we cannot completely rule out the possibility that the wound-phenotypes of *b1b3* are mediated through a JA-independent pathway, the consistency of its phenotypes showing in a number of processes previously shown to be governed by JA pathway strongly suggested that the *b1b3* phenotypes are caused by disrupted JA-Ile metabolism. If we suppose that the phenotypes were due to the yet-to-be discovered alternative functions of 94B1 and 94B3 that is distinct from JA-Ile hydroxylation, then such function should have as significant and broad signaling impact as that of JA-Ile on mediating wound response and insect resistance. Signals with such magnitude of influence on wounding and insect resistance have not been identified apart from JA. In addition, that hypothetical signal must be able to suppress the JA-Ile signals which are highly abundant in the mutant.

The two biggest changes in metabolic profile of JA in *b1b3* were the hyperaccumulation of JA-Ile and the depletion of 12OH-JA-Ile. Since JA-Ile is the

receptor-binding form, its chronic presence in *b1b3* is suspected to be the main culprit behind *b1b3*'s wound phenotypes. Even though plant's response to constitutively raised endogenous JA-Ile levels has not been studied in detail, it generally has been assumed that the situation would result in hyper-activation of JA-regulated defense pathways. This prediction is largely based on observations from plants grown on media supplemented with high levels of exogenous JA. However, exogenous hormone treatment does not always accurately reflect *in vivo* conditions. Continuous exposure of all cell types to large quantities of exogenous JA could lead to complex non-physiological effects. Mutants that constitutively accumulate JA, such as *cev1*, which has mutation in a cellulose synthase gene *CeSA3*, are dwarfed, supporting the view that the constant presence of JA inhibits plant growth (Ellis et al., 2002). The difference between *cev1* and *b1b3*, however, is that whereas *cev1* is exposed to increased levels of JA always starting from as early as the embryonic stage, *b1b3* is not exposed to JA until its biosynthesis is elicited (e.g., by wounding). The context in which plants experience high levels of JA may also play an important role in shaping the final outcomes. For instance, in addition to increased JA, *cev1* is also constitutively overproducing ethylene (ET), an important plant hormone involved in fruit ripening, senescence, growth inhibition, and pathogen defense (Ju et al., 2015). The *coi1* mutation (JA-Ile receptor) in the *cev1* background alone could not suppress the stunted phenotype of *cev1*, rather an additional mutation in the ethylene receptor, ETR1, was needed to restore the WT sizes, indicating that both JA and ET are contributing to the stunted phenotype of *cev1*. Unlike the

cev1 or plants grown on JA-containing media, *b1b3* experiences elevated JA-Ile in the context of repeated tissue damage or insect herbivory, which also elicits pathways that are independent of the JA pathway. It is possible that under such conditions, chronic elevation of JA-Ile levels can have a unique signaling outcome.

How the molecular mechanism works to suppress the JA-mediated wound-response in *b1b3* is not known, but one hypothesis might be that it is mediated through negative feedback mechanisms of the JA-Ile signaling pathway. We found that *JAZ8* and *JAZ10* gene transcripts are up-regulated in wounded *b1b3*. The *JAZ* family proteins are repressors of JA-responsive gene expression (Chini et al., 2007; Thines et al., 2007). Most JAZ proteins are proteolytically destroyed by the SCF^{COI} and 26S protease system in the presence of JA-Ile. However, JAZ8 and the alternative splice variants of JAZ10 proteins are resistant to this degradation (Chung and Howe, 2009; Shyu et al., 2012). The physiological function of these 'stable' JAZs is unclear although their ectopic expression in plants was shown to constitutively repress JA signaling (Chung and Howe, 2009; Shyu et al., 2012). Our data showing that the *JAZ8* and *JAZ10* genes are highly expressed in wounded *b1b3* (Figure 2.13) raise the possibility that these 'stable' JAZs may accumulate to higher levels in the mutant and attenuate JA responses despite high JA-Ile levels. Interestingly, JAZ8 and JAZ10 proteins also physically interact with the bHLH TFs, TT8, GL3, and EGL3, and the R2R3-MYB TFs, MYB75/PAP1 and GL1 (Qi et al., 2011). These TFs are components of the WD-repeat/bHLH/MYB complexes that mediate JA-induced

anthocyanin accumulation and trichome initiation (Khosla et al., 2014). *MYB75*/*PAP1* transcripts were strongly reduced in *b1b3* (Figure 2.13) which may be contributing to the reduction of anthocyanin. Other targets of JAZ proteins include DELLAs in the gibberellin (GA) pathway which is a major hormonal pathway regulating plant growth (Hou et al., 2010; Qi et al., 2014; Yang et al., 2012). JAZ interaction with DELLA proteins has been suggested to explain the antagonistic growth regulation between JA and GA. The abundant JAZ8 and JAZ10 proteins in the wounded *b1b3* may interact with the DELLAs and sequester them away from the GA TFs, resulting in the activation of GA-responsive gene expression and subsequent promotion of plant growth.

An alternative hypothesis is that the dampened wound response of *b1b3* may be through post-transcriptional regulations. The majority of the JA-responsive gene transcripts except for *MYB75*/*PAP1* was induced by wounding and, thus was anti-correlated with the reduced wound-response phenotypes of *b1b3*. Although these transcripts may eventually take a down-turn and repressed in the long run when exposed to chronic JA-Ile under repeated tissue damage (via negative regulators as hypothesized in the previous paragraph), it is equally possible that the regulation lies at the post-transcriptional level. These hypotheses need to be investigated further.

5. Conclusions

JA showcases the importance of oxidative fatty acid metabolism during stress responses in plants. The metabolic pathways to catabolize JA are only

beginning to be elucidated. Our results using mutants defective in JA-Ile turnover show that defects in JA-Ile catabolism can disrupt the normal stress adaptive responses in ways that are not be predictable by existing JA signaling model. Further interrogation of the JA-turnover pathways is likely to uncover previously unrecognized regulatory elements of JA signaling and wound response in plants.

CHAPTER III: INVESTIGATING THE ROLE OF OXIDIZED-JA-ILE AS A SIGNALING MOLECULE IN PLANT STRESS RESPONSE

ABSTRACT

Plant hormone jasmonic acid and its derivatives collectively termed jasmonates (JAs) control immune response against insects and regulate plant development. Among the JA derivatives, jasmonoyl-isoleucine (JA-Ile) is known to be the endogenous bioactive form of JA responsible for JA mediated responses. JA-Ile is further metabolized into other metabolites including 12-hydroxy-JA-Ile (12OH-JA-Ile), upon synthesis following elicitation such as by tissue injury. 12OH-JA-Ile has been reported to be the first metabolite in the catabolic pathway to deactivate JA-Ile signal and has been reported to be synthesized by CYP94 members of the Arabidopsis cytochrome P450s. Contrary to the widely held belief that 12OH-JA-Ile is largely an inactive signal, our genetic analyses have provided indirect evidence that 12OH-JA-Ile may function as an active signal. Consistently, Arabidopsis seedlings treated with 12OH-JA-Ile accumulated anthocyanin and were also increased in leaf trichome cell numbers to levels comparable to that induced by same concentration of JA-Ile. Both anthocyanin and trichomes are anti-herbivory features known to be regulated by JA-Ile. In addition, expression of several JA-Ile responsive marker genes was upregulated by 12OH-JA-Ile. Genome-wide transcript analyses and untargeted metabolomics experiments

showed that 12OH-JA-Ile could mimic a significant part of JA-Ile effects both at the transcriptional and metabolic levels. Mutation in *CORONATINE INSENSITIVE 1* (*COI1*) blocked 12OH-JA-Ile effects on anthocyanin and trichome induction, indicating that 12OH-JA-Ile signals through the common receptor and signaling mechanism as JA-Ile. 12OH-JA-Ile was able to trigger anthocyanin accumulation in tomato seedlings in COI1-dependent manner indicating that 12OH-JA-Ile signaling system is likely to be conserved in the eudicots. Increased endogenous 12OH-JA-Ile levels in a double T-DNA insertion mutant line blocked in 12OH-JA-Ile hydrolysis, *ill6iar3*, and decreased 12OH-JA-Ile either by triggering hydrolysis or oxidation of 12OH-JA-Ile in transgenic line *ILL6-OE* or *CYP94C1-OE* displayed phenotypes proportionate with endogenous 12OH-JA-Ile, indicative of JA-Ile-like signaling in wounded plants. Together, these results show that 12OH-JA-Ile likely plays a role in the JA-regulated wound response in plants.

1. Introduction

Plants use diverse chemicals to regulate their growth and development as well as to survive and adapt to environmental challenges. The lipid-derived hormone jasmonic acid and its many derivatives broadly named in the field as jasmonates (JAs) are such chemical signals more famously known for their important role in plant resistance to insect herbivory (Howe and Jander, 2008; Campos et al., 2014). Production of numerous metabolites with insecticidal and anti-nutritive properties or remodeling epidermal cells into hair-like structures

called trichomes are some of well-known anti-herbivory responses regulated by JA. The JA induced plant responses extend beyond the insect resistance to other processes important to protect plants against diverse biotic and abiotic stresses (Kastir et al., 2008; Koo and Howe, 2009; Wasternack 2015). These stress responses accompany tradeoffs in plant growth which is believed to increase plants' overall fitness (Baldwin 1998; Huot et al., 2013; Shyu and Brutnell, 2015; Zust and Agrawal, 2017).

JA-regulated physiological responses are the results of genome wide transcriptional changes that are directly or indirectly controlled by JA. For example, JA-regulated growth and developmental readjustments are attributed to transcriptional changes in genes related to photosynthetic activity and cell cycle progression (Noir et al., 2013; Attaran et al., 2014). Carbon and metabolite reallocation to increase the mass production of specialized defense compounds at the expense of growth-related metabolism is tightly linked to altered gene expression patterns (Christensen et al., 2013; De Geyter et al., 2012). Expression of several anthocyanin biosynthetic genes encoding dihydroflavonol reductase (DFR), leucoanthocyanidin dioxygenase (LDOX), or UDP-Glc:flavonoid 3-O-glucosyltransferase (UF3GT) are dependent on JA receptor CORONATINE INSENSITIVE 1 (COI1) in Arabidopsis. Transcriptional regulator complex composed of WD-repeat, basic helix-loop-helix (bHLH), and MYB-transcriptional factors (TFs) including MYB75, GLABRA1 (GL1), GLABRA3 GL3), ENHANCER OF GLABRA3 (EGL3), and TRNSPARENT TESTA GLABRA8 (TT8) involved in the control of anthocyanin production and trichome initiation directly

interact with the members of JASMONATE DOMAIN (JAZ) repressors, JAZ1, JAZ8 and JAZ10, in the JA receptor complex (Li et al., 2004; Yoshida et al., 2009; Shan et al., 2009; Qi et al., 2011).

The core JA signaling machinery is composed of jasmonoyl-isoleucine (JA-Ile), JAZ, and COI1 which forms a co-receptor complex through direct ligand-mediated protein-protein interaction (Chini et al., 2007; Thines et al., 2007; Sheard et al., 2010). In the absence of JA-Ile, JAZ proteins bind to bHLH TF MYC2 and its close homologs MYC3 and MYC4 preventing their transcriptional activity (Dombrecht et al., 2007; Fernandez-Calvo et al., 2011; Zhang et al., 2015). In the presence of JA-Ile, JAZ binds to COI1 which is an F-box protein component of Skp1-Cul1-F-box (SCF) E3 ligase complex. COI1 binding to JAZ results in polyubiquitination of JAZ followed by its proteolysis by the 26S proteosomal pathway. Degradation of JAZ releases the transcription factor MYCs activating JA-inducible genes.

The basal level of JA present in the stress free cell is not high enough to trigger defense responses. Wounding or herbivory elicits major increase of JA levels through *de novo* synthesis. The final step of JA-Ile production is the conjugation of jasmonic acid with the amino acid isoleucine (Ile) by cytoplasm-localized aminoacyl synthetase, JASMONATE RESISTANT 1 (JAR1) (Staswick et al., 2002).

Jasmonic acid and JA-Ile are metabolized to a variety of other JA derivatives. Along with the biosynthetic pathways these other metabolic pathways will determine the overall cellular concentration of JA-Ile, and thus their regulation

is expected to have major influences on the final outcomes of JA signaling. One of those pathways recently discovered is mediated by the members of the Arabidopsis cytochrome P450 family, CYP94B1 (B1) and CYP94B3 (B3) (Koo et al., 2011, Kitaoka et al., 2011; Heitz et al., 2012; Koo et al., 2014). These enzymes catalyze the hydroxylation of JA-Ile at the 12th carbon position which is the methyl- or ω-end (hence, called ω-oxidation pathway) of the pentenyl side chain generating 12-hydroxy-JA-Ile (12OH-JA-Ile). 12OH-JA-Ile is further oxidized to 12COOH-JA-Ile by CYP94C1 (C1) and B3 in the same CYP94 clade (Heitz et al., 2012; Koo et al., 2014). Another reported route of JA-Ile metabolism operates by cleaving the amide bond that connects the jasmonic acid moiety with the Ile moiety of JA-Ile. This hydrolysis reaction is catalyzed by ILR1-LIKE6 (ILL6*)* and IAA-ALA Resistant 3 (IAR3) in the auxin amidohydrolase family (Bhosale et al., 2013; Widemann et al., 2013; Woldermariam et al., 2012; Zhang et al., 2016). ILL6 and IAR3 also use 12OH-JA-Ile as a substrate generating 12OH-JA and Ile. Endogenous JA profiling in mutants and transgenic lines of ILL6 and IAR3 indicated that 12OH-JA-Ile is in fact the more preferred substrate of these enzymes (Koo et al., 2014; Zhang et al., 2016). Together with the recently identified JASMONATE OXIDASEs (JOXs) belonging to the 2-oxoglutarate dioxygenase family that catalyzes direct hydroxylation of jasmonic acid (Caarls et al., 2017; Smirnova et al., 2017), hydrolysis of 12OH-JA-Ile is a major pathway to produce 12OH-JA. Other JA derivatives with enzymes identified include volatile form of JA, methyl-JA, synthesized by *S*-ADENOSYL-L-METHIONINE:JASMONIC ACID CARBOXYLMETHYL TRANSFERASE (JMT)

(Seo et al., 2001) and sulfated form of JA, 12-hydroxyjasmonic acid sulfate (12HSO_4-JA), synthesized by HYDROXYJASMONATE SULFOTRANSFERASE 2A (ST2A) (Gidda et al., 2003). In maize, peroxisomal localized *silkless1* (*sk1*) gene encoding a uridine diphosphate (UDP) glycosyltransferase depletes JA and OPDA from flowers (Hayward et al., 2016). Specific enzymes leading to the production of glycosylated JAs have not been identified in Arabidopsis.

In contrast to the firmly established signaling function of JA-Ile, the biological functions of other JA metabolites are largely unknown, besides being considered as catabolic by-product of JA metabolism. Jasmonic acid, MeJA, 12OH-JA, and 12COOH-JA-Ile failed to promote COI1 and JAZ protein-protein interaction (Thines et al., 2007; Koo et al., 2014; Patkar et al., 2015). 12OH-JA and 12-HSO_4-JA are unable to inhibit germination, repress root elongation or activate JA-responsive gene expression (Miersch et al., 2008). However, biological effects of certain JA metabolites have been reported albeit being different from classical JA responses. For instance, 12OH-JA and its *O*-glucoside, were reported to have tuber inducing activity in potatoes (Yoshihara et al., 1989). 12-*O*-Glc-JA mediated leaf movement in nyctinastic plants, such as rain trees (*Samanea saman*) and legumes (*Medicago truncatula*) (Nakamura et al., 2011; Zhou et al., 2012). The rice blast fungus *Magnaporthe oryzae* synthesizes 12OH-JA by its monooxygenase and uses it as a virulence factor during its invasion of host cells (Patkar et al., 2015). Oxidized JA-Ile was suggested to play a signaling role for plant resistance against fungal pathogen *Botrytis cineria* (Aubert et al., 2015).

In this study, we investigated the biological potential of 12OH-JA-Ile as a bona fide signaling molecule. The work was prompted by unexpected phenotypes of CYP94 mutants blocked in 12OH-JA-Ile formation (Poudel et al., 2016). Our results are consistent with the conclusion that 12OH-JA-Ile can trigger many classical JA-dependent responses including JA-responsive marker gene expression, production of anthocyanin and other specialized metabolites, and the formation of trichomes. These effects were dependent on the presence of the JA-Ile receptor COI1 and could be replicated in other plant species.

2. Materials and methods

2.1. Plant materials and growth conditions

Plant material for the experiment consisted of wild type *Arabidopsis thaliana* ecotype Columbia (Col-0), tomato (*Solanum lycopersicum L.*) cv. Micro-Tom and sorghum (*Sorghum bicolor*). Arabidopsis ethylmethane sulfonate mutant *coi1-1* and T-DNA insertion mutants *aos* (SALK_017756) and *ill6-2 iar3-5* have been described earlier (Xie et al., 1998; Bhosale et al., 2013; Zhang et al., 2016; Poudel et al., 2016) and the individual single mutant seeds were obtained from the Arabidopsis Biological Resource Center. *coi1-1* was introgressed to Col-0 to clean out the trichomeless genetic marker *gl1* (Yoshida et al., 2009). Transgenic lines expressing cauliflower mosaic virus (CaMV) *35S* promoter driven *ILL6* construct (*ILL6-OE*) (Zhang et al., 2016) was described previously. Binary vector constructs for generating *CYP94C1-OE* lines were made by PCR-amplifying the full-length *CYP94C1* (At2g27690) open reading frame (ORF) from WT genomic

DNA template using the primer pair 5'-GGACTAGTATGTTACTAATCATATCATTCACCATCG-3' and 5'-TTCTCGAGCTAACTCCTTTCTTGGATCATAACC-3' and ligating the resulting PCR fragment into the *Spe*I and *Xho*I sites of a modified pBI121 vector (Schilmiller et al., 2007), which places the gene under the control of the CaMV *35S* promoter. Resulting construct was transformed into *Agrobacterium tumefaciens* strain C58C1 then to Arabidopsis by the floral dip method (Clough and Bent, 1998). T1 seeds were first screened for their antibiotic resistance on Murashige and Skoog (MS) media containing kanamycin (50 μg mL^{-1}) and vancomycin (100 μg mL^{-1}), and upon transfer to soil were analyzed for mRNA transcript and JA profile. Tomato cv. Micro Tom and *jasmonic acid insensitive1-1* (*jai1-1*) (Li *et al*., 2004) seeds were generously provided by Dr. Gregg Howe from Michigan State University. Plants were grown in growth chambers maintained at 22 °C under long-day photoperiod condition of 16 h light (100–120 μE m^{-2} s^{-1}).

2.2. Anthocyanin induction and measurements

Anthocyanin was extracted in a solvent mixture of methanol (MeOH):water:hydrochloric acid = 85:15:1 (v/v/v) as described earlier (Poudel et al., 2016) and absorbance was measured at 530 nm and 657 nm wavelength using a spectrophotometer. Relative anthocyanin content was determined by A_{530} – (A_{657} x 0.25) and was normalized by the tissue weight (Rabino and Mancinelli, 1986). For tomato and sorghum seedlings, hypocotyl region obtained after

removal of true leaves and roots were grinded briefly with a plastic micro pestle in above extraction solvent and absorbance was taken as described previously.

2.3. Trichome counting

Trichomes were counted on the adaxial surface of the leaf using stereomicroscope (SZ-PT Olympus) as described previously (Poudel et al., 2016) with following modification. Soil grown 17-day-old plants were applied with 5 µL droplet of either mock, 50 µM JA-Ile or 50 µM 12OH-JA-Ile dissolved in water (< 0.01% ethanol) on the surface of leaf number 4 and 5 for two consecutive days. On the third day, an additional 10 µL was applied on the same leaves. Trichomes within 4 x 4 mm^2 area were counted on the 5th day after first application. Each treatment consisted of 6-7 biological replicates.

2.4. Quantification of JA derivatives

JA metabolites were analyzed using Ultra Performance Liquid Chromatography (UPLC) (ACUITY H-class, Waters)-triple quadrupole tandem mass spectrometer (MS/MS) (Xevo T-QS, Waters) system using previously established method (Koo et al., 2014; Poudel et al., 2016). Briefly, frozen leaf tissues weighing between 20-40 mg were grinded with metal beads in TissueLyser II (Quigen) and extracted with 200 µL methanol:water:acetic acid = 70:29:0.5 (v/v/v) solution containing a mixture of dihydro-JA(dhJA) and [$^{13}C_6$]-JA-Ile as internal standards. The resulting tissue extracts were vortexed for 15 min and cleared by centrifugation at 18,000 xg for 25 min in 4 ^{o}C. Seven µL of cleared

supernatant was separated on a UPLC BEH C18 column (1.7 µm, 2.1 × 50 mm; Waters) maintained at 40 °C. The 3-min inlet method consists of a gradient program of 0.1% aqueous formic acid and methanol as a mobile phase with a flow rate of 0.4 mL/min (Koo et al., 2014). MS transitions of *m/z* 209 > 29 for JA, 211 > 59 for dhJA, 225 > 59 for 12OH-JA, 322 > 130 for JA-Ile, 328 > 136 for [13C^6]-JA-Ile, 338 > 130 for 12OH-JA-Ile, and 352 > 130 for 12COOH-JA-Ile was used to detect the respective compounds. MassLynx 4.1 and TargetLynx software (Waters) was used to analyze the data. Concentrations were determined by comparisons to the standard curves generated using known concentrations of analytes.

2.5. Untargeted metabolite profiling

Untargeted metabolite profiling was performed with Bruker maXis impact quadrupole-time-of-flight (QTOF) mass spectrometer coupled to Waters ACQUITY UPLC system according to the methods described in (Lei et al., 2015). 15-d-old Col-0 seedlings grown in Murashige and Skoog (MS) medium were sprayed with mock (0.01% w/v ethanol in water), 50 µM of JA-Ile and 50 µM of 12OH-JA-Ile. Four plants were pooled for each replicate after 72 h of spray. Tissues were freeze dried (Labconco lyophilizer) for 72 h. The tissues were grinded with a metal bead in 2 ml plastic vials previously rinsed with MeOH to avoid plastic contamination. Around 5 mg of dried tissues were extracted in 1 mL of 80% MeOH containing 18 µg/ml umbelliferone as an internal standard. Each treatment consisted of five biological replicates. The samples were sonicated for

5 seconds, agitated for 2 h, centrifuged and transferred to the vial for LC-MS run. Samples were separated on a Waters C18 column (2.1 x 100 mm, BEH C18 column with 1.7-um particles) using a linear gradient of 95%:5% to 30%:70% eluent A:B (A: 0.1% formic acid, B: acetonitrile) over 30 min with the flow rate of 0.56 mL/min and the column temperature of 60 ^{o}C. Mass spectrometry was performed in the negative electrospray ionization mode with the nebulization gas pressure at 43.5 psi, dry gas of 12 L/min, dry temperature of 250 ^{o}C and a capillary voltage of 4000 V. Mass spectral data were collected from 100 and 1500 *m/z*. After data acquisition, samples were auto-calibrated using sodium formate. Data were processed using freely available standalone XCMS software package loaded in 3.3.1 version of R (Smith et al., 2006).

MS/MS fragmentation was performed on the same instrument, column and a mobile phase as untargeted MS method. For the gradient, mobile phase B was increased from 5% to 70% over 30 min, then to 95% over 3 min, held at 95% for 3 min, then was returned to 5% for equilibrium. The flow rate was 0.56 mL/min and the column temperature was 60 ^{o}C. Mass spectrometry was performed in the negative electrospray ionization mode with the nebulization gas pressure at 43.5 psi, dry gas of 12 L/min, dry temperature of 25 ^{o}C and a capillary voltage of 4000V. Mass spectral data were collected from 100 and 1500 m/z and were auto-calibrated using sodium formate after data acquisition.

2.6. RNA analysis

Fully expanded 21-d-old rosette leaves of Col-0 were sprayed with a solution containing Mock (0.01% w/v ethanol in water), 50 μM JA-Ile or 50 μM 12OH-JA-Ile in four biological replicates. Plants were flash frozen in liquid N_2 after 1 h and stored in -80 °C until RNA extraction.

RNA was extracted as described previously (Zhang et al., 2016). Briefly, frozen tissues were finely grinded with a metal ball using TissueLyser II (QIAGEN) and extracted with 1 mL TRIzol (Invitrogen). The RNA was further treated with TURBO DNA-free kit (Ambion) following the company's protocol. RNA quality test based on the absorbance ratio 260/280 and 260/230 was performed on NanoDrop One (Thermo Scientific). One μg of total RNA was reverse transcribed using oligo $(dT)_{20}$ (IDT) primers and Moloney murine leukemia virus (M-MLV) reverse transcriptase (Promega). The resulting cDNA was diluted 10 times and 1 μL was used for semi-quantitative reverse transcription PCR (qRT-PCR) reaction using SsoFast™ EvaGreen® Supermix (Bio-Rad) fluorescent polymerase CFX96 Touch™ real-time PCR detection system (Bio-Rad). *ACTIN8* (AT1G49240) was used as an internal reference gene. Primers used in this study have been described in (Poudel et al., 2016).

For RNA-seq analysis, the integrity of total RNA was first tested on Fragment Analyzer automated electrophoresis system. Three best samples from each treatment with the RNA integrity number (RIN) values ranging from 7.2 to 8.2 were selected. High-throughput sequencing was performed at the University of Missouri DNA Core Facility as follows. Libraries were constructed with

reagents supplied in Illumina's TruSeq mRNA stranded sample preparation kit following the manufacturer's protocol. The protocol involves isolating poly-A containing mRNA from total RNA. The purified RNA is then fragmented followed by synthesis of double-stranded cDNA from the fragmented RNA. Index containing adapters are ligated to the end of the cDNAs and amplified by PCR. The amplified cDNAs were purified by addition of Axyprep Mag PCR Clean-up beads. The final library was evaluated using the Fragment Analyzer automated electrophoresis system, quantified with the Qubit flourometer using the Qubit HS dsDNA assay kit, and diluted according to Illumina's standard sequencing protocol for sequencing on the NextSeq 500 (Illumina). The barcoded samples were multiplexed to run in one of the four NextSeq 500 lanes. Each sample replicate generated about 45 M reads.

RNA-seq informatics analysis of resulting fastq file was conducted using an in-house developed pipeline starting with quality control using fastqc (http://www.bioinformatics.babraham.ac.uk/projects/fastqc/) tool and trim-galore (http://www.bioinformatics.babraham.ac.uk/projects/trim_galore/) tool to remove low quality reads and trim adaptor sequences. The trimmed sequencing reads were then indexed with respect to the *Arabidopsis thaliana* (TAIR10) reference genome using Bowtie2 (Langmead and Salzberg, 2012) short read aligner. Indexed RNA-seq reads were aligned to the reference genome using TopHat (Trapnell et al., 2012), which reports splice junction sites. The aligned reads were then used to quantify the expression level of each gene using the tool Cufflinks (Trapnell et al., 2010) in our in-house pipeline. The quantified expression level is

represented by Fragments Per Kilobase of transcript per Million mapped reads (FPKM) values. The differential expression levels of quantified genes were then calculated using Cuffdiff (Trapnell et al., 2013). The thresholds were set as two-fold (JA-Ile) or 1.5-fold (12OH-JA-Ile) change and *q*-value ≤ 0.05 for the genes to be differentially expressed.

2.7. Plant treatment for wound-induced growth inhibition experiment

Plants were subjected to multiple wounding treatments as previously described (Poudel et al., 2016). Briefly, leaf number 1 and 2 of 17 days old plants were crushed once across the midrib with a hemostat. Leaf number 3 and 4 were wounded once each day on 18th and 19th days. Plants were then not wounded for three days. On 23rd and 24th day, leaf number 5 and 6 was wounded once. Each plant received 10 wounding in total. Plants were then harvested 2-3 days after final wound treatment for fresh weight determination and anthocyanin extraction.

3. Results

3.1. 12OH-JA-Ile induces anthocyanin and trichome formation in a COI1 dependent manner

During our previous study of *cyp94* mutants, it was observed that those mutants were strongly reduced in anthocyanin content and also generated significantly less number of trichomes compared to WT plants in response to wounding. Since the *cyp94* mutants were severely depleted in endogenous

12OH-JA-Ile levels, a question was raised whether 12OH-JA-Ile has a role in wound-induced production of anthocyanin and trichomes.

To directly test this possibility, 10-d-old Arabidopsis seedlings were treated with exogenous 12OH-JA-Ile (50 μM). As a negative control, mock solution consisting of water (<0.01% ethanol) was used. Two positive controls used were an equal amount (50 μM) of JA-Ile and sucrose (100 mM) (Rudell, et al., 2002; Teng et al., 2005; Loreti et al., 2008; Shan et al., 2009). Exogenous treatment of JA is known to induce anthocyanin and trichomes in Arabidopsis (Boughton et al., 2005; Shan et al., 2009; Yoshida et al., 2009). This effect of JA has been reported to be the function of the bioactive form of JA, JA-Ile, and was also found to involve protein-protein interactions between JAZ proteins of the JA pathway and the WD40/bHLH/MYB protein complex of the anthocyanin and trichome biogenesis pathways (Qi et al., 2011). JAZ proteolysis mediated by COI1-dependent polyubiquitination of the JAZ in the presence of JA-Ile releases transcriptional repression on WD40/bHLH/MYB, activating gene expression responsible for the anthocyanin biosynthesis and trichome development. As expected, both JA-Ile and sucrose, another well-known inducer of anthocyanin, induced anthocyanin accumulation within 48 h after treatment (shown are the measurements after 72 h) (Figure 3.1.A). Interestingly, application of 12OH-JA-Ile also induced anthocyanin similar to the level induced by JA-Ile. To see if this anthocyanin inducing activity of 12OH-JA-Ile requires the JA-Ile receptor COI1, *coi1-1* mutants were equally treated side by side with WT plants.

Consistent with the previous report (Shan et al., 2009) *coi1-1* mutation completely abolished anthocyanin induction by JA-Ile. Similarly, no increase in anthocyanin was observed in *coi1-1* plants treated with 12OH-JA-Ile indicating intact COI1 is required also for 12OH-JA-Ile action. As observed by others (Shan et al., 2009) *coi1-1* mutation only partially blocked sucrose induced anthocyanin accumulation showing that *coi1-1* retained metabolic capacity to synthesize anthocyanin biosynthesis.

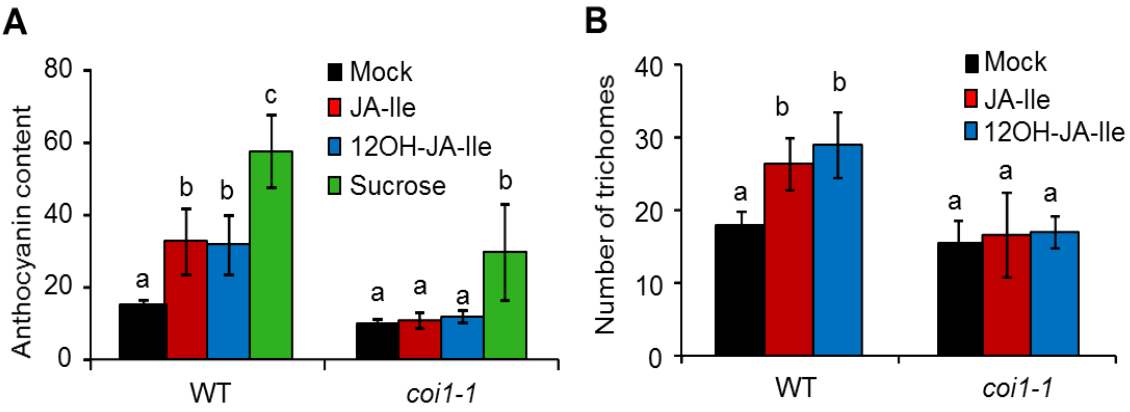

Figure 3.1. Induction of anthocyanin and trichomes by 12OH-JA-Ile. (A) Anthocyanin content in 14-d-old WT and *coi1-1* Arabidopsis seedlings grown on MS media treated with mock, 50 µM JA-Ile, 50 µM 12OH-JA-Ile, or 100 mM sucrose. Homozygous *coi1-1* was pre-selected on MS media containing 20 µM JA. Solution was applied as a spray while sugar treatment was done by transferring plants to a MS media containing 100 mM sucrose. Plants were harvested after 72 h of treatment. (B) Number of trichomes on 22-d-old WT and *coi1-1* leaves. The trichomeless genetic marker *gl1* in *coi1-1* was cleaned by introgression to Col-0. Five µL of the mock, 50 µM JA-Ile or 50 µM 12OH-JA-Ile was applied as droplets on the surface of the 4th and 5th true leaves. After two days, an additional 10 µL was applied on the already treated leaves.

Trichomes within 16 mm^2 area of the treated leaves were counted on the 5th day of application. Each bar is the mean and standard deviation of 6-7 biological replicates. Letters above columns indicate significant differences ($p < 0.05$) compared to WT Mock treatment as determined by Student's *t* test.

Next we tested if 12OH-JA-Ile could also increase the number of trichomes as JA-Ile does. 22-d-old WT and *coi1-1* leaves were treated with 5 µL of mock (0.01% ethanol in water), 50 µM JA-Ile or 50 µM 12OH-JA-Ile as droplets on the leaf surface. After two days an additional 10 µL of same solution was applied on the already treated leaves and number of trichomes was counted on the 5th day of application. Both JA-Ile and 12OH-JA-Ile treatment resulted in significant increases in trichome numbers in WT plants compared to mock treatment (Figure 3.1.B). Similar to the case of anthocyanin induction experiment, neither JA-Ile nor 12OH-JA-Ile was able to induce trichomes in *coi1-1* (Yoshida et al., 2009). These results show that 12OH-JA-Ile can mimic JA-Ile's anthocyanin- and trichome-inducing activity in Arabidopsis and that those responses require JA-Ile receptor COI1.

3.2. Exogenous 12OH-JA-Ile is not metabolized to JA-Ile

The observations that 12OH-JA-Ile can activate anthocyanin biosynthesis and trichome initiation through a pathway that depends on COI1 might be explained if 12OH-JA-Ile is converted back to JA-Ile endogenously by the plant after the exogenous application. Conversion of 12OH-JA-Ile to JA-Ile has never been reported in the literature and nor is an enzymatic step(s) known to catalyze such a reaction.

We tested such possibility by quantifying endogenous JA-Ile levels using LC-MS/MS in the leaves after incubating with exogenous 12OH-JA-Ile. A JA biosynthetic mutant *aos* was used in addition to WT as a control. Same amount of 12OH-JA-Ile (50 µM) as in Figure 3.1 was applied to leaf surface and samples were collected at 3 h, 6 h, and 10 h after the treatment for hormone quantification.

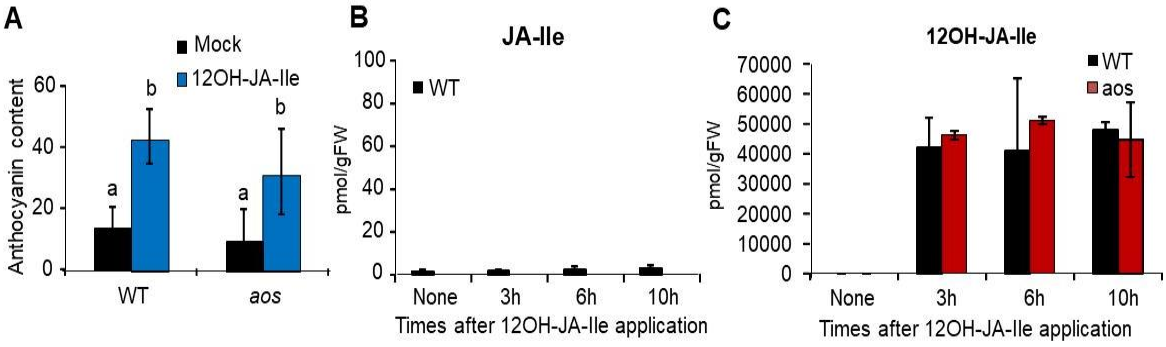

Figure 3.2. Exogenously applied 12OH-JA-Ile is not converted to JA-Ile *in planta*. (A) Anthocyanin content in 19-d-old WT and *aos* plants treated with Mock (0.01% ethanol in water) or 50 µM 12OH-JA-Ile. Leaves were treated similarly to the methods described in Figure 3.1. Each bar graph represents average of 6 biological replicates ± SD. (B-C) JA-Ile (B) and 12OH-JA-Ile (C) content in WT and *aos* leaves applied with 10 µL of 50 µM 12OH-JA-Ile. Leaf tissue samples were harvested 3 h, 6 h, and 10 h post treatment along with those that received mock treatment (None). Each bar graph represents average of 4 biological replicates ± SD. Different letters above the bars denote significant difference ($p < 0.05$; Student's *t* test) compared to mock treated WT. 'ns' denote not significant.

Similar to the results in Figure 3.1.A, 12OH-JA-Ile treatment induced anthocyanin in WT plants compared to the mock treatment (Figure 3.2.A). The 12OH-JA-Ile treatment also induced anthocyanin in *aos* that does not have

endogenous JA. Less than 10 pmol/ gram fresh weight (gFW) JA-Ile was present in mock treated WT and *aos*. No significant rise above this baseline could be detected over 10 hrs (Figure 3.2.B). 12OH-JA-Ile level, on the other hand, remained very high at > 40,000 pmol/gFW in the tissues treated with exogenous 12OH-JA-Ile (Figure 3.2.C). This shows that at least there isn't major conversion of 12OH-JA-Ile to JA-Ile in these leaves. Even if there were minor rise in endogenous JA-Ile that cannot explain the comparable levels of anthocyanin produced in leaves treated with equally high levels (50 μM) of JA-Ile and 12OH-JA-Ile in Figure 3.1.A. Therefore, it is more likely that 12OH-JA-Ile is responsible for increase of anthocyanin in these experiments.

3.3. 12OH-JA-Ile induces JA-Ile responsive marker genes expression through COI1

Since 12OH-JA-Ile treatment triggered a similar effect as JA-Ile in enhancing the production of anthocyanin and trichomes, we next examined whether 12OH-JA-Ile also mimicked the JA-Ile's ability to regulate gene expression. We selected five marker genes– *JAZ8*, *JAZ10*, *OPR3, MYC2,* and *MYB75/PAP1* genes that have previously been established to be expressed in response to JA-Ile (Thines et al., 2007; Chung et al., 2008; Shan et al., 2009; Zhang et al, 2016; Poudel et al., 2016). Fully expanded rosette leaves of 21-d-old WT plants were sprayed with solutions containing Mock (0.01% ethanol in water), 50 μM JA-Ile or 50 μM 12OH-JA-Ile. Total RNA was extracted after 1 h or 8 h (for *MYB75*) of treatment from the above ground tissues and expression of marker

genes were analyzed by semi-quantitative reverse transcriptase-PCR (qRT-PCR). Consistent with the previous reports (Zhang et al, 2016; Poudel et al., 2016), JA-Ile treatment strongly increased transcripts of all five marker genes compared to the mock treatment (Figure 3.3.A and B). 12OH-JA-Ile treatment also significantly increased transcript levels of all of those marker genes relative to the mock treatment. However, the 12OH-JA-Ile treatment induced-marker gene expressions were significantly lower than those by the JA-Ile treatment with the exception of *MYB75* where modest induction equivalent to that by JA-Ile was replicated by 12OH-JA-Ile at both 1 h and 8 h (Figure 3.3.B). Though not strongly supported by the statistics, 12OH-JA-Ile treatment consistently showed trends of higher *MYB75* transcript levels than that by JA-Ile treatment. A similar expression pattern was observed with transcriptome profiling (Figure 3.4). Together, these results indicate that, albeit much weaker, 12OH-JA-Ile is capable of inducing the transcriptional activity of the five JA-Ile-responsive marker genes.

The obvious next question was whether this 12OH-JA-Ile-activated JA-Ile-responsive marker gene expression requires the JA-Ile-receptor COI1. JA-Ile induced expression of the above five marker genes have been shown to be abolished in *coi1-1* mutant (Chung et al., 2008; Shan et al., 2009; Qi et al., 2011). Twenty one-day-old *coi1-1* plants were treated similarly as above WT using equal concentration of mock and 12OH-JA-Ile solutions for 1 h. The qRT-PCR showed that unlike in WT, 12OH-JA-Ile did not induce the five JA-Ile-responsive marker genes in *coi1-1* mutant (Figure 3.3.C). The gene expression levels were either similar to or less than (*OPR3*) the mock treatment. The failure to induce JA-Ile-

responsive gene expression by 12OH-JA-Ile treatment in *coi1-1,* indicates that 12OH-JA-Ile signals through the common JA-Ile signaling system involving COI1.

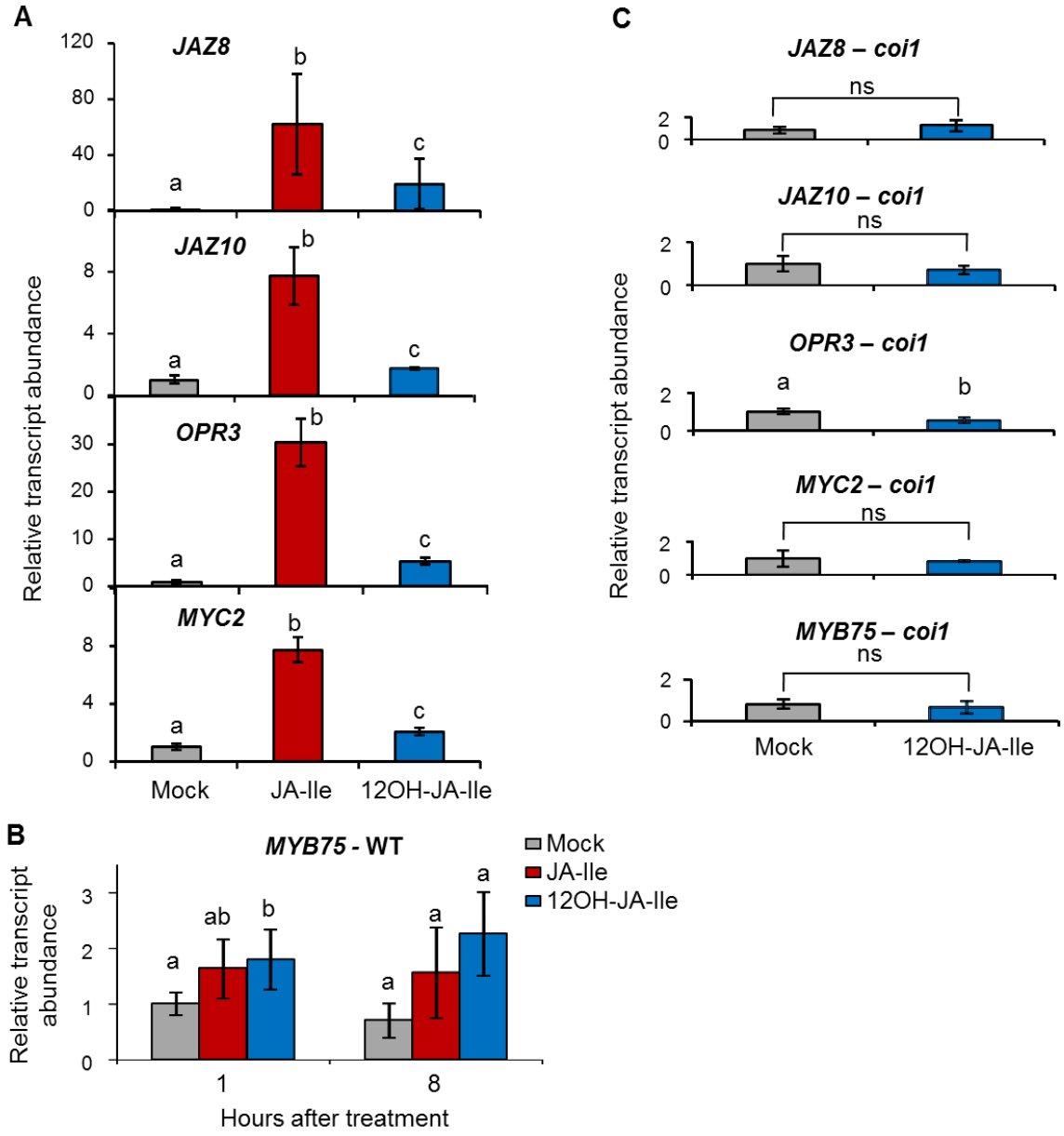

Figure 3.3. 12OH-JA-Ile induces JA-Ile-responsive marker gene expression. qRT-PCR analysis of JA-Ile-responsive marker genes *JAZ8*, *JAZ10*, *OPR3*, *MYC2*, and *MYB75*. Rosette leaves of 21d-old WT (A and B) and *coi1-1* (C) plants were sprayed with Mock (0.01% ethanol in water), 50 µM JA-Ile, or 50 µM 12OH-JA-Ile for either 1 h

(A-C) or 8 h (B). Relative transcript abundance is shown as fold-change compared to the internal reference gene, *ACTIN8*. Each data show mean and SD of four biological replicates. Letters above columns indicate significant differences ($p < 0.05$) as determined by Student's *t* test ('ns'; not significant).

3.4. RNA-seq analysis revealed a broad overlapping set of genes regulated by 12OH-JA-Ile and JA-Ile

After confirming that 12OH-JA-Ile can induce several JA-Ile-responsive marker genes expression by targeted analyses, whole genome transcriptome profiling was performed to study the extent to which 12OH-JA-Ile can influence gene expression. Total RNA isolated from 21-d-old Arabidopsis plants treated for 1 h with JA-Ile and 12OH-JA-Ile in the same manner as those used for qRT-PCR analyses (Figure 3.3) was subject to RNA-seq analysis using NextSeq 500 (Illumina). In total, 4,173 and 673 genes were found to be differentially expressed ($q < 0.05$) by JA-Ile or 12OH-JA-Ile treatment, respectively, compared to the mock treatment. The relative expression of JA-Ile vs. mock and 12OH-JA-Ile vs. mock treatment were used to calculate fold change (FC) between the treatments. Among those, 1,150 and 176 genes changed their expression more than 2-fold by JA-Ile and 12OH-JA-Ile, respectively. The 1,150 genes differentially regulated (≥ 2-fold) by JA-Ile consisted of 786 upregulated and 364 downregulated genes whereas the 176 genes differentially regulated (≥ 2-fold) by 12OH-JA-Ile consisted of 134 upregulated and 42 downregulated genes (Figure 3.4.A, a fold change cutoff of 1.5-fold instead of 2-fold was applied for 12OH-JA-Ile to plot the Venn diagram).

A

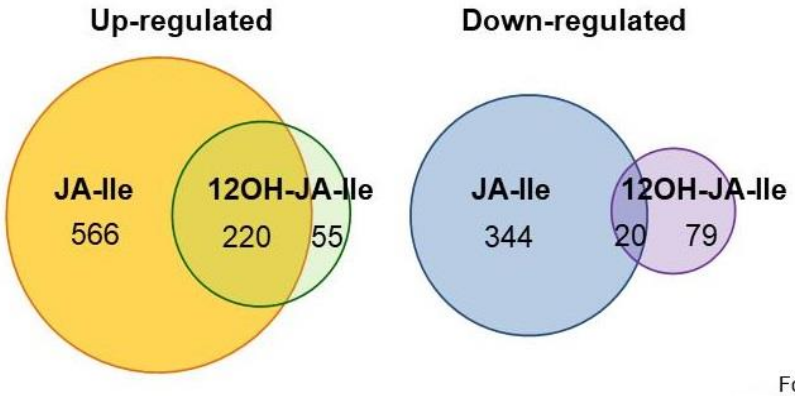

B

Fold change (Log_2 ratio)

0.58 3 7

	Primary Gene Symbol	Gene Locus	Log_2 Fold Change Over Mock	
			JA-Ile	12OH-JA-Ile
JA Metabolism	LIPOXYGENASE 3 (LOX3)	AT1G17420	4.38	1.50
JA Metabolism	LIPOXYGENASE 4 (LOX4)	AT1G72520	2.80	0.76
JA Metabolism	ALLENE OXIDE SYNTHASE (AOS)	AT5G42650	2.96	1.13
JA Metabolism	ALLENE OXIDE CYCLASE 1 (AOC1)	AT3G25760	5.03	1.98
JA Metabolism	ALLENE OXIDE CYCLASE 3 (AOC3)	AT3G25780	4.17	2.13
JA Metabolism	OXOPHYTODIENOATE-REDUCTASE 3 (OPR3)	AT2G06050	5.04	2.52
JA Metabolism	OPC-8:0 COA LIGASE1 (OPCL1)	AT1G20510	2.63	1.16
JA Metabolism	CYTOCHROME P450, FAMILY 94, SUBFAMILY B, POLYPEPTIDE 3 (CYP94B3)	AT3G48520	3.97	2.65
JA Metabolism	IAA-LEUCINE RESISTANT (ILR)-LIKE GENE 6 (ILL6)	AT1G44350	4.23	2.25
JA Metabolism	IAA-ALANINE RESISTANT 3 (IAR3)	AT1G51760	3.51	0.83
JA Metabolism	JASMONIC ACID CARBOXYL METHYLTRANSFERASE (JMT)	AT1G19640	1.93	1.15
JA Metabolism	JASMONATE-INDUCED OXYGENASE 2 (JOX2)	AT5G05600	4.40	1.54
JA Metabolism	JASMONATE-INDUCED OXYGENASE 3 (JOX3)	AT3G55970	2.77	2.86
JA Metabolism	JASMONATE-INDUCED OXYGENASE 4 (JOX4)	AT2G38240	6.88	2.12
JA Metabolism	SULFOTRANSFERASE 2A (ST2A)	AT5G07010	2.76	2.35
JA Signaling	JASMONATE-ZIM-DOMAIN PROTEIN 1 (JAZ1)	AT1G19180	2.51	0.89
JA Signaling	JASMONATE-ZIM-DOMAIN PROTEIN 3 (JAZ3)	AT3G17860	2.09	1.01
JA Signaling	JASMONATE-ZIM-DOMAIN PROTEIN 5 (JAZ5)	AT1G17380	3.98	1.45
JA Signaling	JASMONATE-ZIM-DOMAIN PROTEIN 6 (JAZ6)	AT1G72450	2.14	0.69
JA Signaling	JASMONATE-ZIM-DOMAIN PROTEIN 7 (JAZ7)	AT2G34600	4.02	1.10
JA Signaling	JASMONATE-ZIM-DOMAIN PROTEIN 8 (JAZ8)	AT1G30135	4.95	1.67
JA Signaling	JASMONATE-ZIM-DOMAIN PROTEIN 10 (JAZ10)	AT5G13220	2.88	0.96
JA Signaling	MYC2	AT1G32640	3.42	1.38
Defense	ALKENYL HYDROXALKYL PRODUCING 2 (AOP2)	AT4G03060	3.02	2.51
Defense	MYB DOMAIN PROTEIN 76 (MYB76)	AT5G07700	2.81	2.05
Defense	APS-KINASE 2 (AKN2)	AT4G39940	2.38	1.63
Defense	MYB DOMAIN PROTEIN 34 (MYB34)	AT5G60890	2.33	1.06
Defense	CYTOCHROME P450, FAMILY 79, SUBFAMILY F, POLYPEPTIDE 2 (CYP79F2)	AT1G16400	2.29	1.72
Defense	CYTOCHROME P450, FAMILY 83, SUBFAMILY B, POLYPEPTIDE 1 (CYP83B1)	AT4G31500	2.25	1.00
Defense	SULFOTRANSFERASE 16 (SOT16)	AT1G74100	2.20	1.02
Defense	GAMMA-GLUTAMYL PEPTIDASE 1 (GGP1)	AT4G30530	2.19	0.94
Defense	GLUTATHIONE S-TRANSFERASE F11 (GSTF11)	AT3G03190	2.03	1.87
Defense	UDP-GLUCOSYL TRANSFERASE 74B1 (UGT74B1)	AT1G24100	1.92	1.31
Defense	CYTOCHROME P450, FAMILY 79, SUBFAMILY B, POLYPEPTIDE 2 (CYP79B2)	AT4G39950	1.85	1.09
Defense	CYTOCHROME P450, FAMILY 79, SUBFAMILY B, POLYPEPTIDE 3 (CYP79B3)	AT2G22330	1.85	1.04
Defense	FLAVIN-MONOOXYGENASE GLUCOSINOLATE S-OXYGENASE 1 (FMO GS-OX1)	AT1G65860	1.83	1.33
Defense	ISOPROPYLMALATE ISOMERASE 1 (IPMI1)	AT3G58990	1.81	1.54
Defense	APS KINASE (APK)	AT2G14750	1.78	1.16
Defense	DESULFO-GLUCOSINOLATE SULFOTRANSFERASE 18 (SOT18)	AT1G74090	1.65	1.37
Defense	SULFOTRANSFERASE 17 (SOT17)	AT1G18590	1.63	1.33
Defense	BILE ACID TRANSPORTER 5 (BAT5)	AT4G12030	1.25	0.99
Defense	CYTOCHROME P450 79F1 (CYP79F1)	AT1G16410	1.24	1.06
Defense	SUPERROOT 1 (SUR1)	AT2G20610	1.07	0.63
Defense	similar to ACC oxidase	AT2G25450	1.01	0.62
Defense	VEGETATIVE STORAGE PROTEIN 2 (VSP2)	AT5G24770	1.31	1.26
Defense	PRODUCTION OF ANTHOCYANIN PIGMENT 1 (PAP1)	AT1G56650	1.81	1.66
Defense	TERPENE SYNTHASE 04 (TPS04)	AT1G61120	4.76	1.57

Figure 3.4. RNA-seq analysis of plants treated with JA-Ile and 12OH-JA-Ile. (A) Venn diagrams summarize the partial overlaps between the genes upregulated (left) or downregulated (right) by JA-Ile and 12OH-JA-Ile compared to mock treatment. The

differentially expressed genes are preselected by a $q < 0.05$ and a fold change cutoff of 2 for JA-Ile and 1.5 for 12OH-JA-Ile over mock treatment. (B) Identification of genes induced by JA-Ile and 12OH-JA-Ile in the functional category of JA metabolism, JA signaling, and defense. Heat map shows the fold change (Log2) values of JA-Ile or 12OH-JA-Ile over mock.

Although fewer genes were induced by 12OH-JA-Ile, treatment upregulated significantly higher number of genes compared to mock treatment. Importantly, as much as 75-80% of the genes (100/134 at 2-fold change and 220/275 at 1.5-fold change) upregulated by 12OH-JA-Ile were also upregulated by JA-Ile, indicating that 12OH-JA-Ile is able to induce a subset of JA-Ile responsive genes. Much less overlap, however, was found among the genes that were suppressed by the treatments (22% or 20/99 genes downregulated by 12OH-JA-Ile) (Figure 3.4.A).

Figure 3.4.B displays a list of 47 genes commonly induced by JA-Ile and 12OH-JA-Ile treatments relative to the mock, grouped into three functional categories, ‘JA metabolism’, ‘JA signaling’ and ‘defense’ genes. These genes are classical JA-Ile regulated genes, indicating that 12OH-JA-Ile can induce a significant number of JA-Ile-regulated genes although the inductive potential is much weaker than that of JA-Ile. The overall weaker induction by 12OH-JA-Ile compared to JA-Ile is consistent with the qRT-PCR results (Figure 3.3).

3.5. Untargeted metabolite profiling shows overlapping metabolite induction by JA-Ile and 12OH-JA-Ile

JA-Ile is known to promote specialized metabolite production in plants that constitutes an important component of defense mechanism. Increased anthocyanin, a class of specialized metabolites, together with transcriptional induction of genes involved in specialized metabolite biosynthesis in plants by12OH-JA-Ile treatment, suggested that 12OH-JA-Ile treatment could induce those metabolites like JA-Ile. To directly test this possibility, untargeted metabolite profiling analysis was performed. Methanolic extracts of 15-d-old WT seedlings sprayed with mock (0.01% ethanol in water) or 50 µM each of JA-Ile or 12OH-JA-Ile for 72 h were subjected to UPLC-QTOF-mass spectrometry analyses. The data generated from XCMS had around 800 entries representing different mass to charge ratio (*m*/*z*) and retention times for each sample treatment with five replicates. The relative signal intensities between JA-Ile vs. mock and 12OH-JA-Ile vs. mock treatment were used to calculate fold change (FC) between the treatments. The majority of the metabolites (>80%) remained unchanged upon treatment with either JA-Ile or 12OH-JA-Ile relative to the mock. JA-Ile treatment induced (>1.5 FC over mock; $p < 0.05$) 75 metabolites (Figure 3.5.A). 12OH-JA-Ile treatment also induced less metabolites than by JA-Ile but comparable number (56) of metabolites relative to mock (Figure 3.5.B). The percentage of induced metabolites by both JA-Ile (9%) and 12OH-JA-Ile (7%) treatment were lower than those induced by wound treatment (31%) (Poudel et al., 2016),

suggesting that JA-Ile and 12OH-JA-Ile are responsible for a quarter to one third of the metabolites induced in wounded plants.

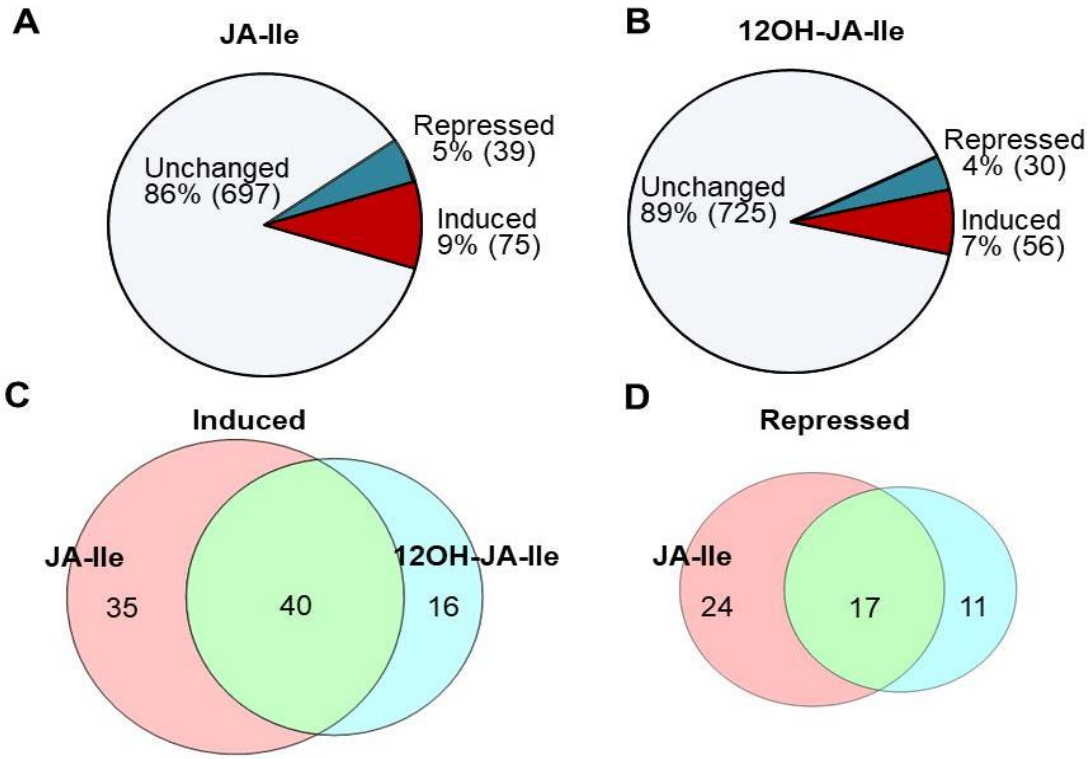

E

1.5 3.9

Metabolites induced by both JA-Ile and 12OH-JA-Ile		
Compound Name	**JA-Ile / Mock**	**12OH-JA-Ile / Mock**
Kaempferol-7-O-glucoside	3.9	2.3
Glucoibarin	3.1	2.9
Glucohirsutin	3.2	2.6
Glucoraphanin	2.6	2.6
7-GlcA tricin	1.6	2
Arginine	1.7	1.6

Induced by JA-Ile only	
Compound Name	**JA-Ile / Mock**
9-hydroperoxy-10E,12Z-octadecadienoic acid	2.1
Genistein	1.6

Induced by 12OH-JA-Ile only	
Compound Name	**12OH-JA-Ile / Mock**
N-Alpha-acetyl-L-ornithine/acetyl ornithine	1.6
7-Glu Chrysoeriol	1.5
Rhoifolin	1.5
4'-O-(2'-E-Feruloyl GluA(1-2)GluA) Apigenin	1.5

Figure 3.5. Untargeted metabolite profiling of plants treated with JA-Ile or 12OH-JA-Ile. Data were obtained from five replicates of 17-d-old Arabidopsis seedlings sprayed with mock (0.01% ethanol in water) or 50 μM each of JA-Ile or 12OH-JA-Ile. (A-B) Distribution of the metabolites induced (fold change (FC) > 1.5), repressed (FC < 0.67) or unchanged (0.67 ≤ FC ≤ 1.5) by (A) JA-Ile and (B) 12OH-JA-Ile relative to mock. (C-D) Venn diagram showing overlaps between the metabolites induced or repressed by JA-Ile and 12OH-JA-Ile. (D) List of metabolites identified by MS/MS and library search. Metabolites showing at least 1.5 FC difference from LC-MS results were subjected to MS/MS analysis followed by matching against in-house and Massbank libraries (Lei et al., 2015). Heat map visualizes the FC values shown in the table.

There was an extensive overlap between the metabolites induced by JA-Ile and 12OH-JA-Ile. Among the 75 induced by JA-Ile and the 56 by 12OH-JA-Ile, 40 metabolites were induced by both treatments (71% of those induced by 12OH-JA-Ile) (Figure 3.5.C). Similar trend was observed with metabolites that were repressed by the treatments. Among 41 and 28 metabolites repressed by JA-Ile and 12OH-JA-Ile treatments, respectively, 17 (61% of 12OH-JA-Ile inducible metabolites) overlapped (Figure 3.5.D). Identities of some of the induced metabolites based on the accurate mass by MS/MS fragmentation pattern is displayed in Figure 3.5.E. Compounds include flavonoids and glucosinolate class of compound known to be regulated by JA.

3.6. Anthocyanin inducing activity of 12OH-JA-Ile in other plant species

Next we tested whether the JA-Ile-like signaling activity of 12OH-JA-Ile is specific for Arabidopsis or conserved in other higher plant species. Tomato and sorghum were chosen to represent dicotyledonous and monocotyledonous species, respectively. For tomato, *jai1-1* mutant was available to be tested along with WT. *jai1-1* is mutated in a tomato version of Arabidopsis *COI1* gene, hence is insensitive to JA-Ile. Since *jai1-1* are sterile and only maintained as heterozygous, homozygous mutants were pre-selected on a filter paper containing MeJA by monitoring absence of anthocyanin accumulation and inhibition of root elongation. Four-d-old WT and *jai1-1* tomato seedlings were treated with 10 µL each of mock (0.01% w/v ethanol in water), JA-Ile (50 µM) or 12OH-JA-Ile (50 µM) solutions for three consecutive days. Anthocyanin was extracted from the hypocotyl region of the seedlings where red coloration primary appears (Figure 3.6). Similar to the Arabidopsis results, both JA-Ile and 12OH-JA-Ile treatments induced several-fold higher anthocyanin in WT tomato seedlings compare to the mock. *jai1-1* mutants which did not respond to MeJA (during preselection) did not respond to neither JA-Ile nor 12OH-JA-Ile (Figure 3.6A and C). Similar tests conducted on 8-d-old sorghum indicated that 12OH-JA-Ile could also induce anthocyanin to a comparable level as that by JA-Ile. These results imply that 12OH-JA-Ile perception and signaling mechanism is conserved in both dicots and monocots and that at least in tomato, the mechanism involves the common JA-Ile receptor system.

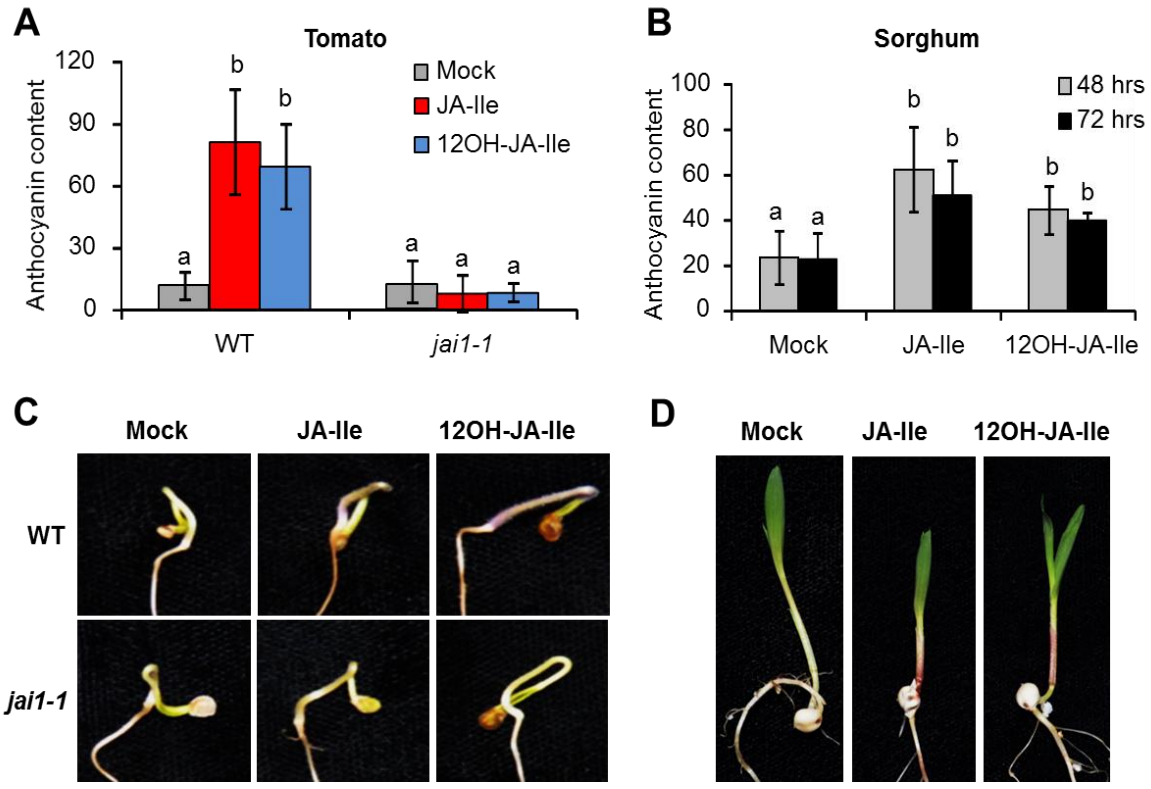

Figure 3.6. 12OH-JA-Ile activity is conserved in other higher plant species. (A and C) Anthocyanin content (A) and photograph image (C) of 9-d old WT and *jai1-1* tomato seedlings treated with mock (0.01% w/v ethanol in water), 50 μM JA-Ile or 50 μM 12OH-JA-Ile. Ten μL of solutions containing each compound was applied to the newly emerging hypocotyl of 4-d old seedlings germinated on wet filter papers once everyday for three consecutive days. Seedlings were harvested on the 5th day after the initial application. Homozygous *jai1-1* was pre-selected by spraying with 500 μM MeJA. (B and D) Anthocyanin content (B) and representative photo image (D) of 8-d old sorghum seedlings at 48 and 72 h after spraying with mock, 50 μM JA-Ile or 50 μM 12OH-JA-Ile. Different letters above bar graphs indicate significant differences (p < 0.05) within the group as determined by Student's *t* test.

3.7. Varying levels of 12OH-JA-Ile created by genetic manipulations correlate with anthocyanin accumulation and plant growth patterns

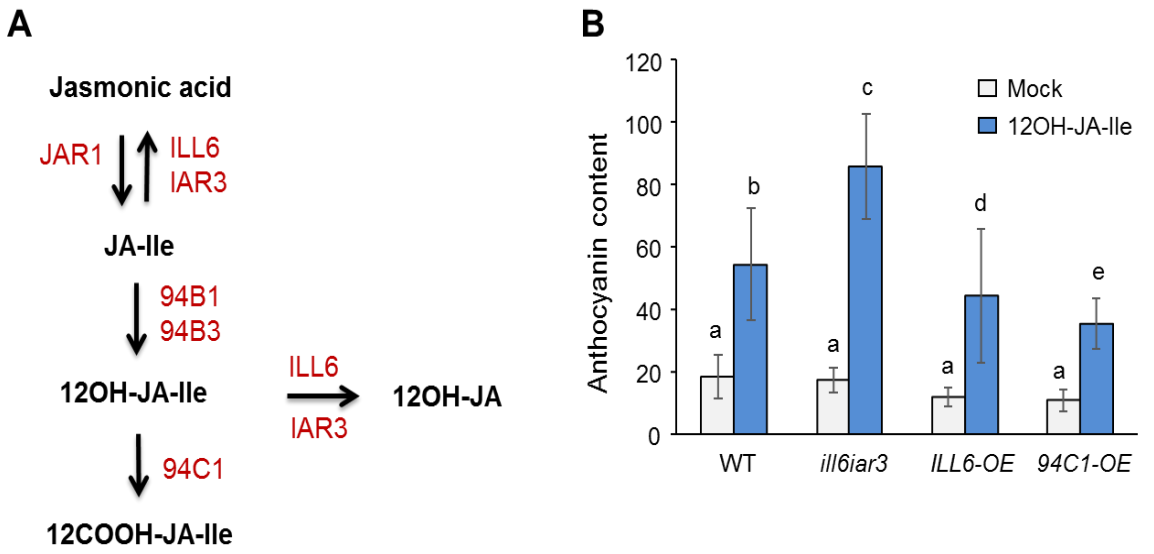

Figure 3.7. Genetic manipulation to decrease or increase 12OH-JA-Ile metabolism correlates with anthocyanin accumulation. (A) Schematic diagram of JA metabolic pathways. (B) Anthocyanin levels in 12-d-old WT, *ill6iar3*, *ILL6-OE*, and *94C1-OE* plants sprayed with mock (0.01% ethanol in water) or 50 μM 12OH-JA-Ile for 72 h. Data represent mean ± SD of 6 biological replicates. Different letters above bar graphs indicate significant differences ($p < 0.05$) as determined by Student's *t* test.

Thus far, we have mainly used pharmacological approach to examine the effects of 12OH-JA-Ile. To seek more *in vivo* evidence that endogenously generated 12OH-JA-Ile could play physiological role in plants, genetic approaches were employed. The double T-DNA insertion mutant, *ill6iar3*, was reported to be blocked in hydrolysis of 12OH-JA-Ile to 12OH-JA, hence the

mutant lines overaccumulate 12OH-JA-Ile in their wounded tissues (Zhang et al., 2016). Along with 12OH-JA-Ile, JA-Ile levels are altered in *ill6iar3* mutants because ILL6 and IAR3 also use JA-Ile as substrate (Figure 3.7.A) (Bhosale et al., 2013; Weidmann et al., 2013; Zhang et al., 2016). However, 12OH-JA-Ile increase is far more dramatic (>3.7 fold WT) than that of JA-Ile (<1.3 fold WT) in wounded *ill6iar3* (Zhang et al., 2016). Conversely, overexpression of either ILL6 or IAR3 results in depletion of 12OH-JA-Ile (Zhang et al., 2016). Alternatively, overexpression of CYP94C1 results in depletion of 12OH-JA-Ile by oxidizing it to 12COOH-JA-Ile (Aubert et al., 2015). First, we tested whether these mutations would change anthocyanin accumulation patterns in response to exogenous 12OH-JA-Ile treatment. Figure 3.7.B shows that exogenous 12OH-JA-Ile treatment raised anthocyanin levels in all genotypes but the degree of increase was higher with *ill6iar3* plants and was lower in lines overexpressing CYP94C1 (*94C1-OE*) and, to a lesser extent, in lines overexpressing ILL6 (*ILL6-OE*) compared to WT. These patterns matched the expected metabolism of 12OH-JA-Ile in those lines.

Next, wounding instead of exogenous compound treatment was used as a means to elicit anthocyanin production in plants. In addition to anthocyanin measurements, plant weight gain (or inhibition) was assessed as an additional JA-dependent wound response phenotype. Both effects of wounding are in large part controlled by JA pathway (Yan et al., 2007; Zhang and Turner, 2008; Shan et al., 2009; Poudel et al., 2016). To control for the variations between independent experiments, WT and mutant lines were always treated side-by-side. Wounding

elicited anthocyanin accumulation in WT plants (Figure 3.8. A, C, and E). However, the induction levels were significantly ($p < 0.05$) higher in *ill6iar3* and were lower in *ILL6-OE* and *94C1-OE*. The degree of effect was less pronounced with wound-induced inhibition of plant growth but the pattern seen with the anthocyanin was conserved also with the growth inhibition phenotype, i.e., *ill6iar3* was more inhibited while *ILL6-OE and 94C1-OE* were less inhibited in their growth compared to WT. These data shows that de-regulation of 12OH-JA-Ile levels affect the two wound responses and further support the *in vivo* action of 12OH-JA-Ile in JA-dependent wound signaling.

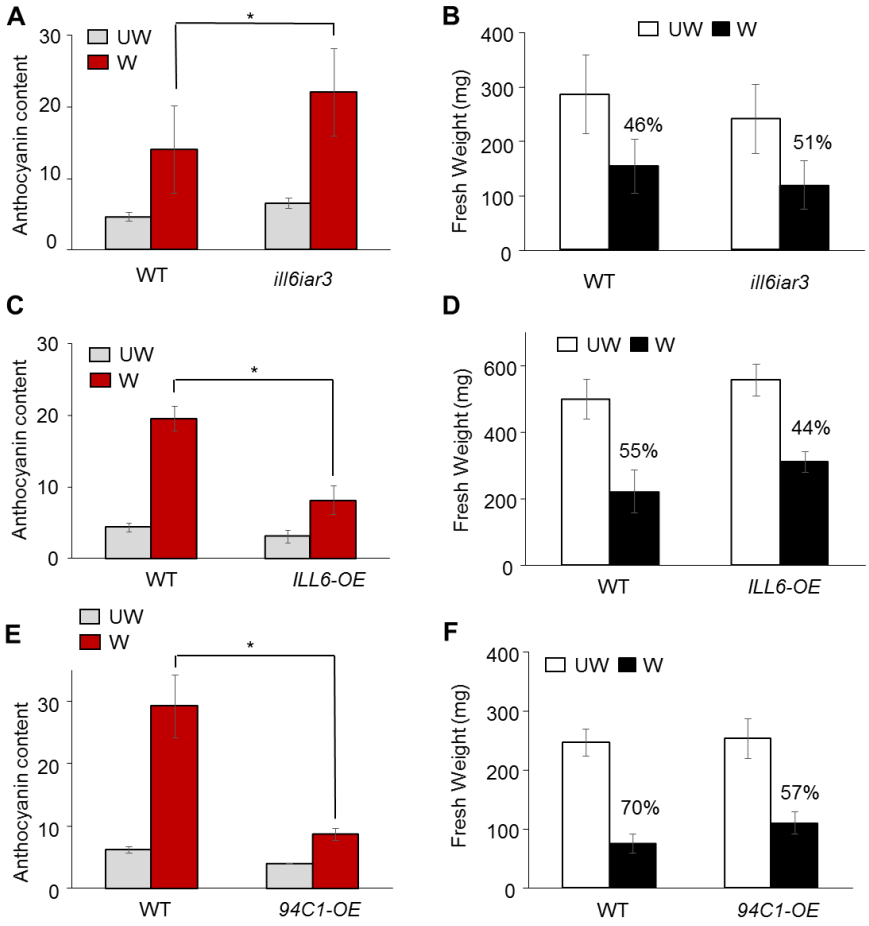

Figure 3.8. Impacts of genetic manipulation changing 12OH-JA-Ile metabolism on JA-dependent wound responses. (A, C, E) Anthocyanin content in wounded and unwounded WT, homozygous double knock-out mutant, *ill6iar3,* and transgenic lines overexpressing *ILL6* (*ILL6-OE)* or *CYP94C1*(*94C1-OE*). Asterisks denote significant differences at $p < 0.05$ (Student's *t* test). (B, D, F) Plant mass (fresh weights in mg) of wounded and unwounded WT, *ill6iar3, ILL6-OE*, and *94C1-OE*. Percent weight changes compared to unwounded plants are displayed above each wounded genotypes. Data represent average ± SD of 6 and 14-17 number of individual plant replicates for anthocyanin and plant fresh mass, respectively.

4. Discussion

In this study we explored the bioactivity of 12OH-JA-Ile on plants' physiological processes. 12OH-JA-Ile is synthesized by 12-hydroxylation of JA-Ile by CYP94 clade P450 enzymes and has been considered only as a catabolic intermediate of JA-Ile. However, the results showed that 12OH-JA-Ile mimics the bioactivity of JA-Ile in many ways including, anthocyanin accumulation, trichome biogenesis, JA-Ile responsive marker gene expression, and specialized metabolite biosynthesis. This and the relatively high concentration of 12OH-JA-Ile (at least as high as or higher than JA-Ile in damaged tissues) together raise the possibility that 12OH-JA-Ile might actually have a role as a *bona fide* signal in processes that have only been attributed to the function of JA-Ile.

The idea that metabolic derivative of a hormone retaining signaling activities of the major active form is not entirely new. For example, a catabolite of the plant hormone abscisic acid (ABA), phaseic acid (PA), was shown to serve an

ABA-like hormonal function (Weng et al., 2016). In this case, PA was perceived by a subset of PYR/PYL/RCAR family members of ABA receptors which was viewed as a functional diversification of the ABA receptor family co-evolving with hormonal metabolism to further improve plants' adaptive plasticity (Weng et al., 2016). Analogous to PA, 12OH-JA-Ile induced molecular and physiological effects that mostly overlapped with that of JA-Ile even though some signs of deviation were detected, e.g., a subset of transcripts and metabolites were uniquely affected by 12OH-JA-Ile. A major difference between ABA and JA in this context is that unlike ABA, where there are at least 14 PYR/PYL/RCR family members serving as soluble receptors for ABA with varying ligand binding properties (Ma et al., 2009; Park et al., 2009) there has not been any evidence of similar functional diversification for COI1. Multiple lines of evidence including the data presented in this paper such as the loss of anthocyanin and trichrome inducing activities of JA-Ile or transcriptional blockage of JA-Ile responsive marker genes in *coi1* mutant is consistent with COI1 being the sole receptor for JA-Ile in Arabidopsis. However, the fact that there are over 600 F-box proteins in Arabidopsis (Xu et al., 2009) combined with the fact that there are 13 JAZ proteins (Thireault et al., 2015) that form co-receptor complexes with COI1 cautions one from denying all possibilities for future expansion of the F-box-JA metabolite-JAZ complex repertoire. It will be interesting to study whether such process may already be taking place in other plant species. 12OH-JA-Ile induced anthocyanin in two other species, tomato and sorghum (Figure 3.6), indicated cross-species conservation of the 12OH-JA-Ile perception and signaling system.

However as for 12OH-JA-Ile, the resemblance between the phenotypes induced by 12OH-JA-Ile and JA-Ile together with the elimination of such effects by the *coi1* mutation, indicate that 12OH-JA-Ile signals through COI1. Same was true for tomato wherein, 12OH-JA-Ile activity was similarly blocked by tomato version of Arabidopsis *coi1* mutation. The physical interaction between 12OH-JA-Ile and COI1-JAZ co-complex shown earlier by *in vitro* protein pull-down experiment further supports the notion that 12OH-JA-Ile signals the same way as JA-Ile does through direct complex formation with COI1-JAZ (Koo et al., 2011). In the earlier interaction study (Koo et al., 2011), more attention was given to the reduced activity of 12OH-JA-Ile compared to JA-Ile which was consistent with the discovery that CYP94B3 is an enzyme that catalyzes the first step towards inactivation of JA-Ile signal. However, it was clear even from that study that 12OH-JA-Ile did retain the ability to promote the JAZ-12OH-JA-Ile-COI1 ternary complex. Later it was also found that further oxidation of 12OH-JA-Ile to 12COOH-JA-Ile completely abolished the co-receptor complex formation (Koo et al., 2014). Consistently, exogenous treatment of Arabidopsis seedlings with 12COOH-JA-Ile did not induce any sign of anthocyanin accumulation (data not shown).

The resolved crystal structure of COI1 bound to JA-Ile and the JAZ degron (a conserved sequence motif in JAZ that directly interacts with and traps JA-Ile in the ligand-binding pocket in COI1) showed that the pentenyl side chain of JA-Ile is packed in the hydrophobic cavity in COI1 formed by five hydrophobic amino acid residues (Sheard et al., 2010). Mutation in one of these residues, A86, to

bulkier side chains (such as Ile) were shown to cause enough steric clash to weaken the ligand binding (Zhang et al., 2015) indicating that there is not enough room to accommodate longer side-arms of JA-Ile such as that with the 12COOH-modification. Our preliminary modeling experiment results are consistent with 12OH- modification being small enough to be accommodated by the hydrophobic cavity (data not shown). These docking simulation studies obviously have their own limitations particularly when considering JAZ proteins are another part of the equation. Based on the crystal structure, the pentenyl side chain of JA-Ile does not directly touch JAZ residues but making it bulkier could indirectly affect other parts of the 12OH-JA-Ile molecule that directly interface with JAZ residues, such as the keto group or the carboxyl group of JA-Ile that coordinates with Ala204 and Arg206 of JAZ, respectively (Sheard et al., 2010).

The weaker interaction between 12OH-JA-Ile and COI1-JAZ is consistent with smaller number of genes that were transcriptionally activated by 12OH-JA-Ile compared to JA-Ile. The degree to which gene expression was induced by 12OH-JA-Ile was also markedly smaller in magnitude than that by JA-Ile as was verified by both qRT-PCR and RNA-seq analyses (Figures 3.3 and 4). Based on this observation it appears to be reasonable to conclude that 12OH-JA-Ile is a weaker signal *per se* than JA-Ile. Given this, it was surprising to observe that the anthocyanin and trichome promoting activity of 12OH-JA-Ile was equivalent to that of JA-Ile. This was also somewhat true for the metabolome where, an overall 11% of the metabolites were changed in abundance by 12OH-JA-Ile compared to 14% by JA-Ile. This indicates that there could be other factors besides receptor

binding affinity and gene transcription to compensate for the weaker activity to ultimately bring about comparable physiological outcomes. Relative abundance of the hormone ligand can be one such factor. More sustained accumulation of 12OH-JA-Ile compared to JA-Ile has been reported in wounded leaves (Koo et al., 2011; Heitz et al., 2012). Tissue- or cell-type specific distribution could also contribute to the specialization of the two hormone derivatives. Oxidized JAs elute earlier than JA or JA-Ile during the reverse phased liquid chromatography due to their increased polarity. 12OH-JA and 12COOH-JA-Ile were overrepresented in the midveins compared to the whole leaf different from JA or JA-Ile and their polarity may have contributed to this differential occurrence (Glauser et al, 2008). At the subcellular level, there could also be variable partitioning among different organellor compartments. Upon synthesis in the peroxisomes, JA is conjugated with -Ile in the cytosol. However, CYP94B3 and CYP94C1, and the amidohydrolases, ILL6 and IAR3, were all shown to be localized to the ER (Koo et al., 2014; Zhang et al., 2016). It is unclear whether difference may exist between JA-Ile and 12OH-JA-Ile regarding their entry into the nucleus and hence access to the COI1-JAZ receptor complex. JA-Ile transport across the nuclear envelope is mediated by a JA transporter (JAT1) (Li et al., 2017). Substrate specificity of JAT1 for 12OH-JA-Ile is unknown but based on its additional function as an efflux carrier of JA at the plasma membrane it appears that JAT1 has broad specificity. Since 12OH-JA-Ile does induce JA-Ile-like phenotypes through COI1, it is clear that 12OH-JA-Ile is entering the nucleus. In addition to JAT1, other multifunctional transporters exist that could

potentially contribute to the 12OH-JA-Ile nuclear entry (Nguyen et al., 2017). On the other hand, exclusion of 12OH-JA-Ile by transporters may partly explain weaker-than-JA-Ile effects of 12OH-JA-Ile.

Alteration of 12OH-JA-Ile levels by genetic means provided wound induced growth and anthocyanin data that are consistent with *in vivo* role of 12OH-JA-Ile in JA signaling. Building the 12OH-JA-Ile pool by blocking its hydrolysis in the *ill6iar3* mutant led to an increase of anthocyanin either by wounding or by exogenous treatment of 12OH-JA-Ile. The same mutation is expected to also build up the JA-Ile pool due to overlapping substrate specificities of ILL6 and IAR3 enzymes for both substrates. However, the impact of the *ill6iar3* mutation on endogenous levels of JAs was much greater for 12OH-JA-Ile (> 3.7 fold WT) than for JA-Ile (<1.3 fold WT) (Zhang et al., 2016), making 12OH-JA-Ile being more likely reason behind the increased anthocyanin levels in the mutant (Figure 3.8). Overexpression of ILL6, on the other hand, was reported to have similar degree of impact on levels of JA-Ile and 12OH-JA-Ile (Zhang et al., 2016), making it difficult to conclude depletion of which of the two compounds is responsible for decreased anthocyanin levels in *ILL6-OE* lines (Figure 3.8). However, similar decrease in anthocyanin was observed in lines overexpressing the *CYP94C1* whose main substrate is 12OH-JA-Ile (Heitz et al., 2012; Poudel et al., 2016). This further supports the endogenous role of 12OH-JA-Ile in wound response.

Despite the JA-Ile-like activities of 12OH-JA-Ile, overwhelming evidence shows that JA-Ile is still the major receptor-active ligand and that the 12-

hydroxylation of JA-Ile is a major passage way for catabolism of JA-Ile. That said, one of the problems that needs to be resolved is the unusual phenotypes displayed by the double loss-of-function mutant *cyp94b1cyp94b3* that is blocked in the 12-hydroxylation step leading to overaccumulation of JA-Ile (3-4 fold of WT) at the expense of 12OH-JA-Ile (< 5% WT) (Koo et al., 2014; Poudel et al., 2016). Characterization of this mutant showed that, despite increased JA-Ile, wounded *cyp94b1cyp94b3* plants displayed phenotypes reminiscent of JA-Ile deficient mutants such as reduced growth inhibition, reduced anthocyanin and defense metabolite accumulation, decrease in trichome number, and increased susceptibility insect herbivory. The mutant responded normally to exogenously applied JA indicating that the JA perception and signaling system is not disrupted. One could hypothesize that depletion of 12OH-JA-Ile is the cause of the various phenotypes but this radical idea is unlikely to be true given the firmly established function of JA-Ile as the major receptor ligand as discussed earlier. Significantly stronger transcriptional response induced by JA-Ile compared to 12OH-JA-Ile (Figure 3.3 and 3.4) is also consistent with such conclusion. Clearly these questions highlight the gaps in our understanding of JA metabolism and signaling.

CHAPTER IV: Novel gain-of-function mutant screen for new genes in the JA metabolic pathway: Characterization of *UGT86A1* and *UGT86A2*

ABSTRACT

In planta overexpression of genes has been widely used in conjunction with loss-of-function mutations to study gene function. In this chapter, a screening strategy inspired by observed JA-resistant phenotypes in most transgenic lines overexpressing negative regulators of the JA pathway genes was used to screen for novel genes in the jasmonate (JA) metabolic pathway. A mutant population generated by Ichikawa and colleagues (2006), randomly expressing full-length Arabidopsis cDNAs was screened for resistance to JA-inhibited root elongation and altered JA profile. Twenty two candidates were selected and the identity of cDNAs potentially responsible for the phenotypes in 10 candidates were determined by PCR and sequencing. A candidate gene encoding UDP-glucosyltransferase *86A1* (*UGT86A1*) and its close homolog *UGT86A2* were further characterized. Transgenic lines overexpressing *UGT86A1* or *UGT86A2* displayed reduced jasmonoyl-isoleucine (JA-Ile) and increased 12-*O*-glucosyl-jasmonic acid (12-*O*-Glc-JA) levels in wounded leaves. Single T-DNA insertion mutants, *ugt86a1* and *ugt86a2*, however, did not show the converse JA profiles compared to the overexpressing lines possibly due to the functional

redundancies of the two genes. In a preliminary *in vitro* enzyme assay, purified GST-fusion proteins of UGT86A1 and UGT86A2 failed to show clear glucosyltransferase activities.

1. Introduction

Plant hormone jasmonate (JA) plays important role in the regulation of plant growth and defense responses. JA is induced by tissue injury inflicted by mechanical wounding, herbivory, or necrotrophic fungal pathogens. Jasmonic acid is activated into an amino acid conjugate form by an acyl-amido synthase, JAR1 to yield JA-Ile (Staswick et al., 2002), which then is perceived by the co-receptor complex, CORONATINE INSENSITIVE 1 (COI1)-JASMONATE ZIM DOMAIN (JAZ), to induce genome wide transcriptional changes (Xie et al., 1998; Kastir et al., 2008; Fonseca et al., 2009).

Plants JA-Ile level drops after few hours of induction indicating its metabolic turnover which is understood as an effort to stop the constant activation of the costly defense traits which can have negative impact on plant growth. Some of the JA turnover pathways discovered in recent years includes cytochrome P450 (CYP) 94B1, 94B3, and 94C1 in the so-called ω-oxidation pathway that catalyze oxidation of JA-Ile to 12OH-JA-Ile and 12COOH-JA-Ile (Koo et al., 2011, Kitaoka et al., 2011; Koo et al., 2014; Heitz et al., 2012). JA-Ile is also hydrolyzed by amidohydrolases, ILL6 and IAR3, into jasmonic acid and –Ile which constitutes a second turnover pathway named as hydrolytic turnover pathway (Woldermariam et al., 2012; Bhosale et al., 2013; Widemann et al.,

2013; Zhang et al., 2016). Other metabolites of JA existing in plants include methyl-JA (MeJA), hydroxy-JA (12-OH-JA), 12-*O*-glucosyl JA (12-*O*-Glc-JA), 12-hydroxysulfate-JA (12HSO_4-JA), and 12HSO_4-JA-Ile (Seo et al., 2001; Miersh et al., 2007; Glauser et al., 2008; Heitz et al., 2012; Kitaoka et al., 2014; Koo et al., 2017). The enzymes that catalyze the formation of these metabolites are known for MeJA and 12OH-JA (Seo et al., 2001; Caarls et al., 2017; Smirnova et al., 2017) but others need to be discovered. Arabidopsis sulfotransferase ST2A was shown to have *in vitro* enzymatic activity to produce 12HSO_4-JA from 12OH-JA substrate but genetic evidence is yet to be provided (Gidda et al., 2003). Given many more derivatives reported to occur in nature, more metabolic pathways are expected (Sembdner and Parthier 1993; Wasternack 2007; Koo 2017)

Many discoveries in JA pathway have been through the forward genetic screening of loss-of-function mutant populations. For example, screening of ethyl methanesulfonate-mutagenized Arabidopsis seed population led to the identification of COI1, JAR1, and MYC2/JAI1/JIN1 (Feys et al., 1994; Staswick et al., 2002; Lorenzo et al., 2004). A T-DNA insertion mutagenesis-based reverse genetic approach has also been instrumental in identifying most of the remaining genes we know in the JA biosynthetic pathway. However, major drawbacks exist for loss-of-function mutant screening strategies, namely, the functional redundancy among enzymes that are encoded by a multigene family requires simultaneous deletion of multiple genes in order to show phenotypic changes (Alonso and Ecker, 2006). In addition, success of loss-of-function mutant screen for the most part depends on recessivity of the mutation, lowering the chance of

identifying gene function through phenotyping (Bouche and Bouchez et al., 2001). Use of dominant mutations has helped overcome some of the limitations related to genetic redundancy and recessiveness (Bolle et al., 2011). Activation tagging which uses the T-DNA fragment inserted together with a constitutive enhancer element such as *Cauliflower Mosaic Virus* (CaMV) 35S promoter into the plant genome has been widely used as a means to generate dominant mutations (Weigel et al., 2000; Nakazawa et al., 2003; Lu et al., 2014) although it has its own disadvantage of often times activating genes away from the insertion site making it difficult to track the gene responsible for the phenotype (Ichikawa et al., 2006). As an alternative strategy to create a gain-of-function population, cDNAs can be cloned into and introduced into plant germlines (LeClere and Bartel, 2001). Improving this further, Ichikawa and colleagues used a pool of sequence-verified full-length cDNA, in place of random cDNAs library to generate an Arabidopsis mutant population which they named the Full length cDNA OvereXpressor (FOX) gene hunting system (Ichikawa et al., 2006).

With the aim to identify new genes involved in JA metabolism, we took semi-forward gain-of-function mutant screening strategy using the FOX gene hunting system. It is called semi-forward or semi-targeted because although the initial screening of the mutant population is based on developmental and biochemical phenotypes, i.e., forward genetic screening, the identification of genes responsible does not rely on traditional map-based cloning. Instead, sequence elements in the vector carrying the cDNA potentially responsible for the gain-of-function phenotype can be identified through PCR-based cloning and

sequencing, hence, “targeted”. A second important rationale behind this genetic screen is that overexpression of negative regulators of the JA pathway will result in JA-resistance (or insensitive) phenotypes as has been observed in most if not all negative regulators in the JA pathway, including those involved in catabolism of JA. For example, overexpression of CYP94B1, CYP94B3, ILL6, and IAR3 all resulted in JA-insensitive phenotypes, such as longer roots on JA containing plates, down-regulation of JA-responsive marker genes, reduced fertility, and increased susceptibility to insect herbivory (Koo et al., 2011; Koo et al., 2014; Zhang et al., 2016). In addition, these transgenic lines had altered JA profiles which separates the gain-of-function symptoms acquired by overexpressing metabolic enzymes from that by overexpressing negative regulators of the JA signaling component, which only results in JA-insensitive phenotypes, but not the characteristic shifts in JA profile (Chini et al., 2007; Thines et al., 2007; Chung et al., 2010; Shyu et al., 2012). Our gain-of-function mutant screen also highlights the power of mass spectrometry-based semi-high throughput JA profiling methodology (Koo et al., 2014).

2. Materials and methods

2.1. Plant materials and growth condition

Columbia-0 was used as wild type (WT). Arabidopsis T1 FOX gene hunting system seeds were obtained from RIKEN institute Japan which comes as a tube with 400 seeds per tube representing 50 lines carrying 50 independent full-length cDNA (8 seeds per line in average). The screen was carried out in two

large batches each containing 20 seed pools (20 pools X 400 seeds = 8000 seeds; 2 batches X 8000 seeds = 160000 seeds). Together, these represent 2,000 independent cDNA expressing lines. Individual seeds were surface-sterilized with bleach and germinated in Murashige and Skoog medium (MS) (Caisson Inc.) containing 25 μM MeJA (Sigma Aldrich). The square plates were vertically positioned to measure root length. Each plate contained 12-15 seeds in two rows with 5 WT seeds in each row as a reference.

Seeds of T-DNA inserted lines *ugt86A1* (CS436685) and *ugt86A2* (SALK_014172C) seeds were obtained from the Arabidopsis Biological Resource Center. T-DNA *ugt86A1* lines were selected for antibiotic (sulphadiazine) resistance on plates. T-DNA presence and homozygosity was confirmed by both genomic DNA PCR and RT-PCR. Primers used in genomic DNA PCR screen for *ugt86A1* were 5' GGGCTACACTGAATTGGTAGCTC 3' 5' TGTTCGACGGAATGCCTGAG 3' and 5' GCTCATGGGCTTTTGCTTAG 3' 5' TGTTCGACGGAATGCCTGAG 3'. That for *ugt86A2* genomic DNA PCR screens were 5' ATTTTGCCGATTTCGGAA 3' 5' CTAATCGACTACATTCCCGGAG 3' and 5' CTAATCGACTACATTCCCGGAG 3' 5' GTCTAAGGTTGGTTTATCTAATGGGAAAGCTTAA 3'. Primers used for RT-PCR to verify absence of transcripts were 5' GCTCATGGGCTTTTGCTTAG3' and 5' TTAGTTTGATGGACTTATTTCTAGTCC 3' for *UGT86A1* gene and for 5' CTAATCGACTACATTCCCGGAG 3' and 5' GTCTAAGGTTGGTTTATCTAATGGGAAAGCTTAA 3' for *UGT86A2* genes. Plants were grown in chambers maintained at 22 °C, long-day (16 hours light)

photoperiod and 100-120 $\mu Em^{-1}s^{-1}$ light intensity. Wounding treatment was given on fully expanded rosette leaves of 24-30-d old soil-grown plants by crushing across the midrib with a pair of hemostats with serrated-tips (Herde et al., 2013).

2.2. Transgenic plants overexpressing *UGT86A1* and *UGT86A2*

Transgenic plants overexpressing *UGT86A1* (At2g3697) and *UGT86A2* (AT2G28080) were created by amplifying each open reading frame using Phusion Taq Polymerase (Thermo Scientific) with 5' CCTCGAGATGGAGAGAGCAAAGTCG 3' and 5' GCTCGAGTTAGTTTGATGGACTTATTTCTAGTCC 3' primers containing restriction enzyme digestion sites *Xho*1 for *UGT86A1* and 5' CGGATCCATGGCGGACGTTAGAAAC 3' and 5' GTCTAAGGTTGGTTTATCTAATGGGAAAGCTTAA 3' containing restriction enzyme digestion sites *BamH*1 and *Xho*1 respectively for *UGT86A2*. The amplified products were purified from agarose gels and cloned into pGEMT-easy vector (Promega) and were sequence verified for the presence of *UGT86A1* and *UGT86A2*. The inserts *UGT86A1* and *UGT86A2* were digested from the entry vector with the respective restriction enzymes following manufacturer's (New England Biolabs) instruction. Additionally, single restriction site digested *UGT86A1* was later treated with calf intestinal phosphatase (NEB) to reduce self-ligation of the vector. *UGT86A2* was digested with *BamH*1 and *Xho*1. The purified inserts were then cloned into pBITS (Schilmiller et al., 2007) vector with the kanamycin resistance gene which places the respective genes behind the

CaMV 35S promoter. Each construct was then transformed into Agrobacterium C58C1 strain. WT Arabidopsis plants were transformed with Agrobacterium harboring each construct using the floral dip method. T1 seeds were screened in Kanamycin containing plates and the resistant lines were grown in soil. Rosette leaves from all the resistant lines were collected for RNA extraction and subsequent gene expression analysis. Wounded leaves (4 h) were also collected for JA-Ile and 12-*O*-Glc-JA extraction.

2.3. DNA extraction and cloning for gain-of-function mutant identification

Tissues from selected lines were collected for DNA extraction using the cetyl trimethyl ammonium bromide (CTAB) method. Briefly, frozen tissues were ground using metal beads in a TissueLyzer II (QIAGEN). Warm CTAB containing fresh mercapto-ethanol was added to ground tissues were applied with and vortexed. After centrifugation, collected supernatant were further extracted with 24:1 chloroform/isoamyl alcohol. The subsequent supernatant was then treated with isopropanol to precipitate DNA. PCR amplification of the transgene used FOX primers 5’ CATTTATTCGGAGAGGTACGTAT 3’ and 5’ GGATTCAATCTTAAGAAACTTTATTGCCAA 3’ designed to flank the gene using Taq-Pro Red Complete (Denville) as a Taq polymerase. PCR amplification condition were as follows: initial one cycle of Taq-DNA-Polymerase activation for 5 min at 95 °C, followed by 39 cycles of 30 sec denaturation at 94 °C, annealing for 30 sec an annealing temperature of 49 °C and extension for 1 min sec at

72°C. PCR products were gel purified and cloned into pGEMT easy vector. The plasmid was sent for sequencing at the DNA core facility, University of Missouri.

2.4. Recombinant protein purification and *in vitro* glucosyl transferase assay

The inserts *UGT86A1* with single *Xho*1 restriction enzyme digestion site and *UGT86A2* with *BamH*I and *Xho*1 restriction sites were digested from the entry vector with the respective restriction enzymes following the manufacturer's (New England Biolabs) instruction. The digestion mixtures were separated on a gel and the inserts were gel-purified using a Gel purification kit (Qiagen). The single enzyme digested *UGT86A1* insert fragment was treated with calf intestinal phosphatase (NEB) to avoid self-ligation by dephosphorylation of 5' and 3' ends. The purified insert DNAs were ligated in pGEX-6p-1 (GE Healthcare) expression vector which places the glutathione-*S*-transferase (GST) at the N-terminus (N-Term) of the cloned genes. The constructs were then transformed into BL21 (DE3) competent cells (NEB). Positive colonies were cultured in liquid LB media overnight until OD600 reached 0.6 when the culture was induced with 0.357 μg of Isopropyl β-D-1-thiogalactopyranoside per mL of culture (1.5 μL/mL of 1mM IPTG) for 3 hours. Total uninduced and induced cells for SDS-PAGE were pelleted immediately, put into ice, mixed with SDS loading buffer, and heated in 100 ^{0}C for 10 min before loading onto the gel.

Protein purification was carried out using GST·Bind™ Kits (Novagen) following the manufacturer's instruction. Protein quantification was done using

Pierce BCA protein assay kit (Thermo Scientific) or by spectrophotometric methods (NanoDrop One Spectrophotometer, Thermo Scientific).

In vitro assay was designed to have three different 1.5, 2 and 2.5 μg concentrations of proteins. Reaction mixture consisted of the component as described previously by (Paul et al., 2011). Briefly, 100 mM Tris-HCl, pH 7.5, 5 mM UDP-Glucose, 0.5 mM aglycone, purified recombinant proteins and JA derivatives (JA-Ile, JA-Ile, 12OH-JA and 12OH-JA-Ile as substrates each 100 pM concentration) in a final volume of 50 μL. The reaction mixture was incubated for 1 hour at 28 ^{o}C. The reaction was stopped by adding 200 μL of 70% methanol containing dihydro-JA as internal standard for LC-MS analysis.

2.5. RNA extraction and gene expression analysis

RNA was extracted using TRIzol reagent (Invitrogen) following the method described by the company. Frozen leaf tissues were ground using metal beads in a TissueLyzer II (QIAGEN). Following the extraction, 1 μg total RNA was reverse transcribed using oligo(dT)$_{20}$ primers and Moloney Murine leukemia virus (M-MLV) reverse transcriptase (Promega). PCR using the cDNA as template was done using Taq-Pro Red Complete (Denville) on a CFX96 Touch^{TM} real-time PCR detection system (Bio-Rad) using primer sets 5'- GCTCATGGGCTTTTGCTTAG -3' and 5' GGACTAGAAATAAGTCCATCAAACTAA 3' for *UGT86A1* and 5' CTAATCGACTACATTCCCGGAG 3' and 5' TTAAGCTTTCCCATTAGATAAACCAACCTTAGAC 3'for *UGT86A2*. *ACTIN8* (At1G49240) gene was used as an internal reference gene.

2.6. JA quantification

JA metabolites were quantified using electrospray ionization tandem triple quadrupole mass spectrometer (Xevo TQ-S, Waters) interfaced with Ultra Performance Liquid Chromatography (UPLC) system (ACUITY H-class, Waters)-triple quadrupole tandem mass spectrometer (MS/MS) (Xevo T-QS, Waters) system as described previously (Koo et al., 2014; Zhang et al., 2016; Poudel et al., 2016). Leaf tissues weighing between 20-40 mg were grinded with metal beads in TissueLyser II (Quigen) and extracted with 200 µL methanol:water:acetic acid = 70:29:0.5 (v/v/v) solution containing dihydro-JA(dhJA) and [$^{13}C_6$]-JA-Ile as an internal standard. The grinded tissue with the extraction solvent was vortexed for 15 min and centrifuged twice at 18000 g speed for 20 min in 4 ^{o}C. Five µL of the resulting supernatant was injected into the UPLC system and separated on a UPLC BEH C18 column (1.7 µm, 2.1 × 50 mm; Waters) maintained at a 0.4 mL/min flow rate and 40 °C. The mobile phase consisted of 0.1% aqueous formic acid and methanol. MS transitions of *m/z*, 209 > 29 for JA, 211 > 59 for dhJA, 225 > 59 for 12OH-JA, 322 > 130 for JA-Ile, 328 > 136 for [$^{13}C_6$]-JA-Ile, 338 > 130 for 12OH-JA-Ile and 500 > 130 12-Glc-JA-Ile was used to detect the respective compounds. Data analysis was done using MassLynx 4.1 and TargetLynx software (Waters) and quantification was based on comparisons to standard curves and internal standards.

3. Results

3.1. Novel gain-of-function mutant screening strategy

With an aim to identify novel genes in the JA metabolic pathway, we carried out a genetic screen. The main idea was to screen for gain-of-function phenotypes that resembled those displayed by transgenic lines overexpressing other known JA metabolic enzymes. Overexpression of *CYP94B1*, *CYP94B3*, *ILL6,* and *IAR3* resulted in the classical JA-resistance phenotypes such as longer-than-WT roots on JA containing media and reduced fertility along with characteristic changes in JA metabolite profile (Koo et al., 2011; Koo et al., 2014; Zhang et al., 2016). These symptoms are caused by increased catabolism of bioactive JA-Ile in lines harboring the transgene. If these dominant symptoms can be exploited in genetic screen of a mutant population randomly expressing full-length cDNAs, we might be able to find other enzymes in the JA metabolic pathway. Figure 4.1 illustrates the overall screening strategy including the number of seeds or lines selected in each step. The FOX gene hunting system was created by transforming Arabidopsis with a sequence-verified full-length cDNA library representing 2000 Arabidopsis genes (Ichikawa et al., 2006).

Figure 1. General work flow of the gain-of-function mutant screening for identification of genes involved in JA metabolism and signaling.

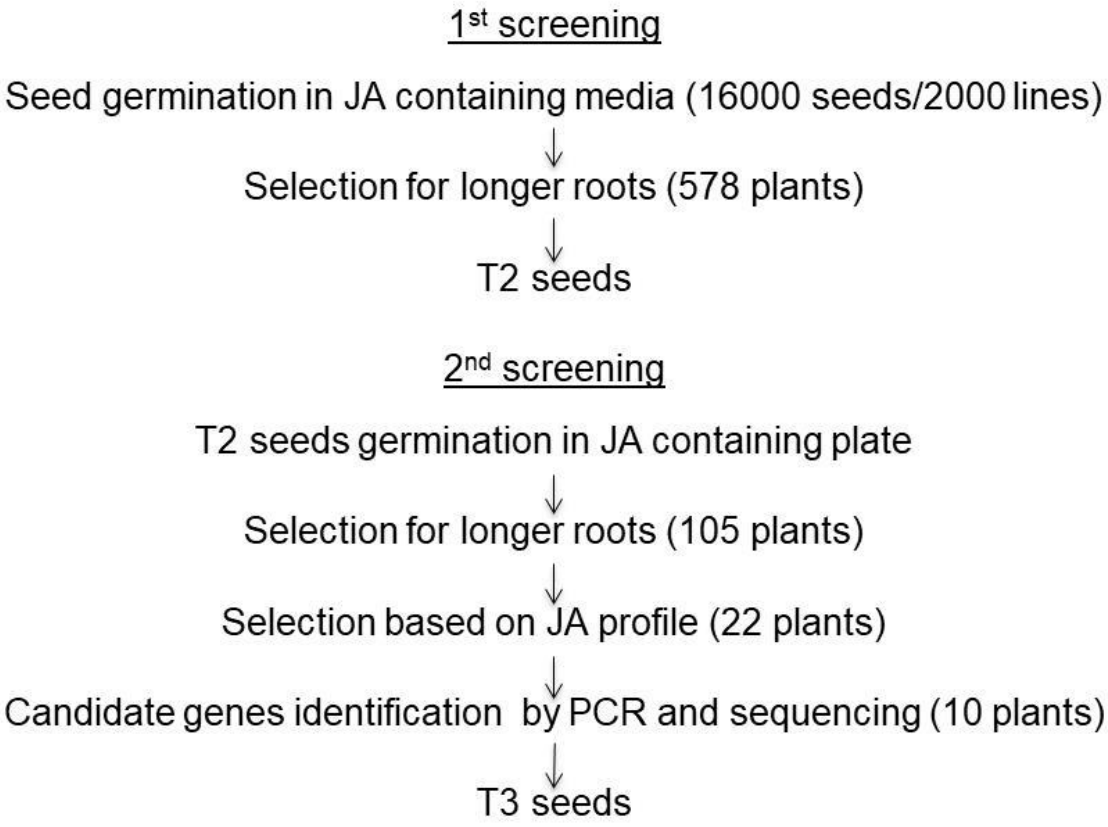

Individual 16,000 T1 seeds representing lines carrying 2,000 cDNA transgenes expressed under CaMV 35S promoter were grown vertically in a solid MS media plates containing 25 μM MeJA. Each plate contained small number of WT seedlings as reference. Among the 16000 seeds, 578 had longer roots than the WT. A less stringent criterion of 1.2 times longer compared to the WT was intended to capture as many candidates, including those with weaker phenotypes. Another reason for lowering the standard was to account for the poor germination observed with the T1 seeds (less than 50%) obtained from the

stock center. Because of the ambiguity created by germination problems, the root length screen was repeated with freshly harvested T2 seeds from the 578 selected T1 lines. Since the T1 lines were not homozygous and expected to segregate with regards to the putative transgene responsible for the phenotype, 15 seeds from each selected line were included in the second screen. As expected, not all the progeny had long roots, indicating that the phenotype is segregating. Average root length of 2-4 seedlings with longer roots was used for evaluation. Out of the 578 T1 lines that were re-screened, 105 passed the second screen with greater than 1.2 times longer root length than WT. Of the selected 105 lines, 2-3 plants per line, were transferred to soil and grown to maturity for JA profiling. Fully expanded rosette leaves were wounded by crushing across the midrib once with serrated-tip hemostats. A tissue sample was taken two hours after wounding and subjected to hormone extraction and analyses. Twenty two of the lines passed the screen with changed JA-Ile content.

3.2. Identification of the candidate genes from FOX screening

An advantage of this mutant screen over a conventional forward genetic screen is that the putative genes responsible for the dominant phenotypes can be readily identified using PCR-based cloning and subsequent sequencing. Primers specific to the pBIG211SF binary vector sequences flanking the full-length cDNA of the candidate genes were used for PCR amplification. In some cases, the PCR did not amplify a band while some lines produced more than one

PCR band. No band could be because of the false positive during screening for the root growth, while double PCR band is due to the insertion of more than one gene. Overall, 10 lines were selected as candidates with identified transgenes potentially contributing to the dominant phenotype. These lines are summarized in Table 1. There were some lines that displayed hypersensitivity to exogenous JA (i.e., shorter roots) that were pursued but were mostly eliminated from current discussion except for one line (21-10) that is shown in Table 1 as an example. Selected lines were named such that the first number represented the tube number where the T1 seeds came from; second number represented the selected T1 seedlings and third number represents the T2 progeny seedlings.

Table 1. Summary of candidates identified from the gain-of-function mutant screening.

	Line #	T1 Root length (fold over WT)	T2 Root length (fold over WT)^	T2 Root length in plain MS	JA-Ile content compared to WT	Gene	Annotation
1	**2-12-2**	1.5	1.8	1.2	half of WT	At2g25940	Vacuolar processing enzyme
2	**4-1-1**	1.8	1.5	1.0	same as WT	At5g50670	SPL13B
3	**4-4-1**	1.5	1.0	1.4	half of WT	At4g29500	Metallopeptidase
4	**5-15** **14-4**	1.5	1.4	1.3	half of WT	At1g79040	Photosystem II
5	**18-3-1** **24-16-1**	1.9	1.0	1.0	18-3: 3/4 WT 24-16: same as WT	At1g56580	Smaller with variable branches
6	**21-1-1**	1.2	1.2	1.0	half of WT	At2g36970	Glucosyl transferase
7	**21-10***	0.7	0.7	0.8	0.25 times higher than WT	At5g06370	Unknown protein/ Lead sensitive
8	**24-10-1**	1.8	1.5	1.0	1/8 of WT	At3g53620	Pyrophosphorylase
9	**28-14-2**	1.8	1.5	1.0	1/4 of WT	At4g16830	Hyaluronan RNA binding deubiquitinating enzymes
10	**31-8-2** **31-17-1**	1.7	1.4	31-8: 1.0 31-17: 1.2	0.25 times higher than WT	At3g51920	Calmodulin

One of the first genes identified through this approach was *JAZ10* (At5g13220), a negative regulator of JA signaling which was previously shown to

cause dominant JA-insensitive phenotypes in overexpressing plants (Chung and Howe, 2009). This candidate was eventually eliminated because it did not pass the criterion of altered JA profile (since it is not a metabolic gene). This, however, indicated that the screening approach was working as expected. Among the sequenced clones, a gene (At1g79040) annotated as “photosystem II” was repeatedly identified in 12 of the lines. Another gene (At3g53620) encoding pyrophosphorylase occurred in 6 lines. Among these, only the lines reduced in JA-Ile are included in the table. Photosystem II and pyrophosphorylase also co-amplified as an additional PCR bands along with other genes in some of the selected lines. Root length in T1 and T2 were not always consistent (Table 1) possibly due to the combined reasons of seed quality, transgene segregation, and experimental variations. However, six lines exhibited consistently longer roots, and they were lines 2-12-2 carrying vacuolar processing enzyme, 4-1-1 carrying metallopeptidase, 6-3-1 carrying protein phosphatase 2C, 21-1-1 carrying glucosyl transferase (*UGT86A1*), 24-10 carrying pyrophosphorylase, 28-14-2 carrying nuclear antigen homolog, 5-15 (and 14-4) photosystem II, and 24-10 carrying pyrophosphorylase (images of representative seedlings are shown in Figure 4.2). The hypersensitive line with shorter roots, line 21-10, was found to carry At5g06370 gene encoding an unknown protein which was later reported to have function in lead tolerance (Fan et al., 2016).

JA-Ile content in the selected lines is shown in Figure 4.3. JA-Ile content in 2-12-2 carrying vacuolar processing enzyme, 4-4-1 carrying metallopeptidase, 5-15 carrying Photosystem II, 18-3 carrying smaller with variable branches, 21-1-1

carrying UDP glucosyl transferase (UGT86A1), 28-14-1 carrying perinuclear and cytoplasmic mRNA binding proteins and 31-17-1 carrying calmodulin were reduced to less than half of the WT.

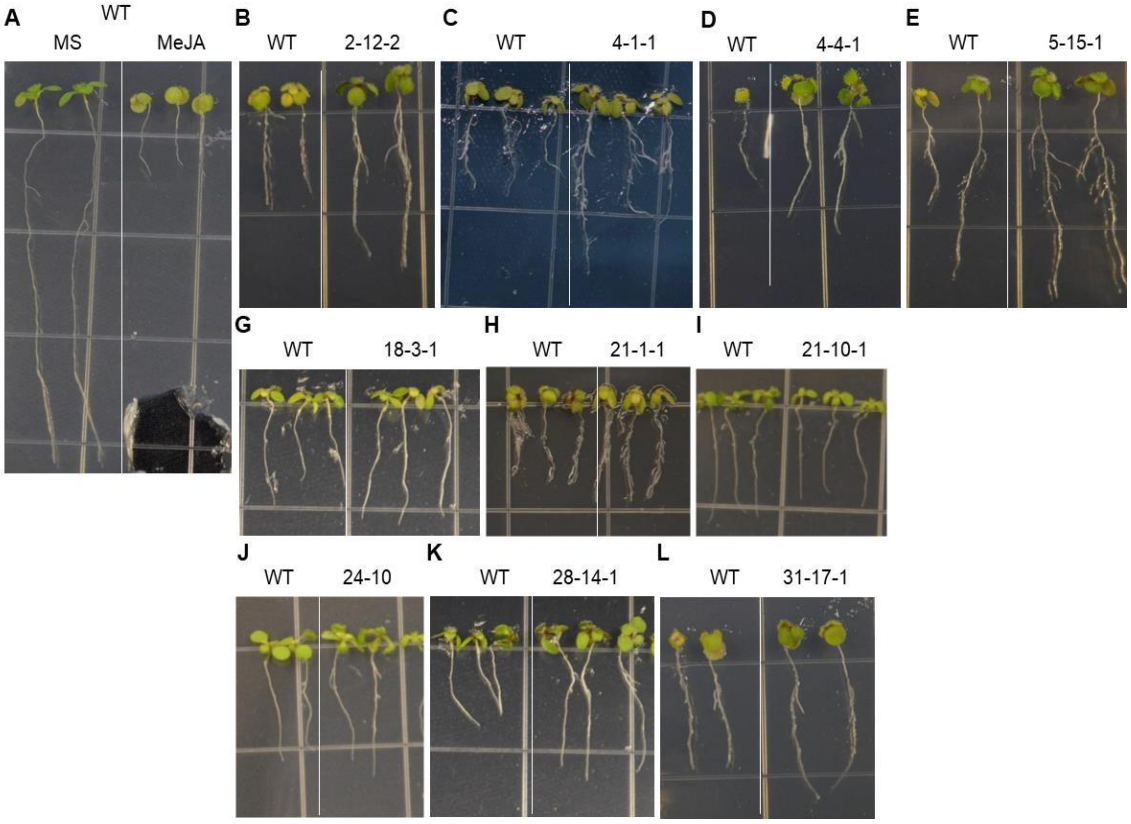

Figure 4.2. Root length screening results of the representative gain-of-function lines (T3). Seedlings were grown on MS plates with (B-L) or without (A, left) 25 μM MeJA for 11-14 days.

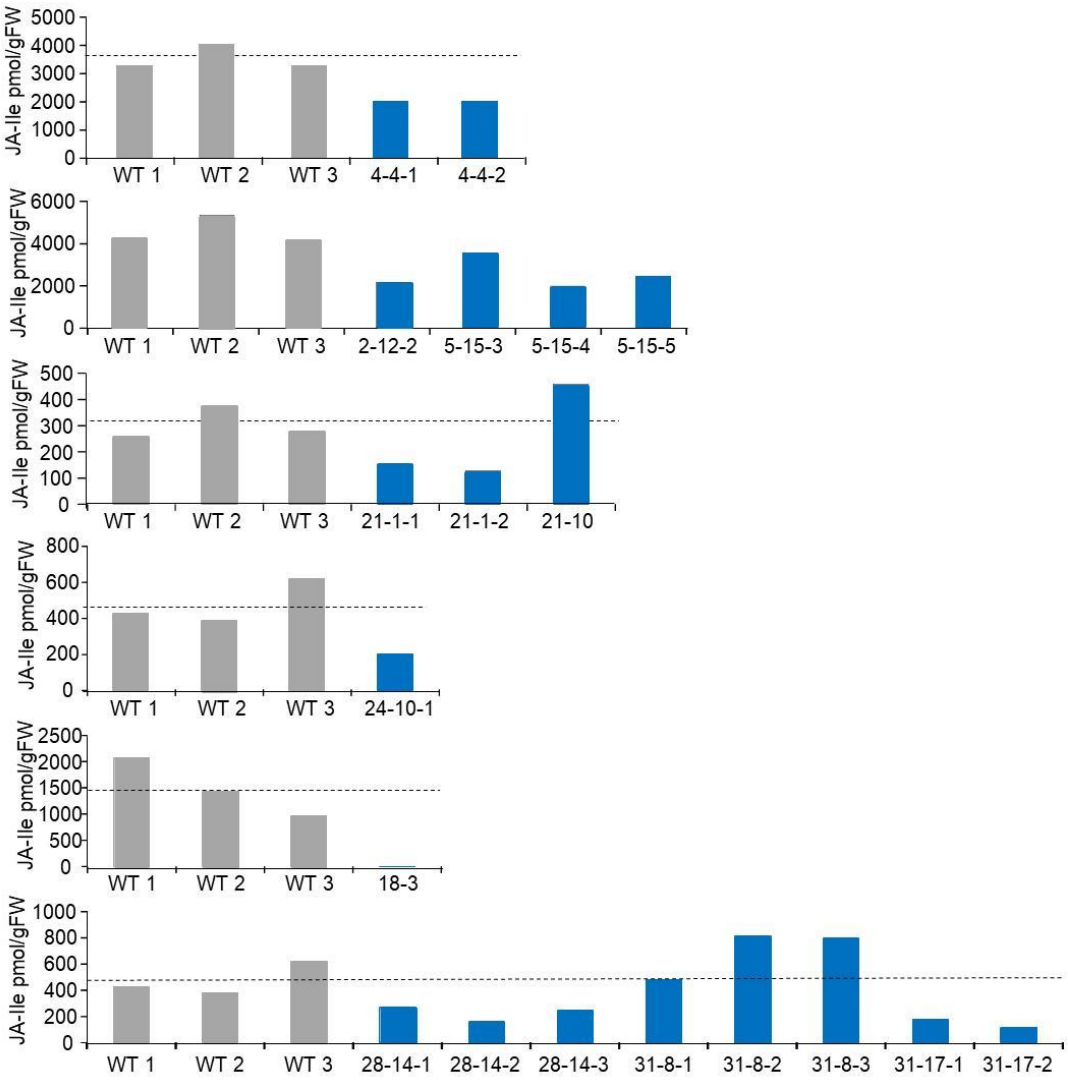

Figure 4.3. JA-Ile content in the wounded leaves of the selected candidates (T2). Wounding was performed by crushing the fully expanded rosette leaves once across the mid vein with a hemostat. Leaves were collected after 2 hours of wounding. JA-Ile content was determined using LC-MS/MS. Dashed lines represents the comparison of the JA-Ile level between WT controls and transgenic lines.

Among the candidate genes/proteins metallopeptidase (line 4-4-1) and UDP-glucosyl transferase (*UGT86A1*) (line 21-1-1) were the two with putative metabolic enzymatic functions. Of the two, *UGT86A1* was chosen for further

characterization. Interestingly, flowers of 21-1-1 lines displayed reduced fertility with many aborted siliques, a hallmark of JA-Ile deficient phenotype (Figure 4.4.B). However, leaves of this mutant also displayed curled phenotype which had been reported previously from plants overexpressing enzyme involved in auxin catabolism (Jin et al., 2013) (Figure 4.4.C).

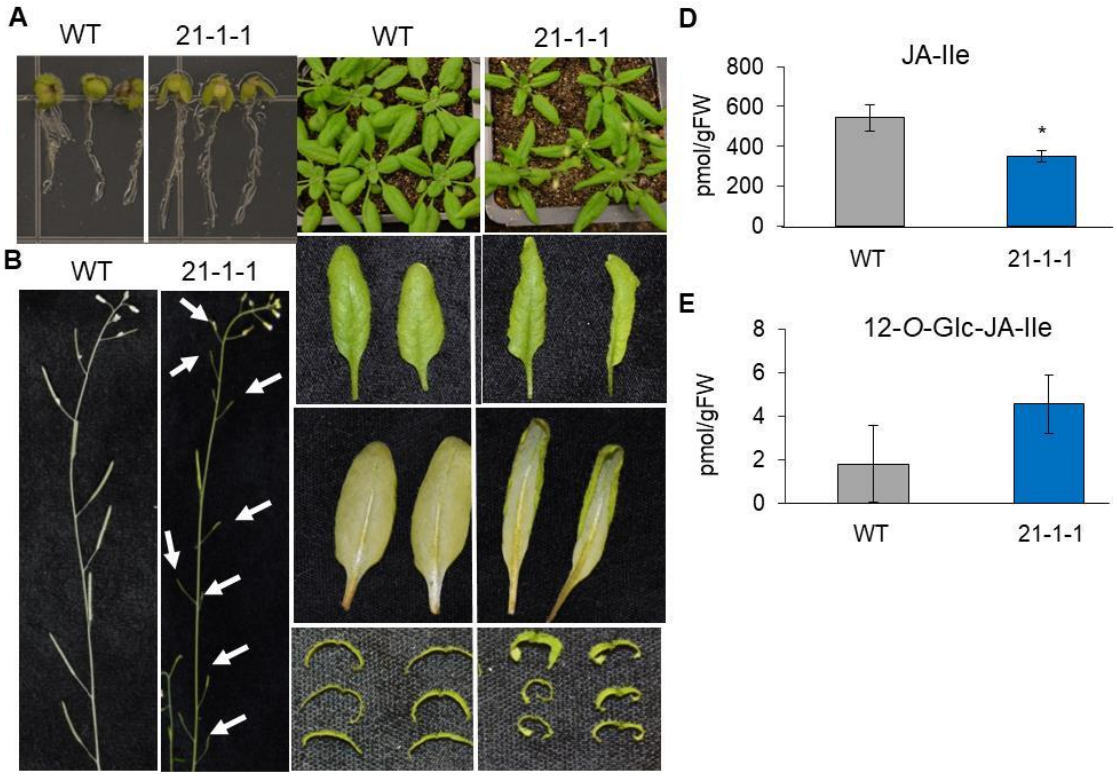

Figure 4.4. Developmental and biochemical phenotype of line 21-1-1 (T3). (A) Line 21-1-1 has slightly longer roots comparted to WT. Seedlings grown for 11 days on MS plate containing 25 µM MeJA. (B) Line 21-1-1 displays reduced fertility with aborted siliques (arrows). (C) Image showing curled leaves of line 21-1-1. (D and E) Line 21-1-1 has lower JA-Ile (C) and higher 12-*O*-Glc-JA-Ile (D) in wounded (2 h) leaves compared to WT. Each data point represents the mean ± SD of three biological replicates. The asterisk denotes a significant difference compared to WT based on the Student's *t* test ($P < 0.05$).

3.3. Characterization of *UGT86A1* and *UGT86A2* in JA metabolism

3.3.1. Ectopic expression of *UGT86A1* and *UGT86A2* in Arabidopsis

UGT86A1 identified from the gain-of-function screen was further characterized to confirm its involvement in JA metabolism. *UGT86A1* belonged to the group K consisting of two gene in Arabidopsis annotated as UDP-glucosyl transferases (Ross et al., 2001). Based on its putative function as a UGT, we hypothesized that the encoded protein may be involved in the synthesis of glucosyl-derivatives of JA. There was one other protein sequence, *UGT86A2* (AT2G28080), grouped together in the clade with 57% sequence identity with UGT86A1 at the protein level. Both *UGT86A1* and *UGT86A2* genes were independently cloned into a plant binary vector under controll of the constitutive *CaMV* 35S promoter and transformed into Arabidopsis. Primary screening of T1 seedlings yielded 21 and 23 kanamycin resistant lines for *UGT86A1* and *UGT86A2*, respectively (named, *UGT86A1-OE* and *UGT86A2-OE*). The resistant

lines were transferred to soil and analyzed for the expression of *UGT86A1* or *UGT86A2* by RT-PCR with *ACTIN8* as a control (Figure 4.5 and 4.6). Several lines displayed visibly increased transcript levels compared to three WT controls. All the 21 and 23 kanamycin resistant lines were analyzed for the JA-Ile and 12-*O*-Glc-JA content in their leaves after 4 hours of wounding. Several lines (*UGT86A1-OE* lines 5, 24, 27, 28 and *UGT86A2-OE* lines 7, 11, 15, 16, 33, 35, 42, 43) with increased gene transcript showed decreased JA-Ile content resembling the pattern displayed by line 21-1-1; however, there were also cases where no obvious correlation between transcript and JA-Ile levels was found (*UGT86A1-OE* lines 1, 18, 22 and *UGT86A2-OE* lines 10, 17, 34, 38, 39) (Figures 4.5A-B, 4.6A-B). There were also lines with increased 12-*O*-Glc-JA content but the transcript-hormone correlation was poor for *UGT86A1-OE* (Figure 4.5.A and C). More correlation was found for *UGT86A2-OE* lines with almost all lines with increased 12-*O*-Glc-JA contents having increased transcripts (Figure 4.6A and C).

Surprisingly, unlike FOX line 21-1-1 no clear defects in flower fertility was observed in any of the *UGT86A1-OE* or *UGT86A2-OE* lines. In addition, the curled leaf phenotypes observed in FOX line 21-1-1 (Figure 4.4.B) did not show in either of the lines. Root length of at least 20 seeds of potential T1 lines of *UGT86A1-OE* and *UGT86A2-OE* grown on MS media containing JA were similar to that of WT root length.

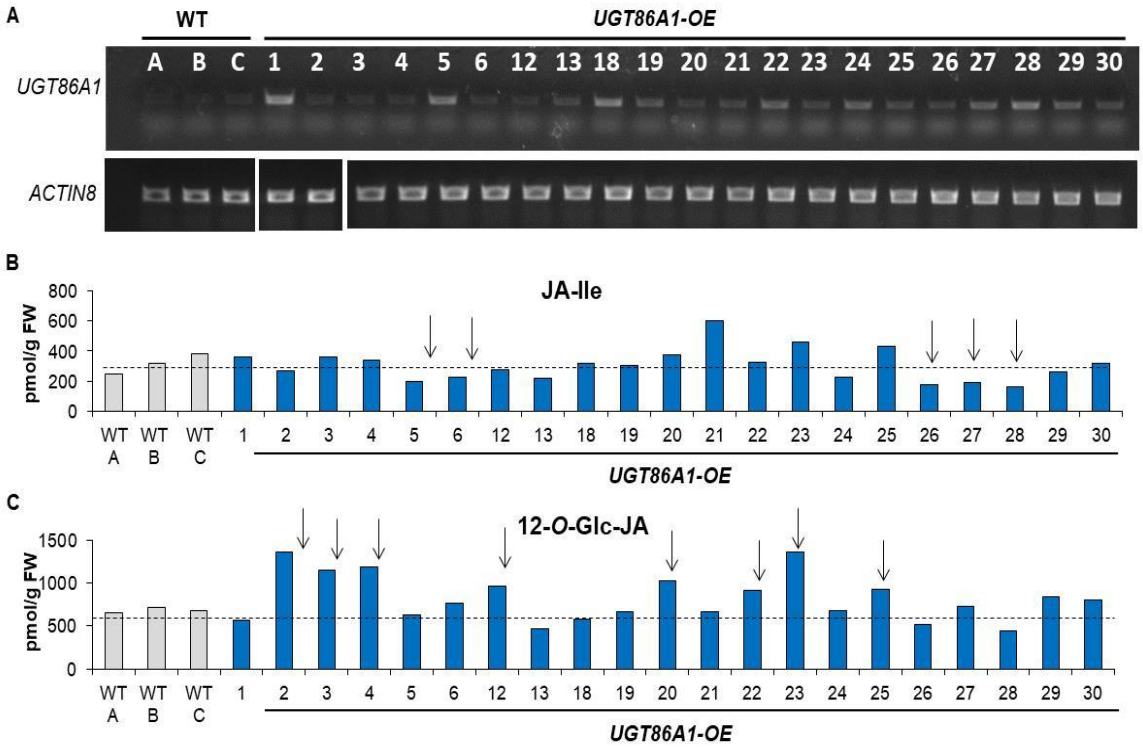

Figure 4.5. T1 screening of transgenic lines (*UGT86A1-OE*) overexpressing *UGT86A1.* (A) RT-PCR measuring transcript abundance of UGT86A1 in the leaves of WT and 21 independent antibiotics (kanamycin) resistant *UGT86A1-OE* lines. *ACTIN8* was used as an internal reference. (B) JA-Ile and (C) 12-*O*-Glc-JA content in the wounded (4 h) leaves of WT and *UGT86A1-OE*. Wounding was performed by crushing the fully expanded rosette leaves twice across the mid vein with a hemostat.

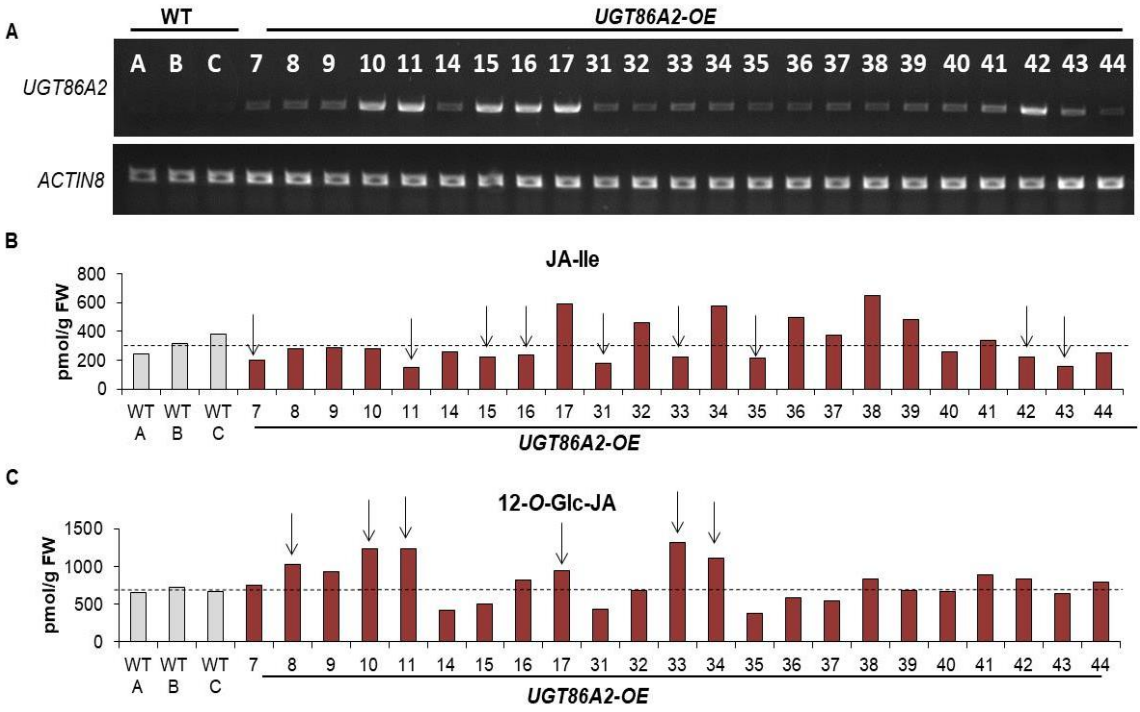

Figure 4.6. T1 screening of transgenic lines (*UGT86A2-OE*) overexpressing *UGT86A2*. (A) RT-PCR measuring transcript abundance of *UGT86A2* in the leaves of WT and 23 independent kanamycin resistant *UGT86A2-OE* lines. *ACTIN8* was used as an internal reference. (B) JA-Ile and (C) 12-*O*-Glc-JA content in the wounded (4 h) leaves of WT and *UGT86A2-OE*. Wounding was performed by crushing the fully expanded rosette leaves twice across the mid vein with a hemostat.

3.3.2. T-DNA insertion knock-outs *ugt86a1* and *ug86a2* display WT JA profile

In addition to overexpression, we also tested T-DNA insertion loss-of-function mutants, *ugt86a1* and *ugt86a2*. *ugt86A1* (CS436685) and *ugt86A2* (SALK_014172C) both have a T-DNA inserted in the second exon, which could be verified by genomic DNA PCR using T-DNA left border specific and gene specific primer pairs. Homozygous *ugt86a1* and *ugt86a2* insertion lines were

further confirmed by RT-PCR which showed no detectable transcripts (Figure 7A). Despite the disruption, hormone analysis on the wounded rosette leaves of knock out lines showed that neither JA-Ile nor 12-*O*-Glc-JA content was significantly altered in *ugt86a1* and *ugt86a2* compared to the WT (Figure 4.7.B and C). There was no change in JA-Ile and 12OH-JA-Ile level in the single knock outs possibly due to the functional redundancies between UGT86A1 and UGT86A2.

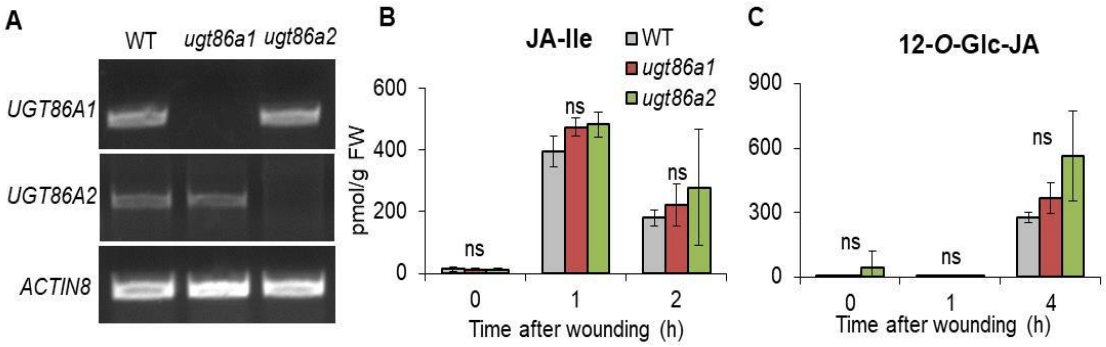

Figure 4.7. Molecular and biochemical characterization of the T-DNA insertion mutants *ugt86a1* and *ugt86a2*. (A) RT-PCR analyses showing the absence of *UGT86A1* or *UGT86A2* transcripts in the unwounded leaves of the *ugt86a1* or *ugt86a2*. (B) Time course of (A) JA-Ile and (B) 12-*O*-Glc-JA accumulation in the wounded leaves of WT, *ugt86a1* and *ugt86a2*. Leaves were wounded twice across the mid rib using a hemostat. Each data point is mean ± SD of three biological replicates.

3.3.3. *In vitro* enzymatic activity of *UGT86A1* and *UGT86A2*

Catalytic activities of UGT86A1 and UGT86A2 were tested using purified recombinant proteins. N-terminal fusions of GST-tagged UGT86A1 and UGT86A2 were expressed in *E. coli* (Figure 4.8). Addition of IPTG to the culture

induced a strong band at around 73 kDa which is smaller than the expected 79 and 80 kDa respectively for GST-fused UGT86A1 and UGT96A2. The smaller size of purified UGT in a SDS gel was also reported for GST-UGT74D1 (Jin et al., 2013). The same 73 kDa proteins were recovered after the purification with GST bind kit (Novagen). Pierce^{TM} BCA protein assay kit (Thermo Scientific) quantified protein concentration for GST-UGT86A1 was 107.9 μg/ml and GST-UGT86A2 was 78.2 μg/ml. For both proteins, the second elution among the three yielded the highest concentration. Three different protein concentrations were used for the *in vitro* UDP-glucosyl transferase assay. Typical reaction components published previously by others (von Saint Paul et al., 2011) were used except for the substrates JA, JA-Ile, 12OH-JA and 12OH-JA-Ile. After 1 h of incubation the reaction mixture was subject to LC-MS analysis for the detection of the presumed products, 12-*O*-Glc-JA. The preliminary assessment showed that there was no obvious increase in the glucosyl derivatives of JA.

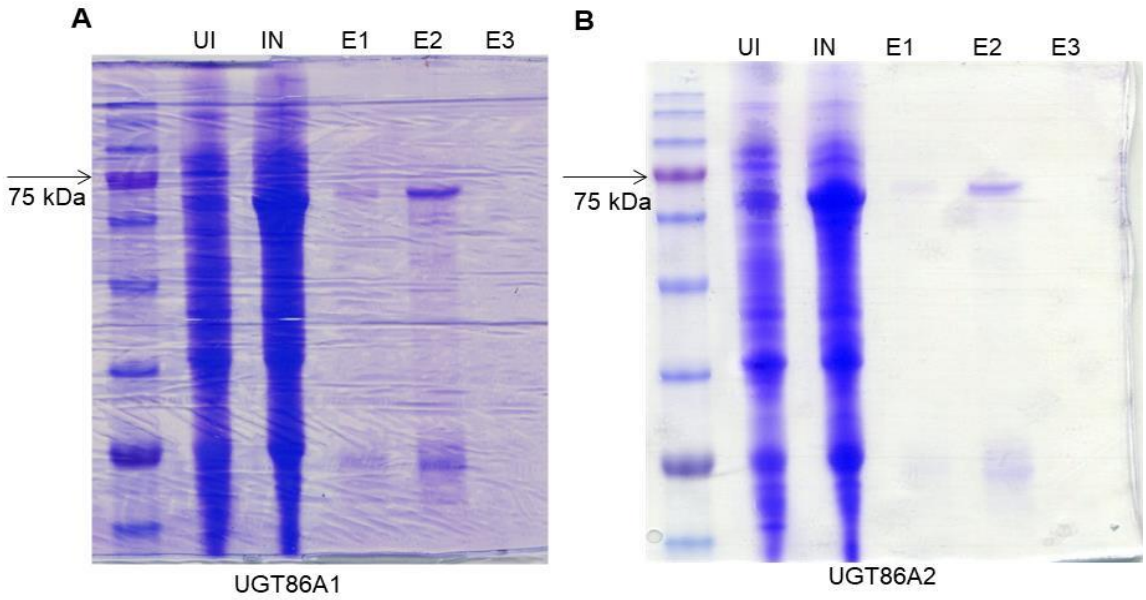

Figure 4.8. Protein purification of N-terminal GST-fused UGT86A1 and UGT86A2 expressed in *E. coli.* Coomassie Blue stain of SDS-PAGE gels containing indicated fractions of (A) GST-UGT86A1 and (B) GST-UGT86A2: UI - uninduced total, IN - induced total, and E - elution.

4. Discussion

Even though there has been success in recent years to identify the enzymes that catalyze JA catabolism, examination of higher order mutants blocked in those enzymes has indicated that there must be additional routes to remove excess JA from cells. We conducted a gain-of-function mutant screening strategy in pursuit of these undiscovered genes involved in JA turnover.

Gain of function mutation has been used to study the function of genes in including the study of JA metabolic enzymes (Yokotani et al., 2008; Sato et al., 2009; Koo et al., 2011; 2014; Zhang et al., 2016). Our screen was inspired by the consensus phenotypes displayed by plants overexpressing catabolic enzymes of

JA, namely, resistance to root growth inhibitory effects of exogenous JA and changes in JA profile. Transgenic plants overexpressing negative regulators in the JA signaling pathway, such as JAZ proteins which are transcriptional repressors, also results in the JA insensitive phenotypes, but can be distinguished from the effects of metabolic enzymes by measuring JA profile. Indeed, one of the first mutants isolated through the root elongation assay was later identified to carry the *JAZ10* gene. This mutant line did not survive subsequent steps of LC-MS based JA profiling. This example demonstrated that our screen scheme is working. However, despite this success, relatively few, (two out 10), gene candidates identified (Table 1) were annotated to encode metabolic enzymes (metallopeptidase and glucosyl transferase). It is unclear how the other eight genes might contribute to altered JA metabolism. It is possible that they are indirectly affecting the expression or activity of JA metabolic enzymes which remains to be determined. Considering the fact that there are about 30 known genes involved in JA metabolism out of 27,000 total protein encoding genes in Arabidopsis genome (TAIR, https://www.arabidopsis.org/) representing about 0.1%, 10 candidates out of 2,000 screened lines (0.5%) is relatively high, and thus, false positives are certainly expected among the selected candidates.

Some of the phenotypes may have been caused by loss-of-function mutations, in a rarer event where the T-DNA “landed” in open reading frame of a gene knocking out the gene function. Although the recessive mutation is less likely to be detected in the T1 screen, they may appear in the segregating T2 population. Inverse PCR may be used to map the surrounding sequences of the

candidate genes. An alternative reason for mismatch between predicted gene function and the mutant phenotype may be that there were extra insertions of more than one cDNA construct. The creators of the FOX lines (Ichikawa et al., 2006) reported an average of 2.7 independent insertion events per line. We have observed cases where PCR amplification using the vector specific primer results in more than one band on DNA gels. Backcrossing the candidate lines with WT will help further verify and clarify the responsible mutation for observed phenotypes. In the case of UGT86A1, we took an alternative approach. Instead of backcrossing and further characterizing the isolated mutant line, new transgenic lines overexpressing *UGT86A1* were created to see if the phenotypes could be replicated. Partial reproducibility of the phenotypes (e.g., reduced JA-Ile) indicated that overexpression of *UGT86A1* may not be the cause of all the phenotypes (e.g., reproductive failure, curled leaves, etc.) displayed by the line 21-1-1.

One of the unexpected complications we faced were variability in germination rates between the seeds which made it difficult to evaluate root length. In an ideal situation controls grown on plain media without JA can in part address the problem but in large scale mutant screening that is time consuming and costly. Most importantly, the mutant seeds with unknown identities cannot be divided into control and test groups. To minimize the problems, the root length screen was divided into two phases, an initial screen followed by a second screen of the progenies of the preselected lines. Since the transgenes are expected to segregate in the following generation, larger number of seeds had to

be examined which negatively impacted the efficiency. In addition, there is inherent variability in root growth on solid media plate caused by factors such as position in the growth chamber that affects light intensity and quality, etc.

One of the unique aspect of this genetic screen was using the LC-MS based JA metabolic profiling. No similar attempt has been reported to date. Significant improvement in LC-MS instrumentation and simplified hormone extraction protocols synergistically allowed semi-high throughput analysis a reality. However, variability still existed among hormone levels. This variability is not likely to be caused by the hormone quantification method rather caused by factors such as, variations in plant morphology or inconsistency in wounding. Ratio between undamaged and damaged tissue in a sample determines JA level if all other factors are constant. Variable leaf sizes interfere with consistent wounding to maintain similar undamaged: damaged cell ratios. The morphological variability may be the gain-of-function phenotype created by overexpression of the transgene but, in some cases, was introduced by accidents such as abiotic stress during transfer of seedlings from MS media plates to soil or infestation with pests in the growth chambers, etc. Careful repetition with proper controls (e.g., including plain media without JA as a negative control) and taking into consideration the above described issues is needed in the future characterization of the candidates. In addition, remainder of the FOX mutant population representing 10,000 cDNAs in total needs to be screened (only 2,000 lines have been screened so far).

In multiple occasions, the cloned transgene from candidate lines turned out to encode photosystem II (At1g79040) and pyro phosphorylase (At3g53620). While it may be possible that overexpression of these genes positively affect root growth, it is possible that these clones are overrepresented in the library used to transform Arabidopsis for creation of the mutant population. However, there is no clear logical explanation as to why that might have happened. Alternatively, the primers used to amplify the transgenes are non-specifically targeting those two genes. However, there is no clear homology between the primers used and the two genes. Besides, if that was the case, then those genes should be amplified in all PCR reaction but that was not the case. The possibility that those two genes have real effects on root growth can be tested by overexpressing those genes in plants. If confirmed, this may be interesting and perhaps can be exploited towards efforts to increase plant productivity. Future screening strategy should take into account the extra insertion and work to remove it by backcrossing with WT.

UGT86A1 was further characterized as a case study to demonstrate the utility of our screen in identifying genes involved in JA metabolism. UGTs catalyze the transfer of glucosyl group from the activated sugar donor UDP-glucose to small hydrophobic molecules (Ross et al., 2001). Examples of UGTs catalyzing biosynthesis of glycosylated forms of other plant hormone such as IAA (Tognetti, 2010; Tanaka et al., 2014), SA (Song et al., 2008), or ABA (Priest et al., 2005) have been discovered. Glucosyl-derivatives of JA are detected in Arabidopsis (Miersch et al., 2008) but the enzymes responsible for such

reactions have not been identified. Recently, maize *silkless* 1 (*sk1*) encoding glucosyltransferase gene was shown to function in JA metabolism (Hayward et al. 2016). Constitutive expression of the *sk1* gene resulted in complete feminization of all flowers, a gain-of-function phenotype caused by depleting JA. No direct UGT enzymatic activity of the protein encoded by the *sk1* gene has been shown. The subcellular localization of the SK1 protein in the peroxisome suggests its substrate to be either jasmonic acid or its precursors in the peroxisome. The Arabidopsis gene with closest sequence homology to the *sk1* gene is *UGT82A1* (At3g22250), the sole member in the subclade. However, UGT82A1 is not predicted to be targeted to the peroxisome. UGT82A1 should be characterized in the future.

Ectopic expression of UGT86A1 and its closet homolog UGT86A2 in Arabidopsis resulted in changes in JA profile. Reduction of JA-Ile levels in the wounded leaves of several independent lines is consistent with reduced JA-Ile levels in the FOX line 21-1-1. This change in JA-Ile profile did not match 100% with the transgene transcript abundance. However, mismatch between transgene expression vs phenotype has been observed even with the genes with known function. The selected T1 lines should be tested in their subsequent T2 generation for reproducibility of the observed biochemical phenotypes. Correlation between glucosyl-derivative of JA and transgene expression was more evident with the *UGT86A2-OE* plants. As mentioned earlier, some of the classical JA-deficient phenotypes such as fertility defects were not clear. Root length inhibition assay is yet to be tested for the selected positive lines. In

addition to the possibility mentioned earlier regarding the additional insertion event of yet another transgene besides *UGT86A1* or the T-DNA insertion event that caused knock-out of an endogenous gene responsible for the phenotypes observed in FOX lines 21-1-1, it is also possible that the expression level of UGT86A1 may be different between *UGT86A1-OE* and FOX 21-1-1. This needs to be tested in plants grown side-by-side in the future. Another possibility is that since glucosylation of JA or 12OH-JA is further downstream in the JA metabolic pathway, it is only having a minor impact on the bioactive JA-Ile levels. It has been reported in the past in the case of mutation in JAR1 enzyme that up to 90% reduction in JA-Ile level may not impact flowering or wound induced JA-Ile-responsive marker gene expression. Based on this, 50% reduction in JA-Ile is unlikely to cause floral defects and the floral defect observed in FOX 21-1-1 may be caused by a separate reason. If UGT86A1 function in JA metabolism is confirmed, this would showcase the power of high throughput LC-MS metabolic profiling as means to identify biochemical mutants that often fail to display visible developmental phenotypes.

Homozygous single T-DNA knockout mutants, *ugt86a1* and *ugt86a2*, failed to alter both JA-Ile and 12-*O*-Glc-JA levels. This result of no change in JA-Ile and 12OH-JA-Ile level in the single knock outs may be due to the functional redundancies between UGT86A1 and UGT86A2. To overcome the potential functional redundancy double homozygous mutant should be created in the future. However, it may be difficult to achieve that goal through genetic crossing between the single mutant lines because the two genes, *UGT86A1* and

UGT86A2, are located very close to each other in the same chromosome with only 8890 base pairs in between. Other gene knock out techniques such as RNA interference (RNAi) or genome editing techniques such as Clustered Regularly Interspaced Short Palindromic Repeats (CRISPR)/CRISPR-associated system 9 (Cas9) may be used in combination with the existing knock-out mutants.

To test *in vitro* glucosyl transferase activity, GST-fusion proteins of UGT86A1 and UGT86A2 were produced in bacteria. Data (Figure 8) demonstrated that such effort was successful. Unfortunately, *in vitro* catalytic activity was not readily detectable. However, the data is still preliminary and lack critical controls. Data presented in Table 2 does not contain negative control, i.e., proteins purified from bacterial strain with empty vector, to compare. More importantly positive controls, such as already identified UGTs involved in gluosyl derivatives of auxin, SA, or ABA, are needed to verify if the assay conditions are optimal. In addition, we have been detecting only 12-*O*-Glc-JA and 12-*O*-Glc-JA-Ile, but UGT86As may be catalyzing glucose esters at the carboxyl-end of JA or JA-Ile. Mass spectrometric methods to detect glucose esters should be established in the future. If the products generated are uncertain, alternative methods to monitor the progression of the assay through depletion of the substrates or UDP-glucose should be considered.

CHAPTER V: CONCLUSIONS AND FUTURE PERSPECTIVES

The plant hormone jasmonate (JA) controls many stress adaptive responses and normal plant growth and development. The field of JA study had a major breakthrough when the molecular receptor for JA was discovered 10 years ago (Chini et al., 2007; Thines et al., 2007). The biosynthetic pathway of JA has been fully elucidated even before the discovery of the molecular receptor in 2007 with the identity of the catalytic enzymes, their encoding genes, expression patterns, associated mutants, and protein structures in some cases (Wasternack and Hause 2013; Koo 2017). However, there are still uncertainties as to how the homeostasis of JA is regulated by its biosynthesis and turnover. This dissertation focused on the issue of JA turnover. What are the dynamics of JA accumulation and how are they affected by the deregulation of JA turnover? What are the enzymes that contribute to the turnover of JA as well as to the biosynthesis of diverse JA metabolites? What are the physiological consequences if JA catabolism is defective? Along the way, surprising observations were made that appeared to contradict the dogma of JA signaling mechanism.

JA-Ile is the bioactive form of JA that signals through the nuclear residing COI1-JAZ co-receptor complex, yet in the *b1b3* mutant with 3-4 fold higher levels of JA-Ile than WT, the plants behaved as if they were deficient in JA-Ile. This was in a way a reflection of emerging evidence in the field that, the JA signaling

pathway is not linear, but rather multifaceted, with multiple pathways converging and diverging to form a complex signaling network (Poudel et al., 2016; Koo 2017). JA-induced gene expression itself is under the control of complex positive and negative feedback regulation. Among the earliest and most strongly induced genes are the *JAZs* that immediately begin to attenuate the JA-induced transcriptional system. Although most of these JAZ proteins are expected to be degraded in the presence of JA-Ile, some non-canonical JAZs including JAZ8 and splice-variants of JAZ10 were reported to resist the degradation. Interestingly, *JAZ8* and *JAZ10* transcripts were found to hyperaccumulate in *b1b3* unlike other *JAZ* transcripts that accumulated to the level of WT. This led to our hypothesis that perhaps these non-canonical JAZs accumulate to high levels in *b1b3* and desensitize the plant against responding to the high levels of JA-Ile. Supporting this hypothesis, JAZ8 and JAZ10 proteins have been reported to be able to interact with and repress components of the WD-repeat/ bHLH/MYB complexes that mediate JA-induced anthocyanin accumulation and trichome initiation such as TT8, GL3, EGL3, MYB75/PAP1 and GL1 (Qi et al., 2011). Consistent with this, *MYB75*/*PAP1* transcripts were strongly reduced in wounded *b1b3* (Chapter II, Figure 2.13) likely contributing to the reduced anthocyanin. In the future the involvement of JAZ8 and JAZ10 in *b1b3*'s wound response should be tested by knocking out their function in *b1b3*. The resulting *b1b3jaz8*, *b1b3jaz10* and/or *b1b3jaz8jaz10* can be tested for WIGI and wound-induced anthocyanin accumulation.

A second hypothesis the present study did not address, but should be studied in the future as a potential cause for the apparent resistance to the wound induced growth inhibition of *b1b3,* is the interplay between JA and the major growth promoting hormone, gibberellic acid (GA) signaling pathway. The physical interaction between JAZ and DELLA proteins has been proposed as a molecular mechanism behind the antagonistic growth regulation between JA and GA (Yang et al., 2012). Similar to JAZs, the DELLA family proteins (five members in *Arabidopsis*) are transcriptional repressors of GA-responsive genes. Their proteolytic removal in the presence of GA activates gene expression by TFs such as PIFs (PHYTOCHROME INTERACTING FACTORs). JAZ interaction with DELLA sequesters DELLA away from PIFs to activate GA-responsive gene transcription, whereas JAZ degradation releases DELLAs to repress PIFs, inhibiting GA-induced growth. We hypothesize that the increased JAZ8 and JAZ10 in *b1b3* sequester DELLAs, preventing them from repressing PIFs and thereby promoting growth. Evidence for the direct binding of JAZ8/JAZ10 with DELLA is lacking, but this could be achieved through JAZ8/JAZ10's heterodimerization with other JAZs that are shown to bind DELLAs (e.g., JAZ1, JAZ3, JAZ9) (Hou et al., 2010; Yang et al., 2012; Qi et al., 2014). If this is true, *b1b3* is expected to be hypersensitive to GA. Removing JAZ8 or JAZ10 from *b1b3* (i.e., in *b1b3jaz8jaz10*) on the other hand will restore its sensitivity to GA back to the normal level.

A third hypothesis is based on the reduced JA metabolite in *b1b3* described in Chapter III. 12OH-JA-Ile, a byproduct of JA-Ile catabolism and

lacking in *b1b3* mutant was investigated for its potential contribution to JA responses as a signaling molecule. The results showed that 12OH-JA-Ile mimics the bioactivity of JA-Ile in many ways including, anthocyanin accumulation, trichome biogenesis, JA-Ile responsive marker gene expression, and specialized metabolite biosynthesis. 12OH-JA-Ile could induce similar effects in tomato and sorghum indicating conservation of the signaling system in other plant species. We found that 12OH-JA-Ile is signaling not through a separate signaling system, but rather through the common COI1-JAZ co-receptors. The reported *in vitro* protein-protein interaction study further supported 12OH-JA-Ile's role as an agonist for JA co-receptors (Koo et al., 2011, Koo et al., 2014). Our preliminary computational modeling studies also are consistent with 12OH-JA-Ile being accommodated by the ligand binding pocket (data not shown). In addition to these docking simulation studies, COI1-JAZ can be crystalized in the future with 12OH-JA-Ile and structure determined by X-ray crystallography. This could lead to structural information that can be used to mutate the amino acid residues that are coordinating 12OH-JA-Ile in the ligand binding pocket to shift its binding affinity toward 12OH-JA-Ile. The engineered plants can be tested if it now will preferentially respond to 12OH-JA-Ile over JA-Ile. Similar studies have been applied to engineer plants to distinguish between JA-Ile and coronatine, a JA-Ile-mimicking virulence factor in *Pseudomonas syringae* (Zhang L et al., 2015) and also in other hormone receptors (e.g., ABA) (Mosquna et al., 2011). Phylogentic sequence analysis can be used to examine whether such mutations in COI1 receptor (or other related F-box proteins) occur in some other plant species.

An important question that needs to be addressed in the future is whether 12OH-JA-Ile fulfills an impactful biological role in plants and whether it is substitutional, redundant or unique compared to JA-Ile. There were transcripts and metabolites that were exclusively changed by 12OH-JA-Ile supporting its COI1-JAZ independent signaling role. However, it is unclear whether those exclusive changes by 12OH-JA-Ile were experimental artefacts unrelated to 12OH-JA-Ile's function. Our genetics approach intended to either increase or deplete 12OH-JA-Ile relative to JA-Ile has so far provided a consistent correlation between 12OH-JA-Ile levels and wound phenotypes (i.e., anthocyanin accumulation). However, the mutants and transgenic lines used still leaves room for ambiguity mainly due to the overlapping substrate specificities of the enzymes that were mutated. Additional lines are being created to obtain more conclusive results. For example, lines overexpressing the CYP94B1 crossed with *cyp94c1* are expected to build up 12OH-JA-Ile pool at the expense of JA-Ile. Normal accumulation of anthocyanin or trichomes in these lines will more clearly demonstrate the definitive *in vivo* role of 12OH-JA-Ile. On the other hand, relative differences in tissue specific occurrence of JA-Ile versus 12OH-JA-Ile may separate their respective function. For instance, we found evidence that hydroxylated JAs are more preferentially found in non-leaf tissues namely stems and petioles (data not shown). Higher resolution map of the tissue specific distribution of JA metabolites are needed in the future. Our preliminary attempts to quantify JA metabolites in phloem sap gave promising results, identifying both JA-Ile and 12OH-JA-Ile in the sample (data not shown). Technical improvement

of such an approach is expected to provide useful information. One hypothesis is that JA-derivatives with oxygen groups will be more polar in their physical properties which may help them to be more easily dissolved in aqueous phloem or xylem saps. This will make them a good candidate as mobile signals for long-distance JA signaling. To lay the foundation for future studies related to the issue of systemic JA signaling, we have created an inducible system where CYP94 enzymes can be expressed conditionally under the control of a chemical inducible promoter and introduced in *b1b3* mutant background. Using this system 12OH-JA-Ile deficiency of *b1b3* can be conditionally complemented by spatially restricted expression of CYP94 transgenes which can be used to assess importance of 12OH-JA-Ile in leaf-to-leaf JA signaling. More work in this regard is needed to further develop the idea.

Despite the JA-Ile-like activities of 12OH-JA-Ile, there seems to be little doubt that JA-Ile is still the major receptor-active ligand. Other experiments in the lab seem to suggest that hyperaccumulation of JA-Ile may not be the direct reason for the weakened wound response of *b1b3*. It is not entirely impossible to imagine that CYP94 enzymes have alternative substrates. If that is the case, the compound should have a major function in wound response because essentially all classical JA-Ile dependent wound response is diminished in the mutant. Such compound (or the lack of such compound) in *b1b3* should also be able to counter the high concentrations of JA-Ile in the mutant.

This study showcases the need to explore the biological activities of other JA metabolites. The list of naturally occurring JA metabolites is long and

functions of those metabolites are uncertain. Identification of the JA metabolic network and isolation of their associated mutants is already helping to delineate the biological function of each JA derivatives (Poudel et al., 2016).

The last part of this dissertation presented the semi-forward mutant screening work performed to identify the additional JA metabolic enzymes in the JA pathway. The UGT86A1 and UGT86A2 candidates identified by the screen were more closely examined as a case study to verify its role in JA metabolism. The result at this point is inconclusive with evidence divided between supporting and rejecting the hypothesis. This needs to be further verified by using a double loss-of-function mutant. Due to close proximity of these 2 genes loci, appraoches other than or in combination with T-DNA insertion mutation should be used. For example, genome editing technology such as CRISPR-Cas9 or RNA interference can be used. The *in vitro* UGT assay should be improved with proper positive and negative controls. The original FOX mutant (line 21-1-1) should be re-examined for additional transgenes besides *UGT86A1*.

Nine out of ten candidates remain to be studied in detail. The majority of these are unlikely to be directly involved in JA metabolism based on their annotated gene description. Root growth response to JA and altered JA profile may be indirect effects of overexpressing those genes in the selected lines. Among the selected candidates is a vacuolar processing enzyme. There hasn't been any report on compartmentalization of the JA metabolites in the vacuoles, although more water soluble derivatives such as glycosylated JA are expected to eventually end up in the vacuoles. The gene encoding vacuolar processing

enzyme has been reported to be induced by wound, salicylic acid, ethylene and to a lesser extent by jasmonic acid stress (Kinosita et al., 1999). Another candidate is the calmodulin 9, a calcium sensor regulating target proteins in various signaling cascades (Megan et al., 2008; Vadassery et al., 2012). Calcium signaling plays important role in wound response and could be necessary for triggering the initial JA responses (Choi et al., 2016). However it is yet to explore how the overexpression of this calmodulin 9, isolated from our screening confers resistance to the JA-mediated root growth inhibition. A metallopeptidase M24 was among the selected candidates. JA-Ile amidohydrolases, ILL6 and IAR3 belong to a subfamily of the metallopeptidase superfamily (Zhang et al., 2016). JA has been reported to be conjugated with an array of small molecules such as amino acids, sugar or ACC that are also detectable in the wounded leaves (Koo et al., 2009; Staswick et al., 2005; Yan et al., 2016). It is possible that the identified metallopeptidase candidate could be involved in hydrolyzing one of those JA conjugates. A recent paper showed that miR156-targeted TF, SQUAMOSA PROMOTER BINDING PROTEIN-LIKE9 (SPL9) interacts with JAZ proteins and is involved in age-dependent decay of JA-response (Mao et al., 2017). A SPL protein homolog, SPL13, was among the candidates identified in our gain-of-function screen. Overexpression of SPL9 was hypothesized to stabilize JAZs and thereby repress JA response. This could potentially explain why SPL13 overexpressing plants were resistant to JA-induced root growth inhibition. Reduction of JA-Ile in these lines may be the result of reduced JA biosynthetic enzyme expression. Additional studies are needed to test this hypothesis.

Photosystem II (PSII) was identified multiple times in lines with longer roots on JA containing media. Although we discounted PSII as an artefact given that there is no clear explanation for such artefact, the possibility of PSII overexpression causing longer roots, perhaps through enhanced photosynthesis, remains. Other candidates, including pyrophosphorylase, an unknown protein, the smaller with variable branches, the protein phosphatase 2C, and RNA binding diubiquinating enzyme need to be characterized. Study of these genes could open up a new direction in the JA field.

References

Acosta, I.F., and Farmer, E.E. (2010). Jasmonates. The Arabidopsis book / American Society of Plant Biologists *8*, e0129.

Afendi, F.M., Okada, T., Yamazaki, M., Hirai-Morita, A., Nakamura, Y., Nakamura, K., Ikeda, S., Takahashi, H., Altaf-Ul-Amin, M., Darusman, L.K., *et al.* (2012). KNApSAcK family databases: integrated metabolite-plant species databases for multifaceted plant research. Plant Cell Physiol *53*, e1.

Alonso, J.M., and Ecker, J.R. (2006). Moving forward in reverse: genetic technologies to enable genome-wide phenomic screens in Arabidopsis. Nat Rev Genet *7*, 524-536.

Andersson, M.X., Hamberg, M., Kourtchenko, O., Brunnstrom, A., McPhail, K.L., Gerwick, W.H., Gobel, C., Feussner, I., and Ellerstrom, M. (2006). Oxylipin profiling of the hypersensitive response in Arabidopsis thaliana. Formation of a novel oxo-phytodienoic acid-containing galactolipid, arabidopside E. J Biol Chem *281*, 31528-31537.

Andreou, A., Brodhun, F., and Feussner, I. (2009). Biosynthesis of oxylipins in non-mammals. Prog Lipid Res *48*, 148-170.

Attaran, E., Major, I.T., Cruz, J.A., Rosa, B.A., Koo, A.J., Chen, J., Kramer, D.M., He, S.Y., and Howe, G.A. (2014). Temporal Dynamics of Growth and Photosynthesis Suppression in Response to Jasmonate Signaling. Plant Physiol *165*, 1302-1314.

Aubert, Y., Widemann, E., Miesch, L., Pinot, F., and Heitz, T. (2015). CYP94-mediated jasmonoyl-isoleucine hormone oxidation shapes jasmonate profiles and attenuates defence responses to Botrytis cinerea infection. J Exp Bot *66*, 3879-3892.

Baker, A., Graham, I.A., Holdsworth, M., Smith, S.M., and Theodoulou, F.L. (2006). Chewing the fat: beta-oxidation in signalling and development. Trends Plant Sci *11*, 124-132.

Baldwin, I.T. (1996). Methyl jasmonate-induced nicotine production in Nicotiana attenuata: Inducing defenses in the field without wounding. Entomol Exp Appl *80*, 213-220.

Baldwin, I.T. (1998). Jasmonate-induced responses are costly but benefit plants under attack in native populations. Proc Natl Acad Sci U S A *95*, 8113-8118.

Ballare, C.L. (2014). Light regulation of plant defense. Annu Rev Plant Biol *65*, 335-363.

Bannenberg, G., Martinez, M., Hamberg, M., and Castresana, C. (2009). Diversity of the enzymatic activity in the lipoxygenase gene family of Arabidopsis thaliana. Lipids *44*, 85-95.

Bartel, B., and Fink, G.R. (1995). ILR1, an amidohydrolase that releases active indole-3-acetic acid from conjugates. Science *268*, 1745-1748.

Bell, E., Creelman, R.A., and Mullet, J.E. (1995). A chloroplast lipoxygenase is required for wound-induced jasmonic acid accumulation in Arabidopsis. Proc Natl Acad Sci USA *92*, 8675-8679.

Berger, C.N., Brown, D.J., Shaw, R.K., Minuzzi, F., Feys, B., and Frankel, G. (2011). Salmonella enterica strains belonging to O serogroup 1,3,19 induce chlorosis and wilting of Arabidopsis thaliana leaves. Environ Microbiol *13*, 1299-1308.

Bhosale, R., Jewell, J.B., Hollunder, J., Koo, A.J., Vuylsteke, M., Michoel, T., Hilson, P., Goossens, A., Howe, G.A., Browse, J.*, et al.* (2013). Predicting gene function from uncontrolled expression variation among individual wild-type Arabidopsis plants. Plant Cell *25*, 2865-2877.

Biggs, A.R. (1985). SUBERIZED BOUNDARY ZONES AND THE CHRONOLOGY OF WOUND RESPONSES IN TREE BARK. Phytopathology *75*, 1191-1195.

Blancaflor, E.B., Kilaru, A., Keereetaweep, J., Khan, B.R., Faure, L., and Chapman, K.D. (2014). N-Acylethanolamines: lipid metabolites with functions in plant growth and development. Plant J *79*, 568-583.

Blee, E. (2002). Impact of phyto-oxylipins in plant defense. Trends Plant Sci *7*, 315-322.

Bolle, C., Schneider, A., and Leister, D. (2011). Perspectives on Systematic Analyses of Gene Function in Arabidopsis thaliana: New Tools, Topics and Trends. Curr Genomics *12*, 1-14.

Boter, M., Ruiz-Rivero, O., Abdeen, A., and Prat, S. (2004). Conserved MYC transcription factors play a key role in jasmonate signaling both in tomato and Arabidopsis. Genes Dev *18*, 1577-1591.

Bottcher, C., and Pollmann, S. (2009). Plant oxylipins: plant responses to 12-oxo-phytodienoic acid are governed by its specific structural and functional properties. FEBS J *276*, 4693-4704.

Bottcher, C., von Roepenack-Lahaye, E., Schmidt, J., Schmotz, C., Neumann, S., Scheel, D., and Clemens, S. (2008). Metabolome analysis of biosynthetic mutants reveals a diversity of metabolic changes and allows identification of a large number of new compounds in Arabidopsis. Plant Physiol *147*, 2107-2120.

Bouche, N., and Bouchez, D. (2001). Arabidopsis gene knockout: phenotypes wanted. Curr Opin Plant Biol *4*, 111-117.

Boughton, A.J., Hoover, K., and Felton, G.W. (2005). Methyl jasmonate application induces increased densities of glandular trichomes on tomato, Lycopersicon esculentum. J Chem Ecol *31*, 2211-2216.

Browse, J. (2009a). Jasmonate passes muster: a receptor and targets for the defense hormone. Annu Rev Plant Biol *60*, 183-205.

Browse, J. (2009b). The power of mutants for investigating jasmonate biosynthesis and signaling. Phytochemistry *70*, 1539-1546.

Buseman, C.M., Tamura, P., Sparks, A.A., Baughman, E.J., Maatta, S., Zhao, J., Roth, M.R., Esch, S.W., Shah, J., Williams, T.D.*, et al.* (2006). Wounding stimulates the accumulation of glycerolipids containing oxophytodienoic acid and dinor-oxophytodienoic acid in Arabidopsis leaves. Plant Physiol *142*, 28-39.

Caarls, L., Elberse, J., Awwanah, M., Ludwig, N.R., de Vries, M., Zeilmaker, T., Van Wees, S.C.M., Schuurink, R.C., and Van den Ackerveken, G. (2017). Arabidopsis JASMONATE-INDUCED OXYGENASES down-regulate plant immunity by hydroxylation and inactivation of the hormone jasmonic acid. Proc Natl Acad Sci U S A *114*, 6388-6393.

Campanella, J.J., Larko, D., and Smalley, J. (2003). A molecular phylogenomic analysis of the ILR1-like family of IAA amidohydrolase genes. Comp Funct Genomics *4*, 584-600.

Campos, M.L., Kang, J.H., and Howe, G.A. (2014). Jasmonate-triggered plant immunity. J Chem Ecol *40*, 657-675.

Campos, M.L., Yoshida, Y., Major, I.T., de Oliveira Ferreira, D., Weraduwage, S.M., Froehlich, J.E., Johnson, B.F., Kramer, D.M., Jander, G., Sharkey, T.D.*, et al.* (2016). Rewiring of jasmonate and phytochrome B signalling uncouples plant growth-defense tradeoffs. Nat Commun *7*, 12570.

Carrera, E., Holman, T., Medhurst, A., Peer, W., Schmuths, H., Footitt, S., Theodoulou, F.L., and Holdsworth, M.J. (2007). Gene expression profiling reveals defined functions of the ATP-binding cassette transporter COMATOSE late in phase II of germination. Plant Physiol *143*, 1669-1679.

Chauvin, A., Caldelari, D., Wolfender, J.L., and Farmer, E.E. (2013). Four 13-lipoxygenases contribute to rapid jasmonate synthesis in wounded Arabidopsis thaliana leaves: a role for lipoxygenase 6 in responses to long-distance wound signals. New Phytol *197*, 566-575.

Chico, J.M., Chini, A., Fonseca, S., and Solano, R. (2008). JAZ repressors set the rhythm in jasmonate signaling. Curr Opin Plant Biol *11*, 486-494.

Chini, A., Fonseca, S., Fernandez, G., Adie, B., Chico, J.M., Lorenzo, O., Garcia-Casado, G., Lopez-Vidriero, I., Lozano, F.M., Ponce, M.R.*, et al.* (2007). The JAZ family of repressors is the missing link in jasmonate signalling. Nature *448*, 666-671.

Choi, W.G., Hilleary, R., Swanson, S.J., Kim, S.H., and Gilroy, S. (2016). Rapid, Long-Distance Electrical and Calcium Signaling in Plants. Annu Rev Plant Biol *67*, 287-307.

Christensen, S.A., Nemchenko, A., Borrego, E., Murray, I., Sobhy, I.S., Bosak, L., DeBlasio, S., Erb, M., Robert, C.A., Vaughn, K.A.*, et al.* (2013). The maize lipoxygenase, ZmLOX10, mediates green leaf volatile, jasmonate and herbivore-induced plant volatile production for defense against insect attack. Plant J *74*, 59-73.

Chung, H.S., and Howe, G.A. (2009). A critical role for the TIFY motif in repression of jasmonate signaling by a stabilized splice variant of the JASMONATE ZIM-domain protein JAZ10 in Arabidopsis. Plant Cell *21*, 131-145.

Chung, H.S., Koo, A.J., Gao, X., Jayanty, S., Thines, B., Jones, A.D., and Howe, G.A. (2008). Regulation and function of Arabidopsis JASMONATE ZIM-domain genes in response to wounding and herbivory. Plant Physiol *146*, 952-964.

Clough, S.J., and Bent, A.F. (1998). Floral dip: a simplified method for Agrobacterium-mediated transformation of Arabidopsis thaliana. Plant J *16*, 735-743.

Cruz Castillo, M., Martinez, C., Buchala, A., Metraux, J.P., and Leon, J. (2004). Gene-specific involvement of beta-oxidation in wound-activated responses in Arabidopsis. Plant Physiol *135*, 85-94.

Davies, R.T., Goetz, D.H., Lasswell, J., Anderson, M.N., and Bartel, B. (1999). IAR3 encodes an auxin conjugate hydrolase from Arabidopsis. Plant Cell *11*, 365-376.

De Geyter, N., Gholami, A., Goormachtig, S., and Goossens, A. (2012). Transcriptional machineries in jasmonate-elicited plant secondary metabolism. Trends Plant Sci *17*, 349-359.

Delker, C., Zolman, B.K., Miersch, O., and Wasternack, C. (2007). Jasmonate biosynthesis in Arabidopsis thaliana requires peroxisomal beta-oxidation enzymes--additional proof by properties of pex6 and aim1. Phytochemistry *68*, 1642-1650.

Demole E, Lederer E, Mercier D. 1962. Isolement et détermination de la structure du jasmonate de méthyle, constituant odorant charactéristique de lèssence de jasmin, Helvetica Chimica Acta, *45,* 675-685.

Devoto, A., Ellis, C., Magusin, A., Chang, H.S., Chilcott, C., Zhu, T., and Turner, J.G. (2005). Expression profiling reveals COI1 to be a key regulator of genes involved in wound- and methyl jasmonate-induced secondary

metabolism, defence, and hormone interactions. Plant Mol Biol *58*, 497-513.

Dombrecht, B., Xue, G.P., Sprague, S.J., Kirkegaard, J.A., Ross, J.J., Reid, J.B., Fitt, G.P., Sewelam, N., Schenk, P.M., Manners, J.M.*, et al.* (2007). MYC2 differentially modulates diverse jasmonate-dependent functions in Arabidopsis. Plant Cell *19*, 2225-2245.

Ellis, C., Karafyllidis, I., Wasternack, C., and Turner, J.G. (2002). The Arabidopsis mutant cev1 links cell wall signaling to jasmonate and ethylene responses. Plant Cell *14*, 1557-1566.

Engelberth, J., Alborn, H.T., Schmelz, E.A., and Tumlinson, J.H. (2004). Airborne signals prime plants against insect herbivore attack. Proc Natl Acad Sci U S A *101*, 1781-1785.

Engelsdorf, T., Horst, R.J., Prols, R., Proschel, M., Dietz, F., Huckelhoven, R., and Voll, L.M. (2013). Reduced carbohydrate availability enhances the susceptibility of Arabidopsis toward Colletotrichum higginsianum. Plant Physiol *162*, 225-238.

Erb, M., Meldau, S., and Howe, G.A. (2012). Role of phytohormones in insect-specific plant reactions. Trends Plant Sci *17*, 250-259.

Fan, T., Yang, L., Wu, X., Ni, J., Jiang, H., Zhang, Q., Fang, L., Sheng, Y., Ren, Y., and Cao, S. (2016). The PSE1 gene modulates lead tolerance in Arabidopsis. J Exp Bot *67*, 4685-4695.

Farmer, E.E., and Ryan, C.A. (1990). Interplant communication: airborne methyl jasmonate induces synthesis of proteinase inhibitors in plant leaves. Proc Natl Acad Sci U S A *87*, 7713-7716.

Farmer, E.E., and Ryan, C.A. (1992). Octadecanoid Precursors Of Jasmonic Acid Activate The Synthesis Of Wound-Inducible Proteinase-Inhibitors. Plant Cell *4*, 129-134.

Farmer, E.E., Gasperini, D., and Acosta, I.F. (2014). The squeeze cell hypothesis for the activation of jasmonate synthesis in response to wounding. New Phytol *204*, 282-288.

Fernandez-Calvo, P., Chini, A., Fernandez-Barbero, G., Chico, J.M., Gimenez-Ibanez, S., Geerinck, J., Eeckhout, D., Schweizer, F., Godoy, M., Franco-Zorrilla, J.M.*, et al.* (2011). The Arabidopsis bHLH transcription factors MYC3 and MYC4 are targets of JAZ repressors and act additively with MYC2 in the activation of jasmonate responses. Plant Cell *23*, 701-715.

Feys, B., Benedetti, C.E., Penfold, C.N., and Turner, J.G. (1994). Arabidopsis Mutants Selected for Resistance to the Phytotoxin Coronatine Are Male Sterile, Insensitive to Methyl Jasmonate, and Resistant to a Bacterial Pathogen. Plant Cell *6*, 751-759.

Figueroa, P., and Browse, J. (2012). The Arabidopsis JAZ2 promoter contains a G-Box and thymidine-rich module that are necessary and sufficient for jasmonate-dependent activation by MYC transcription factors and repression by JAZ proteins. Plant Cell Physiol *53*, 330-343.

Fonseca, S., Chini, A., Hamberg, M., Adie, B., Porzel, A., Kramell, R., Miersch, O., Wasternack, C., and Solano, R. (2009). (+)-7-iso-Jasmonoyl-L-isoleucine is the endogenous bioactive jasmonate. Nat Chem Biol *5*, 344-350.

Footitt, S., Slocombe, S.P., Larner, V., Kurup, S., Wu, Y., Larson, T., Graham, I., Baker, A., and Holdsworth, M. (2002). Control of germination and lipid mobilization by COMATOSE, the Arabidopsis homologue of human ALDP. EMBO J *21*, 2912-2922.

Funk, C.D. (2001). Prostaglandins and leukotrienes: advances in eicosanoid biology. Science *294*, 1871-1875.

Gidda, S.K., Miersch, O., Levitin, A., Schmidt, J., Wasternack, C., and Varin, L. (2003). Biochemical and molecular characterization of a hydroxyjasmonate sulfotransferase from Arabidopsis thaliana. J Biol Chem *278*, 17895-17900.

Glauser, G., Grata, E., Dubugnon, L., Rudaz, S., Farmer, E.E., and Wolfender, J.L. (2008). Spatial and temporal dynamics of jasmonate synthesis and accumulation in Arabidopsis in response to wounding. J Biol Chem *283*, 16400-16407.

Green, J.M., Appel, H., Rehrig, E.M., Harnsomburana, J., Chang, J.F., Balint-Kurti, P., and Shyu, C.R. (2012). PhenoPhyte: a flexible affordable method to quantify 2D phenotypes from imagery. Plant Methods *8*, 1746-4811.

Guranowski, A., Miersch, O., Staswick, P.E., Suza, W., and Wasternack, C. (2007). Substrate specificity and products of side-reactions catalyzed by jasmonate:amino acid synthetase (JAR1). FEBS Lett *581*, 815-820.

Hagen, G., and Guilfoyle, T.J. (1985). Rapid induction of selective transcription by auxins. Mol Cell Biol *5*, 1197-1203.

Halitschke, R., and Baldwin, I.T. (2005). Jasmonates and realted compounds in plant-insect interactions. J Plant Growth Regul *23*, 238-245.

Havko, N.E., Major, I.T., Jewell, J.B., Attaran, E., Browse, J., and Howe, G.A. (2016). Control of Carbon Assimilation and Partitioning by Jasmonate: An Accounting of Growth-Defense Tradeoffs. Plants (Basel) *5*.

Hayward, A.P., Moreno, M.A., Howard, T.P., 3rd, Hague, J., Nelson, K., Heffelfinger, C., Romero, S., Kausch, A.P., Glauser, G., Acosta, I.F.*, et al.* (2016). Control of sexuality by the sk1-encoded UDP-glycosyltransferase of maize. Sci Adv *2*, e1600991.

Heil, M., and Karban, R. (2010). Explaining evolution of plant communication by airborne signals. Trends Ecol Evol *25*, 137-144.

Heil, M., and Ton, J. (2008). Long-distance signalling in plant defence. Trends Plant Sci *13*, 264-272.

Heitz, T., Widemann, E., Lugan, R., Miesch, L., Ullmann, P., Desaubry, L., Holder, E., Grausem, B., Kandel, S., Miesch, M.*, et al.* (2012). Cytochromes P450 CYP94C1 and CYP94B3 catalyze two successive oxidation steps of plant hormone Jasmonoyl-isoleucine for catabolic turnover. J Biol Chem *287*, 6296-6306.

Herde, M., Koo, A.J., and Howe, G.A. (2013). Elicitation of jasmonate-mediated defense responses by mechanical wounding and insect herbivory. Methods Mol Biol *1011*, 51-61.

Hou, X., Lee, L.Y., Xia, K., Yan, Y., and Yu, H. (2010). DELLAs modulate jasmonate signaling via competitive binding to JAZs. Dev Cell *19*, 884-894.

Howe, G.A., and Jander, G. (2008). Plant immunity to insect herbivores. Annu Rev Plant Biol *59*, 41-66.

Howe, G.A., Lee, G.I., Itoh, A., Li, L., and DeRocher, A.E. (2000). Cytochrome P450-dependent metabolism of oxylipins in tomato. Cloning and expression of allene oxide synthase and fatty acid hydroperoxide lyase. Plant Physiol *123*, 711-724.

Huot, B., Yao, J., Montgomery, B.L., and He, S.Y. (2013). Growth-Defense Tradeoffs in Plants: A Balancing Act to Optimize Fitness. Molecular Plant *7*, 1267-1287.

Ichikawa, T., Nakazawa, M., Kawashima, M., Iizumi, H., Kuroda, H., Kondou, Y., Tsuhara, Y., Suzuki, K., Ishikawa, A., Seki, M.*, et al.* (2006). The FOX hunting system: an alternative gain-of-function gene hunting technique. Plant J *48*, 974-985.

Ishiguro, S., Kawai-Oda, A., Ueda, J., Nishida, I., and Okada, K. (2001). The DEFECTIVE IN ANTHER DEHISCIENCE gene encodes a novel phospholipase A1 catalyzing the initial step of jasmonic acid biosynthesis, which synchronizes pollen maturation, anther dehiscence, and flower opening in Arabidopsis. Plant Cell *13*, 2191-2209.

Ishiguro, S., Kawai-Oda, A., Ueda, J., Nishida, I., and Okada, K. (2001). The DEFECTIVE IN ANTHER DEHISCIENCE gene encodes a novel phospholipase A1 catalyzing the initial step of jasmonic acid biosynthesis,

which synchronizes pollen maturation, anther dehiscence, and flower opening in Arabidopsis. Plant Cell *13*, 2191-2209.

Jin, S.H., Ma, X.M., Han, P., Wang, B., Sun, Y.G., Zhang, G.Z., Li, Y.J., and Hou, B.K. (2013). UGT74D1 is a novel auxin glycosyltransferase from Arabidopsis thaliana. PLoS One *8*, e61705.

Ju, C., Van de Poel, B., Cooper, E.D., Thierer, J.H., Gibbons, T.R., Delwiche, C.F., and Chang, C. (2015). Conservation of ethylene as a plant hormone over 450 million years of evolution. Nature Plants *1*, 14004.

Kachroo, A., and Kachroo, P. (2009). Fatty Acid-derived signals in plant defense. Annu Rev Phytopathol *47*, 153-176.

Katsir, L., Chung, H.S., Koo, A.J., and Howe, G.A. (2008a). Jasmonate signaling: a conserved mechanism of hormone sensing. Curr Opin Plant Biol *11*, 428-435.

Katsir, L., Schilmiller, A.L., Staswick, P.E., He, S.Y., and Howe, G.A. (2008). COI1 is a critical component of a receptor for jasmonate and the bacterial virulence factor coronatine. Proc Natl Acad Sci U S A *105*, 7100-7105.

Kerchev, P.I., Fenton, B., Foyer, C.H., and Hancock, R.D. (2012). Plant responses to insect herbivory: interactions between photosynthesis, reactive oxygen species and hormonal signalling pathways. Plant Cell Environ *35*, 441-453.

Khosla, A., Paper, J.M., Boehler, A.P., Bradley, A.M., Neumann, T.R., and Schrick, K. (2014). HD-Zip Proteins GL2 and HDG11 Have Redundant

Functions in Arabidopsis Trichomes, and GL2 Activates a Positive Feedback Loop via MYB23. Plant Cell *26*, 2184-2200.

Kinoshita, T., Yamada, K., Hiraiwa, N., Kondo, M., Nishimura, M., and Hara-Nishimura, I. (1999). Vacuolar processing enzyme is up-regulated in the lytic vacuoles of vegetative tissues during senescence and under various stressed conditions. The Plant Journal *19*, 43-53.

Kitaoka, N., Matsubara, T., Sato, M., Takahashi, K., Wakuta, S., Kawaide, H., Matsui, H., Nabeta, K., and Matsuura, H. (2011). Arabidopsis CYP94B3 encodes jasmonyl-L-isoleucine 12-hydroxylase, a key enzyme in the oxidative catabolism of jasmonate. Plant Cell Physiol *52*, 1757-1765.

Kliebenstein, D., Pedersen, D., Barker, B., and Mitchell-Olds, T. (2002a). Comparative analysis of quantitative trait loci controlling glucosinolates, myrosinase and insect resistance in Arabidapsis thaliana. Genetics *161*, 325-332.

Kliebenstein, D.J., Figuth, A., and Mitchell-Olds, T. (2002b). Genetic architecture of plastic methyl jasmonate responses in Arabidopsis thaliana. Genetics *161*, 1685-1696.

Koo, A.J. (2017). Metabolism of the plant hormone jasmonate: a sentinel for tissue damage and master regulator of stress response. Phytochemistry Reviews.

Koo, A.J., and Howe, G.A. (2009). The wound hormone jasmonate. Phytochemistry *70*, 1571-1580.

Koo, A.J., and Howe, G.A. (2012). Catabolism and deactivation of the lipid-derived hormone jasmonoyl-isoleucine. Front Plant Sci *3*, 19.

Koo, A.J., Chung, H.S., Kobayashi, Y., and Howe, G.A. (2006). Identification of a peroxisomal acyl-activating enzyme involved in the biosynthesis of jasmonic acid in Arabidopsis. J Biol Chem *281*, 33511-33520.

Koo, A.J., Cooke, T.F., and Howe, G.A. (2011). Cytochrome P450 CYP94B3 mediates catabolism and inactivation of the plant hormone jasmonoyl-L-isoleucine. Proc Natl Acad Sci U S A *108*, 9298-9303.

Koo, A.J., Gao, X., Jones, A.D., and Howe, G.A. (2009). A rapid wound signal activates the systemic synthesis of bioactive jasmonates in Arabidopsis. Plant J *59*, 974-986.

Koo, A.J., Thireault, C., Zemelis, S., Poudel, A.N., Zhang, T., Kitaoka, N., Brandizzi, F., Matsuura, H., and Howe, G.A. (2014). Endoplasmic Reticulum-associated Inactivation of the Hormone Jasmonoyl-l-Isoleucine by Multiple Members of the Cytochrome P450 94 Family in Arabidopsis. J Biol Chem *289*, 29728-29738.

Langmead, B., and Salzberg, S.L. (2012). Fast gapped-read alignment with Bowtie 2. Nat Methods *9*, 357-359.

Laudert, D., Pfannschmidt, U., Lottspeich, F., Hollander-Czytko, H., and Weiler, E.W. (1996). Cloning, molecular and functional characterization of Arabidopsis thaliana allene oxide synthase (CYP 74), the first enzyme of the octadecanoid pathway to jasmonates. Plant Mol Biol *31*, 323-335.

LeClere, S., and Bartel, B. (2001). A library of Arabidopsis 35S-cDNA lines for identifying novel mutants. Plant Molecular Biology *46*, 695-703.

Lei, Z., Jing, L., Qiu, F., Zhang, H., Huhman, D., Zhou, Z., and Sumner, L.W. (2015). Construction of an Ultrahigh Pressure Liquid Chromatography-Tandem Mass Spectral Library of Plant Natural Products and Comparative Spectral Analyses. Anal Chem *87*, 7373-7381.

León, J., Rojo, E., and Sánchez-Serrano, J.J. (2001). Wound signalling in plants. J Exp Bot *52*, 1-9.

Leone, M., Keller, M.M., Cerrudo, I., and Ballare, C.L. (2014). To grow or defend? Low red : far-red ratios reduce jasmonate sensitivity in Arabidopsis seedlings by promoting DELLA degradation and increasing JAZ10 stability. New Phytol *204*, 355-367.

Li, L., Li, C., Lee, G.I., and Howe, G.A. (2002). Distinct roles for jasmonate synthesis and action in the systemic wound response of tomato. Proc Natl Acad Sci USA *99*, 6416-6421.

Li, L., Zhao, Y., McCaig, B.C., Wingerd, B.A., Wang, J., Whalon, M.E., Pichersky, E., and Howe, G.A. (2004). The tomato homolog of CORONATINE-INSENSITIVE1 is required for the maternal control of seed maturation, jasmonate-signaled defense responses, and glandular trichome development. Plant Cell *16*, 126-143.

Lorenzo, O., and Solano, R. (2005). Molecular players regulating the jasmonate signalling network. Curr Opin Plant Biol *8*, 532-540.

Lorenzo, O., Chico, J.M., Sanchez-Serrano, J.J., and Solano, R. (2004). JASMONATE-INSENSITIVE1 encodes a MYC transcription factor essential to discriminate between different jasmonate-regulated defense responses in Arabidopsis. Plant Cell *16*, 1938-1950.

Loreti, E., Povero, G., Novi, G., Solfanelli, C., Alpi, A., and Perata, P. (2008). Gibberellins, jasmonate and abscisic acid modulate the sucrose-induced expression of anthocyanin biosynthetic genes in Arabidopsis. New Phytol *179*, 1004-1016.

Lu, G., Wang, X., Liu, J., Yu, K., Gao, Y., Liu, H., Wang, C., Wang, W., Wang, G., Liu, M.*, et al.* (2014). Application of T-DNA activation tagging to identify glutamate receptor-like genes that enhance drought tolerance in plants. Plant Cell Rep *33*, 617-631.

Ludwig-Muller, J. (2011). Auxin conjugates: their role for plant development and in the evolution of land plants. J Exp Bot *62*, 1757-1773.

Ma, Y., Szostkiewicz, I., Korte, A., Moes, D., Yang, Y., Christmann, A., and Grill, E. (2009). Regulators of PP2C phosphatase activity function as abscisic acid sensors. Science *324*, 1064-1068.

Magnan, F., Ranty, B., Charpenteau, M., Sotta, B., Galaud, J.-P., and Aldon, D. (2008). Mutations in AtCML9, a calmodulin-like protein from Arabidopsis thaliana, alter plant responses to abiotic stress and abscisic acid. The Plant Journal *56*, 575-589.

Mao, Y.B., Liu, Y.Q., Chen, D.Y., Chen, F.Y., Fang, X., Hong, G.J., Wang, L.J., Wang, J.W., and Chen, X.Y. (2017). Jasmonate response decay and

defense metabolite accumulation contributes to age-regulated dynamics of plant insect resistance. Nat Commun *8*, 13925.

Martin, D., Tholl, D., Gershenzon, J., and Bohlmann, J. (2002). Methyl jasmonate induces traumatic resin ducts, terpenoid resin biosynthesis, and terpenoid accumulation in developing xylem of Norway spruce stems. Plant Physiol *129*, 1003-1018.

Matsuura, H., Ohkubo, Y., and Yoshihara, T. (2001). Occurrence of 11-hydroxyjasmonic acid glucoside in leaflets of potato plants (Solanum tuberosum L.). Biosci Biotechnol Biochem *65*, 378-382.

McConn, M., and Browse, J. (1996). The Critical Requirement for Linolenic Acid Is Pollen Development, Not Photosynthesis, in an Arabidopsis Mutant. The Plant Cell *8*, 403-416.

Memelink, J. (2009). Regulation of gene expression by jasmonate hormones. Phytochemistry *70*, 1560-1570.

Miersch, O., Neumerkel, J., Dippe, M., Stenzel, I., and Wasternack, C. (2008). Hydroxylated jasmonates are commonly occurring metabolites of jasmonic acid and contribute to a partial switch-off in jasmonate signaling. New Phytol *177*, 114-127.

Miersch, O., Weichert, H., Stenzel, I., Hause, B., Maucher, H., Feussner, I., and Wasternack, C. (2004). Constitutive overexpression of allene oxide cyclase in tomato (Lycopersicon esculentum cv. Lukullus) elevates levels of some jasmonates and octadecanoids in flower organs but not in leaves. Phytochemistry *65*, 847-856.

Mita, S., Murano, N., Akaike, M., and Nakamura, K. (1997). Mutants of Arabidopsis thaliana with pleiotropic effects on the expression of the gene for beta-amylase and on the accumulation of anthocyanin that are inducible by sugars. Plant J *11*, 841-851.

Mithofer, A., and Boland, W. (2012). Plant defense against herbivores: chemical aspects. Annu Rev Plant Biol *63*, 431-450.

Mitra, S., and Baldwin, I.T. (2014). RuBPCase activase (RCA) mediates growth-defense trade-offs: silencing RCA redirects jasmonic acid (JA) flux from JA-isoleucine to methyl jasmonate (MeJA) to attenuate induced defense responses in Nicotiana attenuata. New Phytol *201*, 1385-1395.

Moreno, I., Sun, C.C., and Ivanov, R. (2009). Far-field condition for light-emitting diode arrays. Appl Opt *48*, 1190-1197.

Mosquna, A., Peterson, F.C., Park, S.Y., Lozano-Juste, J., Volkman, B.F., and Cutler, S.R. (2011). Potent and selective activation of abscisic acid receptors in vivo by mutational stabilization of their agonist-bound conformation. Proc Natl Acad Sci U S A *108*, 20838-20843.

Nabity, P.D., Zavala, J.A., and DeLucia, E.H. (2013). Herbivore induction of jasmonic acid and chemical defences reduce photosynthesis in Nicotiana attenuata. J Exp Bot *64*, 685-694.

Nakagawa, T., Kurose, T., Hino, T., Tanaka, K., Kawamukai, M., Niwa, Y., Toyooka, K., Matsuoka, K., Jinbo, T., and Kimura, T. (2007). Development of series of gateway binary vectors, pGWBs, for realizing efficient

construction of fusion genes for plant transformation. J Biosci Bioeng *104*, 34-41.

Nakamura, Y., Mithofer, A., Kombrink, E., Boland, W., Hamamoto, S., Uozumi, N., Tohma, K., and Ueda, M. (2011). 12-hydroxyjasmonic acid glucoside is a COI1-JAZ-independent activator of leaf-closing movement in Samanea saman. Plant Physiol *155*, 1226-1236.

Nakata, M., Mitsuda, N., Herde, M., Koo, A.J., Moreno, J.E., Suzuki, K., Howe, G.A., and Ohme-Takagi, M. (2013). A bHLH-type transcription factor, ABA-INDUCIBLE BHLH-TYPE TRANSCRIPTION FACTOR/JA-ASSOCIATED MYC2-LIKE1, acts as a repressor to negatively regulate jasmonate signaling in arabidopsis. Plant Cell *25*, 1641-1656.

Nakazawa, M., Ichikawa, T., Ishikawa, A., Kobayashi, H., Tsuhara, Y., Kawashima, M., Suzuki, K., Muto, S., and Matsui, M. (2003). Activation tagging, a novel tool to dissect the functions of a gene family. Plant J *34*, 741-750.

Nilsson, A.K., Johansson, O.N., Fahlberg, P., Kommuri, M., Topel, M., Bodin, L.J., Sikora, P., Modarres, M., Ekengren, S., Nguyen, C.T.*, et al.* (2015). Acylated monogalactosyl diacylglycerol: Prevalence in the plant kingdom and identification of an enzyme catalyzing galactolipid head group acylation in Arabidopsis thaliana. Plant J *13*, 13072.

Noir, S., Bomer, M., Takahashi, N., Ishida, T., Tsui, T.L., Balbi, V., Shanahan, H., Sugimoto, K., and Devoto, A. (2013). Jasmonate controls leaf growth by

repressing cell proliferation and the onset of endoreduplication while maintaining a potential stand-by mode. Plant Physiol *161*, 1930-1951.

O'Byrne, P.M., Israel, E., and Drazen, J.M. (1997). Antileukotrienes in the Treatment of Asthma. Annals of Internal Medicine *127*, 472-480.

Ohnmeiss, T.E., and Baldwin, I.T. (1994). The Allometry of Nitrogen Allocation to Growth and an Inducible Defense under Nitrogen-Limited Growth. Ecology *75*, 995-1002.

Park, S., Gidda, S.K., James, C.N., Horn, P.J., Khuu, N., Seay, D.C., Keereetaweep, J., Chapman, K.D., Mullen, R.T., and Dyer, J.M. (2013). The alpha/beta hydrolase CGI-58 and peroxisomal transport protein PXA1 coregulate lipid homeostasis and signaling in Arabidopsis. Plant Cell *25*, 1726-1739.

Park, S.Y., Fung, P., Nishimura, N., Jensen, D.R., Fujii, H., Zhao, Y., Lumba, S., Santiago, J., Rodrigues, A., Chow, T.F.*, et al.* (2009). Abscisic acid inhibits type 2C protein phosphatases via the PYR/PYL family of START proteins. Science *324*, 1068-1071.

Patkar, R.N., Benke, P.I., Qu, Z., Chen, Y.Y., Yang, F., Swarup, S., and Naqvi, N.I. (2015). A fungal monooxygenase-derived jasmonate attenuates host innate immunity. Nat Chem Biol *11*, 733-740.

Pauwels, L., Barbero, G.F., Geerinck, J., Tilleman, S., Grunewald, W., Perez, A.C., Chico, J.M., Bossche, R.V., Sewell, J., Gil, E.*, et al.* (2010). NINJA connects the co-repressor TOPLESS to jasmonate signalling. Nature *464*, 788-791.

Pauwels, L., Inze, D., and Goossens, A. (2009). Jasmonate-inducible gene: what does it mean? Trends Plant Sci *14*, 87-91.

Pauwels, L., Morreel, K., De Witte, E., Lammertyn, F., Van Montagu, M., Boerjan, W., Inze, D., and Goossens, A. (2008). Mapping methyl jasmonate-mediated transcriptional reprogramming of metabolism and cell cycle progression in cultured Arabidopsis cells. Proc Natl Acad Sci U S A *105*, 1380-1385.

Poudel, A.N., Zhang, T., Kwasniewski, M., Nakabayashi, R., Saito, K., and Koo, A.J. (2016). Mutations in jasmonoyl-L-isoleucine-12-hydroxylases suppress multiple JA-dependent wound responses in Arabidopsis thaliana. Biochim Biophys Acta *1861*, 1396-1408.

Pourcel, L., Irani, N.G., Koo, A.J.K., Bohorquez-Restrepo, A., Howe, G.A., and Grotewold, E. (2013). A chemical complementation approach reveals genes and interactions of flavonoids with other pathways. Plant J *74*, 383-397.

Priest, D.M., Ambrose, S.J., Vaistij, F.E., Elias, L., Higgins, G.S., Ross, A.R., Abrams, S.R., and Bowles, D.J. (2006). Use of the glucosyltransferase UGT71B6 to disturb abscisic acid homeostasis in Arabidopsis thaliana. Plant J *46*, 492-502.

Qi, T., Huang, H., Wu, D., Yan, J., Qi, Y., Song, S., and Xie, D. (2014). Arabidopsis DELLA and JAZ proteins bind the WD-repeat/bHLH/MYB complex to modulate gibberellin and jasmonate signaling synergy. Plant Cell *26*, 1118-1133.

Qi, T., Song, S., Ren, Q., Wu, D., Huang, H., Chen, Y., Fan, M., Peng, W., Ren, C., and Xie, D. (2011). The Jasmonate-ZIM-domain proteins interact with the WD-Repeat/bHLH/MYB complexes to regulate Jasmonate-mediated anthocyanin accumulation and trichome initiation in Arabidopsis thaliana. Plant Cell *23*, 1795-1814.

Rabino, I., and Mancinelli, A.L. (1986). Light, temperature, and anthocyanin production. Plant Physiol *81*, 922-924.

Reymond, P., Weber, H., Damond, M., and Farmer, E.E. (2000). Differential gene expression in response to mechanical wounding and insect feeding in Arabidopsis. Plant Cell *12*, 707-720.

Ross, J., Li, Y., Lim, E.K., and Bowles, D.J. (2001). Higher plant glycosyltransferases. Genome Biol *2*.

Rudell, D. R.; Mattheis, J. P.; Fan, X.; Fellman, J. K. Methyl jasmonate enhances anthocyanin accumulation and modifies production of phenolics and pigments in “Fuji” apples J. Am. Soc. Hortic. Sci. 2002, *127*, 435 - 441

Sanders, P.M., Lee, P.Y., Biesgen, C., Boone, J.D., Beals, T.P., Weiler, E.W., and Goldberg, R.B. (2000). The arabidopsis DELAYED DEHISCENCE1 gene encodes an enzyme in the jasmonic acid synthesis pathway. Plant Cell *12*, 1041-1061.

Santner, A., and Estelle, M. (2009). Recent advances and emerging trends in plant hormone signalling. Nature *459*, 1071-1078.

Sasaki-Sekimoto, Y., Jikumaru, Y., Obayashi, T., Saito, H., Masuda, S., Kamiya, Y., Ohta, H., and Shirasu, K. (2013). Basic helix-loop-helix transcription

factors JASMONATE-ASSOCIATED MYC2-LIKE1 (JAM1), JAM2, and JAM3 are negative regulators of jasmonate responses in Arabidopsis. Plant Physiol *163*, 291-304.

Sato, T., Maekawa, S., Yasuda, S., Sonoda, Y., Katoh, E., Ichikawa, T., Nakazawa, M., Seki, M., Shinozaki, K., Matsui, M.*, et al.* (2009). CNI1/ATL31, a RING-type ubiquitin ligase that functions in the carbon/nitrogen response for growth phase transition in Arabidopsis seedlings. Plant J *60*, 852-864.

Schaller, F. (2001). Enzymes of the biosynthesis of octadecanoid-derived signalling molecules. J Exp Bot *52*, 11-23.

Schaller, F., Biesgen, C., Mussig, C., Altmann, T., and Weiler, E.W. (2000). 12-Oxophytodienoate reductase 3 (OPR3) is the isoenzyme involved in jasmonate biosynthesis. Planta *210*, 979-984.

Schilmiller, A.L., Koo, A.J., and Howe, G.A. (2007). Functional diversification of acyl-coenzyme A oxidases in jasmonic acid biosynthesis and action. Plant Physiol *143*, 812-824.

Schneider, K., Kienow, L., Schmelzer, E., Colby, T., Bartsch, M., Miersch, O., Wasternack, C., Kombrink, E., and Stuible, H.P. (2005). A new type of peroxisomal Acyl-coenzyme A synthetase from arabidopsis thaliana has the catalytic capacity to activate biosynthetic precursors of jasmonic acid. J Biol Chem *280*, 13962-13972.

Sembdner, G., and Parthier, B. (1993). The Biochemistry and the Physiological and Molecular Actions of Jasmonates. Annual Review of Plant Physiology and Plant Molecular Biology *44*, 569-589.

Seo, H.S., Song, J.T., Cheong, J.J., Lee, Y.H., Lee, Y.W., Hwang, I., Lee, J.S., and Choi, Y.D. (2001). Jasmonic acid carboxyl methyltransferase: a key enzyme for jasmonate-regulated plant responses. Proc Natl Acad Sci U S A *98*, 4788-4793.

Shah, J. (2005). Lipids, lipases, and lipid-modifying enzymes in plant disease resistance. Annu Rev Phytopathol *43*, 229-260.

Shan, X., Zhang, Y., Peng, W., Wang, Z., and Xie, D. (2009). Molecular mechanism for jasmonate-induction of anthocyanin accumulation in Arabidopsis. J Exp Bot *60*, 3849-3860.

Sheard, L.B., Tan, X., Mao, H., Withers, J., Ben-Nissan, G., Hinds, T.R., Kobayashi, Y., Hsu, F.F., Sharon, M., Browse, J.*, et al.* (2010). Jasmonate perception by inositol-phosphate-potentiated COI1-JAZ co-receptor. Nature *468*, 400-405.

Shyu, C., and Brutnell, T.P. (2015). Growth-defence balance in grass biomass production: the role of jasmonates. J Exp Bot *66*, 4165-4176.

Shyu, C., Figueroa, P., Depew, C.L., Cooke, T.F., Sheard, L.B., Moreno, J.E., Katsir, L., Zheng, N., Browse, J., and Howe, G.A. (2012). JAZ8 lacks a canonical degron and has an EAR motif that mediates transcriptional repression of jasmonate responses in Arabidopsis. Plant Cell *24*, 536-550.

Shyu, C., Figueroa, P., Depew, C.L., Cooke, T.F., Sheard, L.B., Moreno, J.E., Katsir, L., Zheng, N., Browse, J., and Howe, G.A. (2012). JAZ8 lacks a canonical degron and has an EAR motif that mediates transcriptional repression of jasmonate responses in Arabidopsis. Plant Cell *24*, 536-550.

Smirnova, E., Marquis, V., Poirier, L., Aubert, Y., Zumsteg, J., Menard, R., Miesch, L., and Heitz, T. (2017). Jasmonic Acid Oxidase 2 Hydroxylates Jasmonic Acid and Represses Basal Defense and Resistance Responses against Botrytis cinerea Infection. Mol Plant *10*, 1159-1173.

Smith, C.A., Want, E.J., O'Maille, G., Abagyan, R., and Siuzdak, G. (2006). XCMS: processing mass spectrometry data for metabolite profiling using nonlinear peak alignment, matching, and identification. Anal Chem *78*, 779-787.

Sonderby, I.E., Geu-Flores, F., and Halkier, B.A. (2010). Biosynthesis of glucosinolates--gene discovery and beyond. Trends Plant Sci *15*, 283-290.

Song, J.T., Koo, Y.J., Seo, H.S., Kim, M.C., Choi, Y.D., and Kim, J.H. (2008). Overexpression of AtSGT1, an Arabidopsis salicylic acid glucosyltransferase, leads to increased susceptibility to Pseudomonas syringae. Phytochemistry *69*, 1128-1134.

Staswick, P.E., and Tiryaki, I. (2004). The oxylipin signal jasmonic acid is activated by an enzyme that conjugates it to isoleucine in Arabidopsis. Plant Cell *16*, 2117-2127.

Staswick, P.E., Serban, B., Rowe, M., Tiryaki, I., Maldonado, M.T., Maldonado, M.C., and Suza, W. (2005). Characterization of an Arabidopsis enzyme

family that conjugates amino acids to indole-3-acetic acid. Plant Cell *17*, 616-627.

Staswick, P.E., Tiryaki, I., and Rowe, M.L. (2002). Jasmonate response locus JAR1 and several related Arabidopsis genes encode enzymes of the firefly luciferase superfamily that show activity on jasmonic, salicylic, and indole-3-acetic acids in an assay for adenylation. Plant Cell *14*, 1405-1415.

Stenzel, I., Hause, B., Miersch, O., Kurz, T., Maucher, H., Weichert, H., Ziegler, J., Feussner, I., and Wasternack, C. (2003). Jasmonate biosynthesis and the allene oxide cyclase family of Arabidopsis thaliana. Plant Mol Biol *51*, 895-911.

Stintzi, A., and Browse, J. (2000). The Arabidopsis male-sterile mutant, opr3, lacks the 12-oxophytodienoic acid reductase required for jasmonate synthesis. Proc Natl Acad Sci U S A *97*, 10625-10630.

Stintzi, A., Weber, H., Reymond, P., Browse, J., and Farmer, E.E. (2001). Plant defense in the absence of jasmonic acid: the role of cyclopentenones. Proc Natl Acad Sci USA *98*, 12837-12842.

Strassner, J., Schaller, F., Frick, U.B., Howe, G.A., Weiler, E.W., Amrhein, N., Macheroux, P., and Schaller, A. (2002). Characterization and cDNA-microarray expression analysis of 12-oxophytodienoate reductases reveals differential roles for octadecanoid biosynthesis in the local versus the systemic wound response. Plant J *32*, 585-601.

Suza, W.P., Rowe, M.L., Hamberg, M., and Staswick, P.E. (2010). A tomato enzyme synthesizes (+)-7-iso-jasmonoyl-L-isoleucine in wounded leaves. Planta *231*, 717-728.

Tamura, M., Tsuji, Y., Kusunose, T., Okazawa, A., Kamimura, N., Mori, T., Nakabayashi, R., Hishiyama, S., Fukuhara, Y., Hara, H.*, et al.* (2014). Successful expression of a novel bacterial gene for pinoresinol reductase and its effect on lignan biosynthesis in transgenic Arabidopsis thaliana. Appl Microbiol Biotechnol *98*, 8165-8177.

Tanaka, K., Hayashi, K., Natsume, M., Kamiya, Y., Sakakibara, H., Kawaide, H., and Kasahara, H. (2014). UGT74D1 catalyzes the glucosylation of 2-oxindole-3-acetic acid in the auxin metabolic pathway in Arabidopsis. Plant Cell Physiol *55*, 218-228.

Teng, S., Keurentjes, J., Bentsink, L., Koornneef, M., and Smeekens, S. (2005). Sucrose-specific induction of anthocyanin biosynthesis in Arabidopsis requires the MYB75/PAP1 gene. Plant Physiol *139*, 1840-1852.

Thaler, J.S., Farag, M.A., Pare, P.W., and Dicke, M. (2002). Jasmonate-deficient plants have reduced direct and indirect defences against herbivores. Ecol Lett *5*, 764-774.

Theodoulou, F.L., Job, K., Slocombe, S.P., Footitt, S., Holdsworth, M., Baker, A., Larson, T.R., and Graham, I.A. (2005). Jasmonoic acid levels are reduced in COMATOSE ATP-binding cassette transporter mutants. Implications for transport of jasmonate precursors into peroxisomes. Plant Physiol *137*, 835-840.

Thines, B., Katsir, L., Melotto, M., Niu, Y., Mandaokar, A., Liu, G., Nomura, K., He, S.Y., Howe, G.A., and Browse, J. (2007). JAZ repressor proteins are targets of the SCF(COI1) complex during jasmonate signalling. Nature *448*, 661-665.

Thireault, C., Shyu, C., Yoshida, Y., St Aubin, B., Campos, M.L., and Howe, G.A. (2015). Repression of jasmonate signaling by a non-TIFY JAZ protein in Arabidopsis. Plant J *82*, 669-679.

Tognetti, V.B., Van Aken, O., Morreel, K., Vandenbroucke, K., van de Cotte, B., De Clercq, I., Chiwocha, S., Fenske, R., Prinsen, E., Boerjan, W.*, et al.* (2010). Perturbation of indole-3-butyric acid homeostasis by the UDP-glucosyltransferase UGT74E2 modulates Arabidopsis architecture and water stress tolerance. Plant Cell *22*, 2660-2679.

Tohge, T., Nishiyama, Y., Hirai, M.Y., Yano, M., Nakajima, J.-i., Awazuhara, M., Inoue, E., Takahashi, H., Goodenowe, D.B., Kitayama, M.*, et al.* (2005). Functional genomics by integrated analysis of metabolome and transcriptome of Arabidopsis plants over-expressing an MYB transcription factor. Plant J *42*, 218-235.

Trapnell, C., Hendrickson, D.G., Sauvageau, M., Goff, L., Rinn, J.L., and Pachter, L. (2013). Differential analysis of gene regulation at transcript resolution with RNA-seq. Nat Biotechnol *31*, 46-53.

Trapnell, C., Roberts, A., Goff, L., Pertea, G., Kim, D., Kelley, D.R., Pimentel, H., Salzberg, S.L., Rinn, J.L., and Pachter, L. (2012). Differential gene and

transcript expression analysis of RNA-seq experiments with TopHat and Cufflinks. Nat Protoc *7*, 562-578.

Trapnell, C., Williams, B.A., Pertea, G., Mortazavi, A., Kwan, G., van Baren, M.J., Salzberg, S.L., Wold, B.J., and Pachter, L. (2010). Transcript assembly and quantification by RNA-Seq reveals unannotated transcripts and isoform switching during cell differentiation. Nat Biotechnol *28*, 511-515.

Tsukaya, H., Ohshima, T., Naito, S., Chino, M., and Komeda, Y. (1991). Sugar-Dependent Expression of the CHS-A Gene for Chalcone Synthase from Petunia in Transgenic Arabidopsis. Plant Physiol *97*, 1414-1421.

Ullmann-Zeunert, L., Stanton, M.A., Wielsch, N., Bartram, S., Hummert, C., Svatos, A., Baldwin, I.T., and Groten, K. (2013). Quantification of growth-defense trade-offs in a common currency: nitrogen required for phenolamide biosynthesis is not derived from ribulose-1,5-bisphosphate carboxylase/oxygenase turnover. Plant J *75*, 417-429.

Vadassery, J., Scholz, S.S., and Mithofer, A. (2012). Multiple calmodulin-like proteins in Arabidopsis are induced by insect-derived (Spodoptera littoralis) oral secretion. Plant Signal Behav *7*, 1277-1280.

von Saint Paul, V., Zhang, W., Kanawati, B., Geist, B., Faus-Kessler, T., Schmitt-Kopplin, P., and Schaffner, A.R. (2011). The Arabidopsis glucosyltransferase UGT76B1 conjugates isoleucic acid and modulates plant defense and senescence. Plant Cell *23*, 4124-4145.

Wang, X. (2004). Lipid signaling. Curr Opin Plant Biol *7*, 329-336.

Wasternack, C. (2007). Jasmonates: an update on biosynthesis, signal transduction and action in plant stress response, growth and development. Ann Bot *100*, 681-697.

Wasternack, C. (2015). How Jasmonates Earned their Laurels: Past and Present. Journal of Plant Growth Regulation *34*, 761-794.

Wasternack, C., and Hause, B. (2013). Jasmonates: biosynthesis, perception, signal transduction and action in plant stress response, growth and development. An update to the 2007 review in Annals of Botany. Ann Bot *111*, 1021-1058.

Weigel, D., Ahn, J.H., Blazquez, M.A., Borevitz, J.O., Christensen, S.K., Fankhauser, C., Ferrandiz, C., Kardailsky, I., Malancharuvil, E.J., Neff, M.M.*, et al.* (2000). Activation tagging in Arabidopsis. Plant Physiol *122*, 1003-1013.

Weng, J.K., Ye, M., Li, B., and Noel, J.P. (2016). Co-evolution of Hormone Metabolism and Signaling Networks Expands Plant Adaptive Plasticity. Cell *166*, 881-893.

Widemann, E., Miesch, L., Lugan, R., Holder, E., Heinrich, C., Aubert, Y., Miesch, M., Pinot, F., and Heitz, T. (2013). The amidohydrolases IAR3 and ILL6 contribute to jasmonoyl-isoleucine hormone turnover and generate 12-hydroxyjasmonic acid upon wounding in Arabidopsis leaves. J Biol Chem *288*, 31701-31714.

Withers, J., Yao, J., Mecey, C., Howe, G.A., Melotto, M., and He, S.Y. (2012). Transcription factor-dependent nuclear localization of a transcriptional

repressor in jasmonate hormone signaling. Proc Natl Acad Sci U S A *109*, 20148-20153.

Woldemariam, M.G., Onkokesung, N., Baldwin, I.T., and Galis, I. (2012). Jasmonoyl-L-isoleucine hydrolase 1 (JIH1) regulates jasmonoyl-L-isoleucine levels and attenuates plant defenses against herbivores. Plant J *72*, 758-767.

Wu, J., and Baldwin, I.T. (2010). New insights into plant responses to the attack from insect herbivores. Annu Rev Genet *44*, 1-24.

Xie, D.X., Feys, B.F., James, S., Nieto-Rostro, M., and Turner, J.G. (1998). COI1: an Arabidopsis gene required for jasmonate-regulated defense and fertility. Science *280*, 1091-1094.

Xu, G., Ma, H., Nei, M., and Kong, H. (2009). Evolution of F-box genes in plants: different modes of sequence divergence and their relationships with functional diversification. Proc Natl Acad Sci U S A *106*, 835-840.

Yan, J., Li, S., Gu, M., Yao, R., Li, Y., Chen, J., Yang, M., Tong, J., Xiao, L., Nan, F.*, et al.* (2016). Endogenous Bioactive Jasmonate Is Composed of a Set of (+)-7-iso-JA-Amino Acid Conjugates. Plant Physiol *172*, 2154-2164.

Yan, Y., Stolz, S., Chetelat, A., Reymond, P., Pagni, M., Dubugnon, L., and Farmer, E.E. (2007). A downstream mediator in the growth repression limb of the jasmonate pathway. Plant Cell *19*, 2470-2483.

Yang, D.L., Yao, J., Mei, C.S., Tong, X.H., Zeng, L.J., Li, Q., Xiao, L.T., Sun, T.P., Li, J., Deng, X.W.*, et al.* (2012). Plant hormone jasmonate prioritizes

defense over growth by interfering with gibberellin signaling cascade. Proc Natl Acad Sci U S A *109*, E1192-1200.

Yokotani, N., Ichikawa, T., Kondou, Y., Matsui, M., Hirochika, H., Iwabuchi, M., and Oda, K. (2008). Expression of rice heat stress transcription factor OsHsfA2e enhances tolerance to environmental stresses in transgenic Arabidopsis. Planta *227*, 957-967.

Yoshida, Y., Sano, R., Wada, T., Takabayashi, J., and Okada, K. (2009). Jasmonic acid control of GLABRA3 links inducible defense and trichome patterning in Arabidopsis. Development *136*, 1039-1048.

Yoshihara, T., Omir, E.-S.A., Koshino, H., Sakamura, S., Kkuta, Y., and Koda, Y. (2014). Structure of a Tuber-inducing Stimulus from Potato Leaves (Solanum tuberosumL.). Agricultural and Biological Chemistry *53*, 2835-2837.

Zhang, F., Yao, J., Ke, J., Zhang, L., Lam, V.Q., Xin, X.F., Zhou, X.E., Chen, J., Brunzelle, J., Griffin, P.R.*, et al.* (2015). Structural basis of JAZ repression of MYC transcription factors in jasmonate signalling. Nature *525*, 269-273.

Zhang, L., Zhang, F., Melotto, M., Yao, J., and He, S.Y. (2017). Jasmonate signaling and manipulation by pathogens and insects. J Exp Bot *68*, 1371-1385.

Zhang, T., Poudel, A.N., Jewell, J.B., Kitaoka, N., Staswick, P., Matsuura, H., and Koo, A.J. (2016). Hormone crosstalk in wound stress response: wound-inducible amidohydrolases can simultaneously regulate jasmonate and auxin homeostasis in Arabidopsis thaliana. J Exp Bot *67*, 2107-2120.

Zhang, Y., and Turner, J.G. (2008). Wound-induced endogenous jasmonates stunt plant growth by inhibiting mitosis. PLoS One *3*, e3699.

Zhao, Y., Thilmony, R., Bender, C.L., Schaller, A., He, S.Y., and Howe, G.A. (2003). Virulence systems of Pseudomonas syringae pv. tomato promote bacterial speck disease in tomato by targeting the jasmonate signaling pathway. Plant J *36*, 485-499.

Zhou, C., Han, L., Fu, C., Chai, M., Zhang, W., Li, G., Tang, Y., and Wang, Z.Y. (2012). Identification and characterization of petiolule-like pulvinus mutants with abolished nyctinastic leaf movement in the model legume Medicago truncatula. New Phytol *196*, 92-100.

Ziegler, J., Stenzel, I., Hause, B., Maucher, H., Hamberg, M., Grimm, R., Ganal, M., and Wasternack, C. (2000). Molecular cloning of allene oxide cyclase. The enzyme establishing the stereochemistry of octadecanoids and jasmonates. J Biol Chem *275*, 19132-19138.

Zolman, B.K., Silva, I.D., and Bartel, B. (2001). The Arabidopsis pxa1 mutant is defective in an ATP-binding cassette transporter-like protein required for peroxisomal fatty acid beta-oxidation. Plant Physiol *127*, 1266-1278.

Züst, T., and Agrawal, A.A. (2017). Trade-Offs Between Plant Growth and Defense Against Insect Herbivory: An Emerging Mechanistic Synthesis. Annual Review of Plant Biology *68*, 513-534.

VITA

Arati Nepal Poudel was born on July 29, 1980 in Kathmandu, Nepal. She is the daughter of Mr. Sitaram Nepal and Mrs. Laxmi Thapa Nepal. Arati did her Bachelor of Agriculture from Institute of Agriculture and Animal Science, Tribhuwan University in 2004. She did her Masters majoring in Soil and Plant Science from the same University in 2006. She spent a following two years as a Lecturer at Himalayan College of Science and Technology and as a Soil Scientist at Ministry of Agriculture, Government of Nepal. In 2008, she began her further study at the University of Miyazaki, Japan under the Japanese Government Scholarship. Her interest in understanding molecular mechanism underlying plant stress response, led her to join Division of Plant Sciences in 2013. She finished her Doctoral degree supervised by Dr. Abraham J Koo in December 2017. She has authored and co-authored several peer-reviewed research articles and seeks to continue the research in plant science in the future.